See pages 30-31.

ISSN: 08 84-8157

NEOTECTONICS An International Journal of Crustal Dynamics Volume 1 Number 1 March 1986 Published by JOHN WILEY & SONS

NEOTECTONICS

An International Journal of Crustal Dynamics

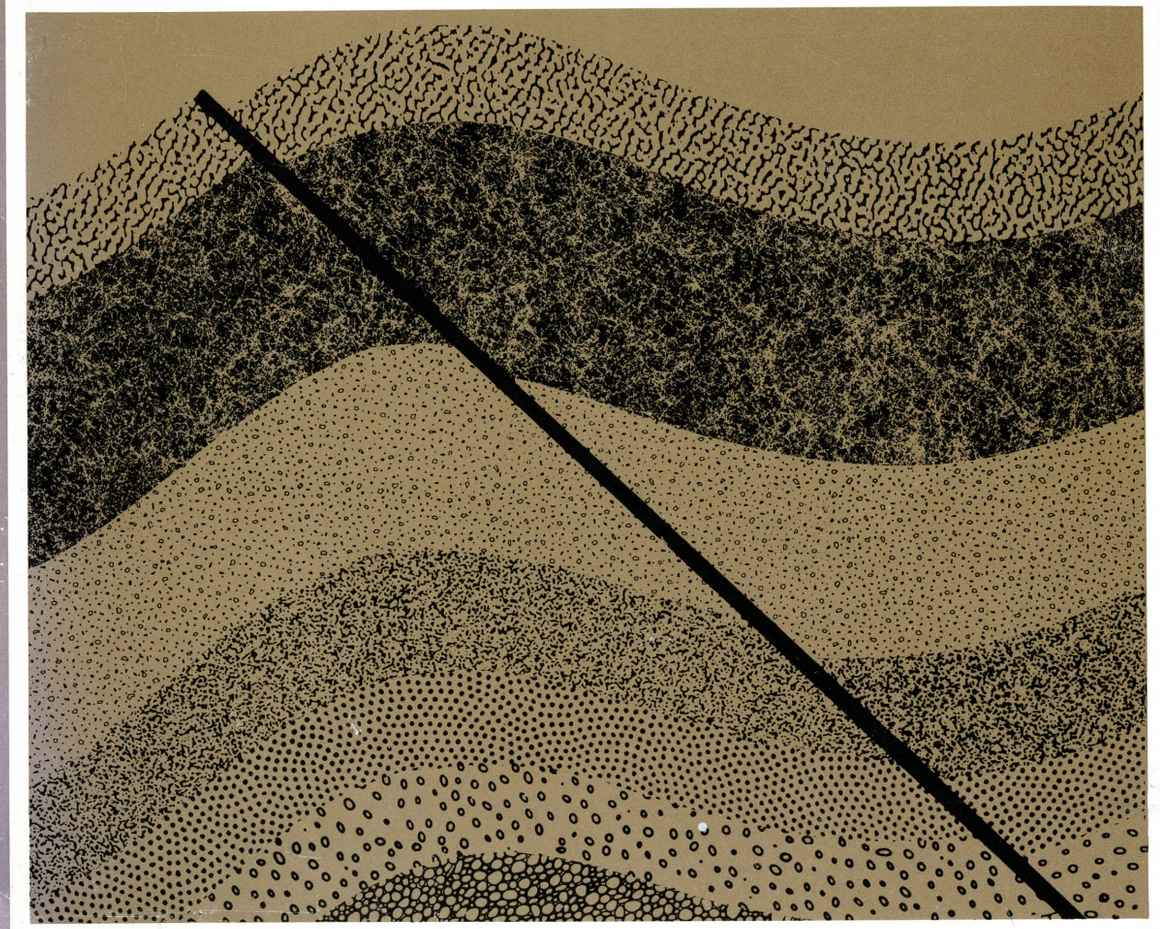

Margaret Anne Winslow, Editor-in-Chief

Volume 1 Number 1 March 1986

Published by JOHN WILEY & SONS

New York • Chichester • Brisbane • Toronto • Singapore

Neotectonics: An International Journal of Crustal Dynamics

Margaret Anne Winslow, *Editor-in-Chief*

Editorial Board

Stephen F. Barrett, *Amoco Production Company (International)*
John F. Dewey, *University of Durham, England*
Rhodes W. Fairbridge, *Columbia University, U.S.A.*
Hugues Faure, *Laboratoire de Geologie du Quaternaire, France*
Mark Hempton, *Bellaire Research Center, U.S.A.*
Daniel E. Karig, *Cornell University, U.S.A.*
Peter Mattson, Ph.D., *Queens College, U.S.A.*
N.-A. Mörner, Ph.D., *Geological Institute, Sweden*
Walter S. Newman, Ph.D., *Queens College, U.S.A.*
Luc Ortlieb, Ph.D., *Office de la Recherche Scientifique et Technique, France*
Robert Speed, Ph.D., *Northwestern University, U.S.A.*
Pavet Vyskocil, *International Center on Recent Crustal Movements, Czechoslovakia*
Robert S. Yeats, Ph.D., *Oregon State University, U.S.A.*

NEW from Wiley in January 1986

GEOARCHAEOLOGY
An International Journal

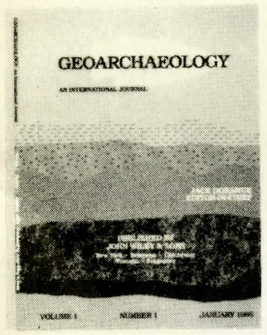

Editor-in-Chief: Jack Donahue, Ph.D.
Department of Anthropology, University of Pittsburgh

GEOARCHAEOLOGY is the only journal to explore the critical interface between archaeology and the earth sciences. Recognizing that the fields are integrally aligned, the journal's interdisciplinary approach aims to promote better understanding of methodologies and applications of common interest to: • archaelolgists • paleontologists • and soil scientists.

GEOARCHAEOLOGY publishes all new information that reflects the interrelatedness of the fields, with emphasis on: • original research reports on the *environmental* setting of archaeological sites and *material analysis* of artifacts • synthesis discussing broader aspects of geoarchaeology, and • methods papers describing new *techniques* and *equipment.*

In addition, GEOARCHAEOLOGY features: Book Reviews, Meeting Notes, Professional News, and Calendars of Events.

Don't miss out on this exciting resource in your field.
Order your subscription to GEOARCHAEOLOGY today.
Volume 1, January 1986 Quarterly $96
(Outside U.S. add $16 for surface postage and handling, or $52 for airmail delivery.)

YES, please enter my subscription to the quarterly, GEOARCHAEOLOGY: An International Journal, with Volume 1, 1986 (four issues) for $96. (Outside U.S. please add $16 for surface postage and handling or $52 for airmail delivery.)

NOTE: Subscriptions are entered on a calendar-year basis only—four issues per year. Your first issue will arrive after payment is received.

Members of certain societies are entitled to a discount on GEOARCHAEOLOGY. Write to us for details.

☐ Check enclosed (U.S. currency only). ☐ Bill me.
Charge to my:
☐ MasterCard. ☐ Visa. ☐ American Express.

Card No. _____ Exp. date _____
Signature _____
Name _____
Institution/Company _____
Address _____
City/State _____ Zip _____
Country _____

Subscription Department
John Wiley & Sons
605 Third Avenue
New York, New York 10158-0012

For faster service, call TOLL-FREE
1-800-526-5368.

In New Jersey, call collect
201-342-6707.

6-0844

NEOTECTONICS:
An International Journal of Crustal Dynamics
Volume 1, Number 1 March 1986

CONTENTS

Editorial 1

Recurrent Late Quaternary Movement on the Strawberry Normal Fault, Basin and Range–Colorado Plateau Transition Zone, Utah
A. R. Nelson and R. B. VanArsdale 7

Origin of the Yaracuy Basin, Boconó-Morón Fault System, Venezuela
C. Schubert 39

Determination of the Land Uplift from Old Water Marks and Tide Gauge Data at Ratan and Lövgrundet/Björn, Sweden
L. E. Sjöberg 51

Secular Crustal Strain in Eastern Taiwan and Its Neotectonic Implication
H. Sato, M. Kosuga, and H. C. Sheu 61

Possible Differential Uplift of New River Terraces in Southwestern Virginia
H. H. Mills 75

Neotectonic Movements on a Passive Continental Margin: Salvador Region, Brazil
L. Martin, J.-M. Flexor, A. C. S. P. Bittencourt, and J. M. L. Dominguez 87

Information for Contributors 105

Neotectonics: An International Journal of Crustal Dynamics (ISSN: 0884-8157) is published quarterly, one volume per year, by John Wiley & Sons, Inc., 605 Third Avenue, New York, New York 10158.
Copyright © 1986 by John Wiley & Sons, Inc. All rights reserved. Reproduction or translation of any part of this work beyond that permitted by Sections 107 or 108 of the United States Copyright Law without the permission of the copyright owner is unlawful.
Second-class postage pending at New York, New York, and at additional mailing offices.
The code and the copyright notice appearing at the bottom of the first page of an article in this journal indicate the copyright owner's consent that copies of the article may be made for personal or internal use, or for the personal or internal use of specific clients, on the condition that the copier pay for copying beyond that permitted by Sections 107 or 108 of the U.S. Copyright Law. The per-copy fee for each article is $4.00 and is to be paid through the Copyright Clearance Center, Inc., 21 Congress St., Salem, MA 01970.
This consent does not extend to other kinds of copying, such as copying for general distribution, for advertising or promotional purposes, for creating new collective work, or for resale. Such permission requests and other permission inquiries should be addressed to the Publisher, Wiley Journals.
Subscription price: $96.00 per year. Postage and handling outside U.S.A.: $19.00 (surface mail); $63.00 (air mail). Back volumes, microfilm, and microfiche are available for previous years. Request price list from publisher. Allow four weeks to process a change of address.
Claims for undelivered copies will only be accepted after the following issue has been received. Please enclose mailing label or cite your subscriber reference number in order to expedite handling. Missing copies will be supplied when losses have been sustained in transit and where reserve stock will permit.
Postmaster: Send address changes to Neotectonics, Subscription Department, John Wiley & Sons, Inc., 605 Third Avenue, New York, New York 10158.
Advertising: Inquiries concerning advertising should be forwarded to Dora Castiblanco, Advertising Sales, John Wiley & Sons, Periodicals Division, 605 Third Avenue, New York, NY 10158, (212)692-6026.
Manuscripts: should be submitted in triplicate and accompanied by an executed Copyright Transfer Form to the Editorial Office, *Neotectonics*, Margaret A. Winslow, Editor-in-Chief, Dept. of Earth and Planetary Sciences, Science Building, J-106, City College of New York, Convent Avenue at 137th Street, New York, NY 10031.
Information for Contributors appears in the first and last issue of each volume. **All other correspondence** should be addressed to the Journals Department, John Wiley & Sons, Inc. 605 Third Avenue, New York, New York 10158, U.S.A.

Editorial

Neotectonics: Concepts, Definitions, and Significance

Neotectonics is the study of new, living, or recent earth movements. Bloom (1978, p. 22) paraphrased the Soviet and eastern European definition of neotectonics as "the study of earth movements of the Quaternary Period and the later part of the Tertiary Period, including those in progress at the present time."

The term "neotectonics" was originally cited in Mescherikov (1968) as defined by V.A. Obruchev in 1948. Mescherikov used this term to describe the Soviet theory that ancient cratons are subjected to cyclic or episodic uplift and subsidence with amplitudes of 10 to 100 meters, wavelengths of hundreds to thousands of kilometers, and rates of less than one to 10 millimeters per year. Support for this theory comes from precise leveling surveys, which have an accuracy of 10^{-7} or 1 mm in 10 km. However, much, if not all, of the data cited in support of this theory were obtained from areas which are responding to postglacial rebound or subsidence, are located near isostatically adjusting mountain belts, or are in tectonically active regions. Therefore, these long wavelength, slowly moving "undulations" may have other tectonic, eustatic, or isostatic explanations. However, as Bloom (1978) points out, such oscillations should be considered "a factor in geomorphic analysis," as large scale features "might be subtly influenced."

Similar to the terms "tectonics," "orogeny," and "epeirogeny," there are various "working definitions" of neotectonics used by researchers in the field. Wegmann (1955) defined neotectonics as "lebendige Tektonik," which means living tectonics. The present consensus of opinion is as follows: neotectonics means new, living, recent, or active tectonics. It includes Miocene to Recent earth movements, of local to plate scale, especially those associated with regional tectonism. This broad concept encompasses vertical and horizontal motions and their results, tilting, isostatic adjustments, seismotectonics, geodetic measurements and theory, tectonic geomorphology, lithospheric mechanics, Neogene to present-day plate motions, and volcanotectonics.

A neotectonics study needn't focus on seismically active areas. The movements may have initiated and finished within the Neogene, for

Neotectonics: An International Journal of Crustal Dynamics, Vol. 1, 1–5 (1986)
© 1986 John Wiley & Sons, Inc. CCC 0884-8157/86/010001-05$04.00

example. Furthermore, the movements can combine input from postglacial isostatic and eustatic adjustments, vertical movements of large-scale crustal blocks, such as occur in pre-Neogene age mountain ranges, epeirogenic movements, as well as Neogene to Recent plate motions. Therefore, a particular study area can have a complex tectonic history and still be suitably classified as a "neotectonic study" if any of the movements occurred in Neogene to recent times.

Neotectonics assessments are also important in legal definitions. For example, the new international definition of "boundary" in off-shore or in poorly mapped onshore regions speaks of "natural prolongations" or "extensions" of features. When these features are young or active, especially seismically, they are more readily identifiable, and have been used in recent international disputes. In addition, environmental impact statements are required, by federal regulations, before the construction of large buildings, dams, and power plants can begin. Such studies require the identification and assessment of "capable" faults and other structures. These are defined as structural features that have had or could be expected to have seismic activity or movement during the time of human occupation. Other uses of the term "capable" have age limits between 100 and 35,000 years. Such structures may not be "active" according to the usage of tectonicists: presently moving or deforming as a direct result or consequence of plate motions or proximity to a magmatic source. However, even Paleozoic or other faults can have seismic activity associated with them due to isostatic adjustments or because of indirect responses to present-day regional stress fields, basement topography, or past loading history. All such faults are considered legally "capable" if they have any record of earthquake activity or motion during human history.

Other terms necessary to the neotectonics vocabulary are "recent crustal movements" or "recent vertical crustal movements," RVCMs. RVCM was defined by the International Union of Geodesy (part of the International Union of Geodesy and Geophysics, IUGG) as instrumentally determined movements during the present century (Mescherikov, 1968; Boulanger et al., 1975; Pavoni and Green, 1975). RVCMs are documented by precision leveling, seismicity, and by sea level monitors. Such movements are generally restricted to vertical movements with respect to a datum, usually sea level, or tilting determined by leveling lines. However, triangulation networks in Japan, California, and Alaska, for example, can monitor horizontal as well as vertical strains. Another important term used in neotectonic studies was derived from the field of geomorphology: morphostructure, a topographic landform developed as a consequence of neotectonism (Gerasimov, 1946; Gerasimov and Mescherikov, 1968).

EARLY AND MODERN OBSERVATIONS OF NEOTECTONISM

Vertical crustal motions have been observed since remote antiquity and were recorded by Aristotle, Strabo, and Pliny the Elder, among others (Fairbridge, 1981). Repeated floodings of coastal lowlands in actively subsiding areas of the Netherlands, southeastern England, and the Po delta of Italy have been documented since the Middle Ages. Vertical movements of sometimes very great velocity have been documented in the unstable volcanic regions such as near Pozzuoli and the Bay of Naples (Lyell, 1875; and others). Most continuous and well known are the postglacial isostatic uplift regions of the Scandinavian and Canadian shields; less known are the broad belts of slow subsidence which mark the periglacial "marginal bulge" regions in the U. S. Atlantic states and in the southern North Sea and Baltic Sea (Walcott, 1975). Global isostatic adjustments to variations in glacio-eustatic water loading and ice unloading have been calculated by Farrell and Clark (1976). Even on "stable" cratons modest motions are detected, which can be amplified along edges of the "passive" or "trailing-edge" plate margins (Faure, 1972; Sleep and Snell, 1976).

NEOTECTONIC RATES

Geodetically determined rates of vertical uplift are 1 to 10 mm/yr, which are about one order of magnitude lower than horizontal motions associated with actively driving plates (1–10 cm/yr). Typical estimates for epeirogeny or broad crustal warping, on the other hand, are 1 to 10 mm/1000 years. Mescherikov (1968) pointed out that in the shield and platform regions the wavelength of these undulations is of the order of 500–1000 km, with rates averaging less than 1–2 mm/yr, whereas in recent orogenic belts, e.g., Japan, the wavelengths are shorter, 50–250 km, and the rates up to 10 times higher (Hatori et al., 1973).

GLOBAL AND EXTRATERRESTRIAL CONTRIBUTIONS

Explanations of epeirogenic rates include mantle pulses accompanying flow. Based on sea level studies and gravity measurements from satellites, Mörner (1976) has proposed that fluctuations in the earth's core are involved. Hillaire-Marcel and Fairbridge (1978) demonstrate data from Hudson Bay beach-ridge cycles that hint at a celestial component. Believed to contribute to the sometimes trigger-like or rapid mechanisms of RVCMs and neotectonic movements are earth tides set up by celestial mechanics (Fairbridge, 1981). Such celestial cycles cause

gravitational effects due to the orbits of the earth–moon pair and of the major and minor planets. These earth tides are known to correlate to a certain extent with seismic activity, some volcanic behavior, and geyser activity (Fairbridge, 1981).

CONCLUSIONS

Neotectonics groups together the "liveliest" fields of geology and geophysics in that many of the study areas experience active movements, seismic, and/or volcanic activity during the length of the research program, and certainly during human history. Neotectonics, however, includes any vertical or horizontal movements that began or continued during Neogene to recent times, including isostatic adjustments presently occurring in pre-Neogene orogenic belts, coastal warping associated with sea level changes glacio-eustatic effects, uplift and seismicity near magmatic sources, and possible long wavelength epeirogenic movements that appear to affect continental interiors.

As Fairbridge (1978) points out, "neotectonics' intrinsic scientific interest remains, not merely as an aspect of actualism—'the study of the present is the key to the past', but also because it interacts closely with a number of other fields."

This inaugural issue of *Neotectonics* and future already assembled ones present a diverse sampling from this fairly new specialty in the earth sciences and cover a wide range of disciplines and geographic locations. *Neotectonics* plans to present current research, new ideas and methodologies, reviews of study areas and techniques, current theories, and field applications.

I invite your contributions, comments, and editorial assistance. The response so far has been overwhelming.

I look forward to hearing from you,

Margaret Anne Winslow, Editor

References

Bloom A. L. (1978). *Geomorphology, A systematic analysis of late Cenozoic landforms.* New Jersey: Prentice-Hall, 510 pp.

Boulanger, et al. (1975). Summary map of the recent vertical crustal movements for Eastern Europe, in *Problems of Recent Crustal Movements* (Fourth Internat. Symposium, USSR, 1971). Tallinn: Valgus Publ., 31–41.

Fairbridge, R. W. (1978). Neotectonics, in *Encyclopedia of Structural Geology*, Van Nostrand-Reinhold.

Fairbridge, R. W. (1981). The concept of Neotectonics, an introduction. *Zeitschrift furr Geomorphologie, Supplementband* **40**, VII–XII, Dec. 1981.
Farrell, W. E., and Clark, J. (1976). On post-glacial sea level. *Geophys. J., Roy. Astron. Soc.* **46**, 647–667.
Faure, H. (1972). Paléodynamique du craton africain. *Intern. Geol. Congr., 24th.* Montreal, Sect. 3, 44–50.
Hatori, K. et al., (1973). Explanatory text of the Quaternary Tectonic Map of Japan, Tokyo: National Research Center for Disaster Prevention, 167 pp. (Maps separately, 1969).
Hillaire-Marcel, C., and Fairbridge, R. W. (1978). Isostasy and eustasy of Hudson Bay, *Geology* **8**, 117–122.
Lyell, C., (1875). *Principles of Geology*, 12th ed. 2 Vols. London: J. Murray.
Mescherikov, Y. A. (1968). Neotectonics, in R. W. Fairbridge (Ed), *Encyclopedia of Geomorphology*. New York: Reinhold, 768–773.
Mörner, N. A. (1976). Eustasy and geoid changes. *J. Geol.* **84**, 123–151.
Pavoni, N., and Green, R. (Eds.) (1975). *Recent Crustal Movements, Tectonophysics*, **29**, 1–551 (also: reprinted as *Developments in Geotectonics*, No. 9).
Walcott, R. I. (1975). Recent and late Quaternary changes in water level. *EOS (Trans. Am. Geophys. Union)* **56** (2), 62–72.
Wegmann, E. (1955). Lebendige Tektonik, eine Uebersicht. *Geol. Rundschau* **43** (1), 4–34.

Recurrent Late Quaternary Movement on the Strawberry Normal Fault, Basin and Range–Colorado Plateau Transition Zone, Utah

Alan R. Nelson*

D-1632, Seismotectonic Section, Engineering and Research Center, U.S. Bureau of Reclamation, Denver, CO 80225, and Institute of Arctic and Alpine Research, University of Colorado, Boulder, CO 80309

Roy B. VanArsdale

Department of Geology, University of Arkansas, Fayetteville, AR 72701

Strawberry Valley lies 40 km east of the Wasatch fault, within the transition zone between the Basin and Range and Colorado Plateau Provinces in central Utah. Geologic mapping and valley geomorphology suggest that Strawberry Valley is a half-graben bounded on the east by the Strawberry normal fault. Two trenches excavated across a 7-m-high fault scarp in alluvium, subsidiary to the main trace of the Strawberry fault, expose a record of 2 to 3 fault events, each of 1 to 2 m stratigraphic displacement, over the last 15,000 to 30,000 yr, but with smaller net vertical tectonic displacements due to graben formation and backtilting. Age estimates based on soils suggest that the last surface displacement event occurred during the early to mid-Holocene. These displacement and age data suggest that recurrence rates for earthquakes large enough to produce surface ruptures on the Strawberry fault are in the range of 5000 to 15,000 yr. Subsidiary fault slip rates calculated from estimated displacement across the 7-m scarp are 0.04 to 0.17 mm/yr, while minimum longer-term late Quaternary rates on the main fault are 0.03 to 0.06 mm/yr based on ^{14}C and amino acid dating of alluvial plain cores 15 km to the south. These rates suggest a slip rate for the Strawberry fault, at most half, and probably an order of magnitude less than latest Pleistocene and Holocene rates for the Wasatch fault. Recurrence rates and the amount of displacement per event are less than for the Wasatch fault, but are similar to estimates for other faults in the eastern Basin and Range. Recurrent late Pleistocene and Holocene displacement on the Strawberry fault suggests that the late Quaternary extensional stress regime of the Basin and Range extends at least this far east in central Utah.

INTRODUCTION

Paleoseismologic and other geologic studies demonstrate continuing Quaternary faulting in the eastern Basin and Range physiographic province (Anderson, 1979; Swan et al., 1980; Hamblin et al., 1981;

*Present address: U.S. Geological Survey, MS 966, P.O. Box 25046, Denver, CO 80225.

Neotectonics: An International Journal of Crustal Dynamics, Vol. 1, 7-37 (1986)
© 1986 John Wiley & Sons, Inc. CCC 0884-8157/86/010007-31$04.00

Nakata et al., 1982; Crone and Harding, 1984). Recent geophysical data and structural interpretations suggest a transition zone between the Basin and Range and Colorado Plateau Provinces that extends 50 to 100 km east of the Wasatch fault in central Utah (Shuey et al., 1973; Zoback, 1983; Smith and Bruhn, 1984). The easternmost extent of proven late Quaternary surface faulting in the transition zone south of Cache Valley (85 km north of Salt Lake City; see Fig. 1), has been along the Wasatch fault (Schwartz and Coppersmith, 1984), although present-day seismicity appears concentrated in a north–south zone 15 to 30 km east of the Wasatch fault (Arabasz et al., 1980). "Back-valley" basins (so termed by Gilbert, 1928, p. 58), such as Kamas, Heber, Round, and Strawberry Valleys, lie within this area east of the crest of the Wasatch Mountains and south of Cache Valley (Fig. 1). The morphology, distribution, and lithology of Quaternary deposits in the back valleys suggest that the east–west extensional faulting characteristic of the late Tertiary of the region (Gilbert, 1928; Eardley, 1944; Hopkins and Bruhn, 1983) extends into the Quaternary within the eastern Wasatch Mountains (Nelson and Krinsky, 1982; Sullivan and Nelson, 1983). However, back-valley faults are not generally marked by scarps in unconsolidated late Quaternary deposits except along the east side of Strawberry Valley (VanArsdale, 1979a, b; Sullivan and Nelson, 1983).

Here we document late Pleistocene and Holocene movement on the normal fault that forms the eastern margin of the easternmost back valley, Strawberry Valley (Fig. 1). An understanding of present and future crustal responses to tectonic stress in the Great Basin, including its eastern transition zone, requires detailed mapping of Quaternary faults with emphasis on fault recurrence. Although such studies help constrain theoretical work (for example, Zandt and Owens, 1980; Smith and Bruhn, 1984), the number of large reservoirs in the back-valley area, several near population centers, also makes earthquake recurrence studies socially and economically important.

STRUCTURE AND TECTONIC GEOMORPHOLOGY OF STRAWBERRY VALLEY

In the northern part of Strawberry Valley, sedimentary rocks ranging from Pennsylvanian to Tertiary age are exposed (Fig. 1). Geosynclinal rocks were thrust eastward over shelf rocks along the Strawberry Valley thrust fault in latest Cretaceous to Paleocene time (Bissell, 1952, 1959; Astin, 1977). The imbricate thrust slices exposed in the northern part of the valley are believed to project southward under the Tertiary sediments of Strawberry Valley (Astin, 1977; VanArsdale, 1979a).

The Strawberry normal fault bounds the eastern side of Strawberry Valley. The fault forms a single bedrock scarp, 100 to 230 m high, from its southern end, northward to the area of Trout Creek (Fig. 1). Deforma-

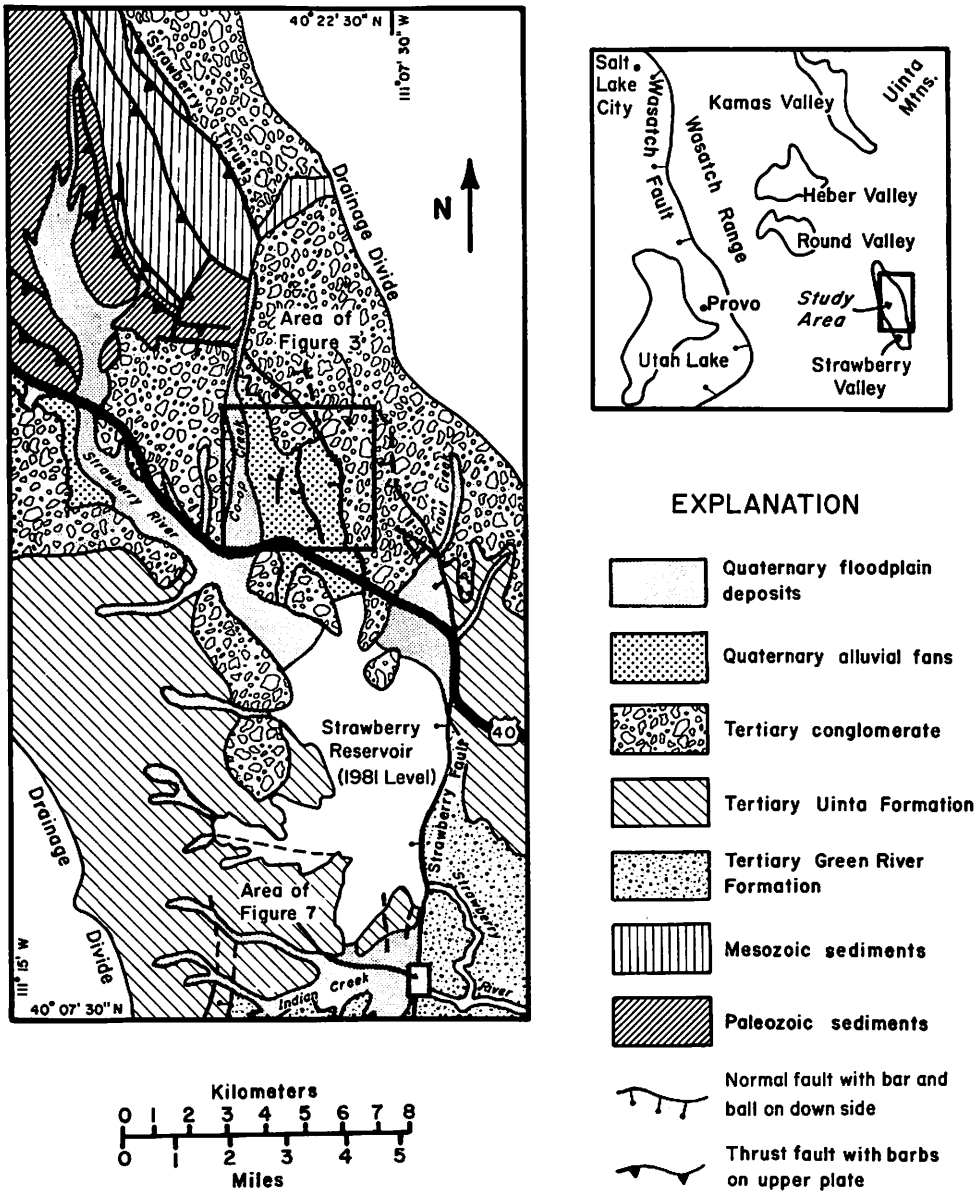

Figure 1. Geologic map of Strawberry Valley, a back valley east of the Wasatch fault, in the transition zone between the Basin and Range and Colorado Plateau Provinces in central Utah. Boxes outline the areas mapped in more detail near trench (Fig. 3) and coring (Fig. 7) sites. The leading edge of the Charleston-Strawberry-Nebo thrust underlies Strawberry Valley, which is bounded on the east by the Strawberry normal fault.

tion along the fault is principally confined to the fault zone and downthrown block, with drag folding particularly evident near Indian Creek in the southern part of Strawberry Valley (Figs. 2 and 7). Near Indian Creek the contact between the Uinta and Green River Formations is downdropped 180 m down-to-the-west. Scarp height decreases

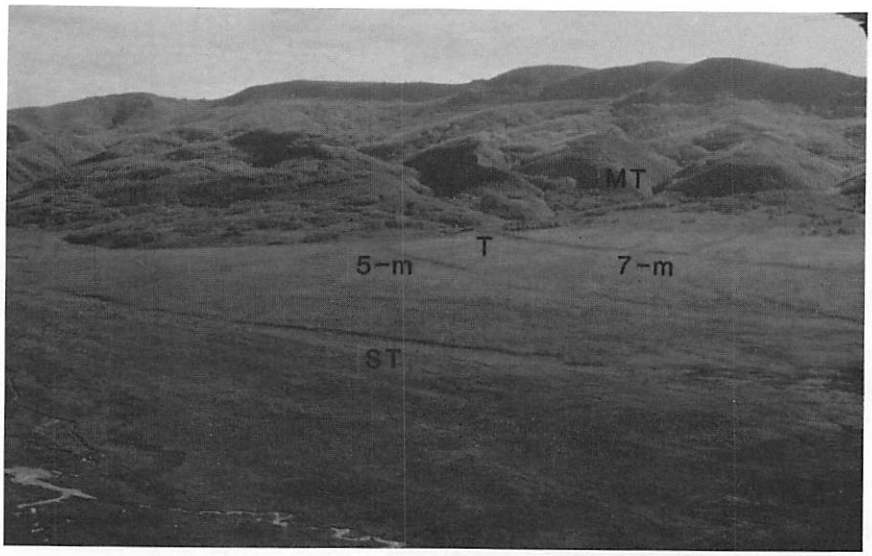

Figure 2. Eastward view of the alluvial fans between the Strawberry fault and Co-op Creek north of Strawberry Reservoir (Figs. 1 and 3) showing the two fault scarps on the fan surface (labeled 5-m and 7-m) and the main trace (MT) of the Strawberry fault (in shadow just above the fans). The terrace scarp along Co-op Creek (ST) is stream cut. Trench 1 (T) was located at the north end of the 7-m scarp.

from 180 m at Indian Creek to zero, 10.5 km south of the reservoir. Near Trout Creek, deformation within the fault zone consists of an asymmetrical graben with sandstone beds within the graben dipping 25° west. Further north, near Co-op Creek, the Strawberry fault forms multiple scarps in alluvial fans and bedrock across a zone 5 km wide (Figs. 1 and 2). Near Co-op Creek the main fault, marked by a 200-m-high escarpment, juxtaposes Quaternary alluvial fan sediments and Tertiary conglomerate. The scarps in the alluvial fans, about 1.3 km west of the main scarp, can be traced for only 3 km and are <7 m high. Near its northern end the fault swings westward through the Tertiary conglomerate, whereupon the scarp becomes difficult to follow.

Absence of a continuous north-trending, down-to-the-east fault on the west side of the valley suggests that Strawberry Valley is a tilted (half-graben) block and that the Strawberry fault is the sole basin-bounding normal fault (Threet, 1959; VanArsdale, 1979a). The fault may be listric and may merge at depth with the southern continuation of the Strawberry thrust fault (VanArsdale, 1979a; Royse, 1983).

The half-graben structural style of Strawberry Valley is reflected in certain of its geomorphic features. Easterly rotation of the Strawberry Valley block resulted in the cutting of narrow canyons on the east (uplifted) side of the valley where Indian Creek and the Strawberry River cross the Strawberry fault (Fig. 1) and in deposition of extensive alluvial fan complexes near Co-op Creek on the downthrown side of the fault. Aggradation of Indian Creek and the Strawberry River on the

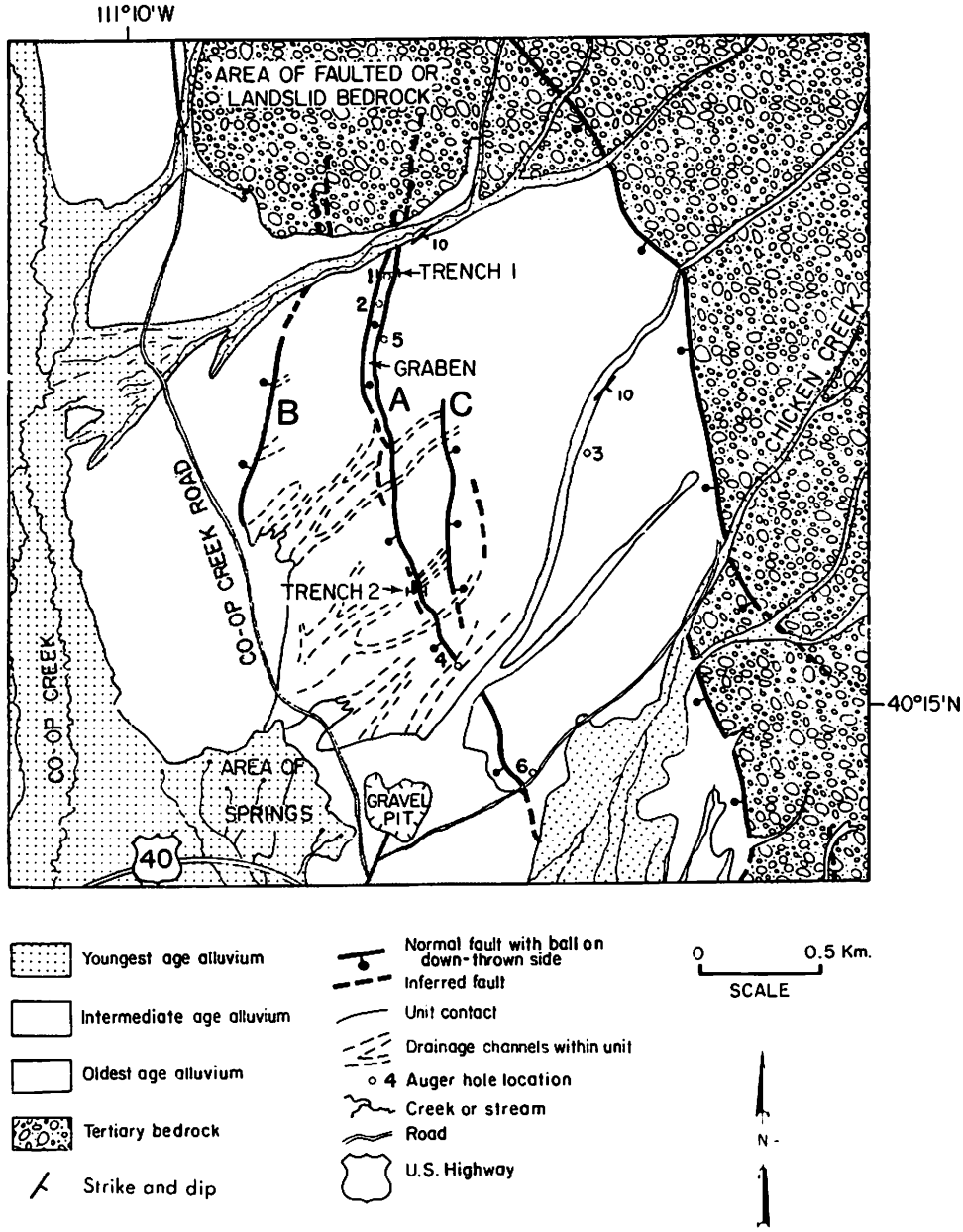

Figure 3. Geologic map of the alluvial fans and fault scarps east of Co-op Creek and north of Strawberry Reservoir (Fig. 1). The 7-m scarp (A) with trenches CC-1 and CC-2 (Figs. 4 and 6), the 5-m scarp (B), the 2-m scarp (C), auger holes, and drainage channels on the fans are shown. The main trace of the Strawberry fault is marked by the en echelon scarps that bound bedrock on the eastern edge of the oldest alluvium. The small drainage channels on the fans are not shown.

rotated block is indicated by the thick alluvial fill west of the fault and alluvial drowning of bedrock inliers in the center of the valley adjacent to Strawberry Reservoir. Fault scarps on the alluvial fans near Co-op Creek reflect primarily down-to-the-west displacement (Figs. 2 and 3).

The only evidence suggestive of separate segments on the Strawberry fault is the en echelon pattern of the main trace of the fault north of Strawberry Reservoir (Fig. 1). The linearity and similar height and steepness of the bedrock escarpment along most of the length of the fault suggest that displacement events of similar size and recurrence have been evenly distributed along the fault during the Quaternary. Thus, the geology or geomorphology of the fault zone cannot be used to subdivide the fault into separate segments with differing fault histories. However, this does not necessarily imply that the entire length of the fault ruptured during each surface faulting event.

Based on their north–south orientation, limited length (Fig. 3), and height relative to the main scarp, the scarps in the alluvial fan sediments near Co-op Creek appear to mark subsidiary faults with much less total displacement than the main fault. Although these scarps may represent most of the displacement within the fault zone during the fault events which produced them, it is more likely that larger displacements occurred on the main fault during these events. Small facets on the scarp or other signs of late Quaternary displacement were not found on the main trace of the fault, but erosion obscures evidence of this type in less than a few thousand years. Topographic profiles down the axis of the alluvial fans show no evidence of warping of the fan surfaces, but small (<3 m) amounts of localized deformation would not be noticeable. For these reasons, we cannot assume that the displacement represented by the scarps was the total displacement in the fault zone during the events which produced the scarps.

Asymmetry in the shape of the drainage channels on the alluvial fans near Co-op Creek (Fig. 3) suggests that the block on which the fans rest may have been tilted to the south during faulting. The largest streams, which begin in the mountains east of the fans, have symmetric cross sections, are deeply incised into the fans, and have smooth profiles where they cross the two prominent fault scarps. Large channels that begin on the fans have asymmetrical cross sections (steep southern banks and gentle northern banks), but also have smooth channel profiles where they cross the scarps. Conversely, small channels which begin on the fans also have asymmetric cross sections, but have knickpoints in their profiles just above each of the two scarps. The greater erosional capacity of the larger streams has apparently removed any knickpoints in their channel profiles at the scarps, whereas the smaller streams have not been able to regrade their profiles. Small alluvial fans have been deposited at the base of scarps where the small fan channels have been vertically displaced. Bedrock exposed in the two large channels has been

tilted 10° to the southeast (Fig. 3) suggesting that the asymmetry of some channels may be the result of greater stream incision against the southern channel banks due to tilting of the fan complex down to the south. Microclimatic control of slope processes is an alternative explanation of channel asymmetry (e.g., Dohrenwend, 1978), but because of the southeastern dip of the bedrock we favor a tectonic interpretation.

Morphometric analysis of profiles across fault scarps on alluvium is a widely used method of estimating the recency of fault movement in the Basin and Range Province (Nash, 1980; Colman and Watson, 1983; Hanks et al., 1984; Mayer, 1984). The sharp crests and steep slopes of the scarps and the small, displaced drainage channels on the alluvial fans (Figs. 2 and 3) suggest that the scarps are probably <100,000 yr old. Topographic profiles across the scarps are smooth, with no apparent facets, suggesting the scarps are not the result of multiple displacement events less than a few thousand years old. Following Wallace (1977) and Bucknam and Anderson (1979), we attempted to use the relation between a fault scarp's height and its maximum scarp–slope angle to estimate the age of the alluvial fan scarps (VanArsdale, 1979a; Nelson and Martin, 1982). However, because (1) there is such large scatter in our data from the alluvial fan scarps (correlation coefficient, r, of 0.60), (2) the scarps are the product of multiple fault events (discussed below), and (3) flows from Co-op Creek were periodically diverted down the graben, eroding portions of the 7-m scarp, our height-maximum-angle data are not suitable for comparisons with other scarp data sets.

SLIP RATES AND RECURRENCE INTERVALS ON THE STRAWBERRY FAULT

The fault scarps crossing the alluvial fan complex near Co-op Creek and the alluvial plain sediments near Indian Creek (Fig. 1) were trenched and cored, respectively, to estimate the age and size of late Quaternary displacement events on the fault (Figs. 5 and 8). Because no scarps in unconsolidated deposits were evident along the main trace of the Strawberry fault, two backhoe trenches were excavated across the subsidiary, 7-m-high, easternmost scarp at the north edge of the Co-op Creek alluvial fans (Fig. 3). Lithology, degree of stratification, degree of soil development, sharpness of stratigraphic unit contacts, the geometry of units, and the relationship of unit contacts to the present ground surface were used to interpret the genesis of units.

Co-op Creek Trench One

Trench one (CC-1) exposed stratified alluvial fan deposits, including braided steam and debris flow deposits, in the upthrown block and along the western third of the trench in the downthrown block (units 1 through

7, Fig. 4). Based on projections of the 3–4° slope of the fan surface, which were measured from topographic profiles extending well above and below the trench site, the net vertical tectonic displacement of unit 7 (methods of Swan et al., 1980) across the graben (stations 32–68, Fig. 4) is only about 1.2 ± 0.2 m, although the scarp is 7 m high. In the main graben, alluvial fan units 1–5 have been dropped below the bottom of the trench and may have been partially eroded by streams flowing through the graben (see discussion below). However, because unit 8 at station 45 extends to the base of our excavation (see note 4, Fig. 4), units 1 and 2 appear to be displaced at least 6 m. In the main graben portion of the trench (between stations 33 and 63, Fig. 4) we interpret moderately sorted, poorly to moderately stratified units (8 and 10) as alluvium. These units were apparently derived from fan alluvium and scarp-derived colluvium that was reworked by intermittent streams flowing from the drainage which presently truncates the graben on the north (Fig. 3) down the axis of the graben.

Age of Faulted Deposits

The degree of soil development is our best evidence with which to assess the age of the alluvial fan surface. The soil developed on unit 7 has an argillic B horizon (unit 7B) of variable thickness, averaging 60 cm thick (profile 1, Table I, Fig. 4). Clay coats the clasts to a greater degree in this horizon than in others, although all coarse units probably contain some infiltrated clay. Above unit 7B are eluvial units (7E, 16) of similar lithology, but with very little clay. Along most of the trench these units are interpreted as alluvial fan deposits with E and BA horizons developed on them from which clay has been eluviated into the Bt, although in some areas they are clearly colluvial. The thickness of these units is quite variable, perhaps due to increased eluviation through coarser zones in unit 7 or to ground disturbance by burrowing or tree-uprooting. Carbonate with stage I morphology (Gile et al., 1966), related to the present soil profile, has accumulated well below the B horizon in unit 5 (Fig. 4). Similar alluvial fan sediments with argillic horizons were encountered in auger holes 3, 4, 5, and 6 elsewhere on the fan surface (Fig. 3) indicating much of the fan surface is about the same age as the area near CC-1.

Assessment of the age of this soil is difficult because of the lack of independently dated soils on similar materials in the region with which to compare it. Comparison of the argillic horizon in this profile with those described from glacial deposits in the Rocky Mountain region (Madole, 1976; Pierce, 1979; Shroba and Birkeland, 1983) suggests a Bull Lake (about 60,000 to 150,000 yr) to older Pinedale (about 30,000 to 70,000 yr) age (nomenclature and ages of Porter et al., 1983). However, the criteria of Shroba (1980, 1982) for soils along the Wasatch Front (45 km to the

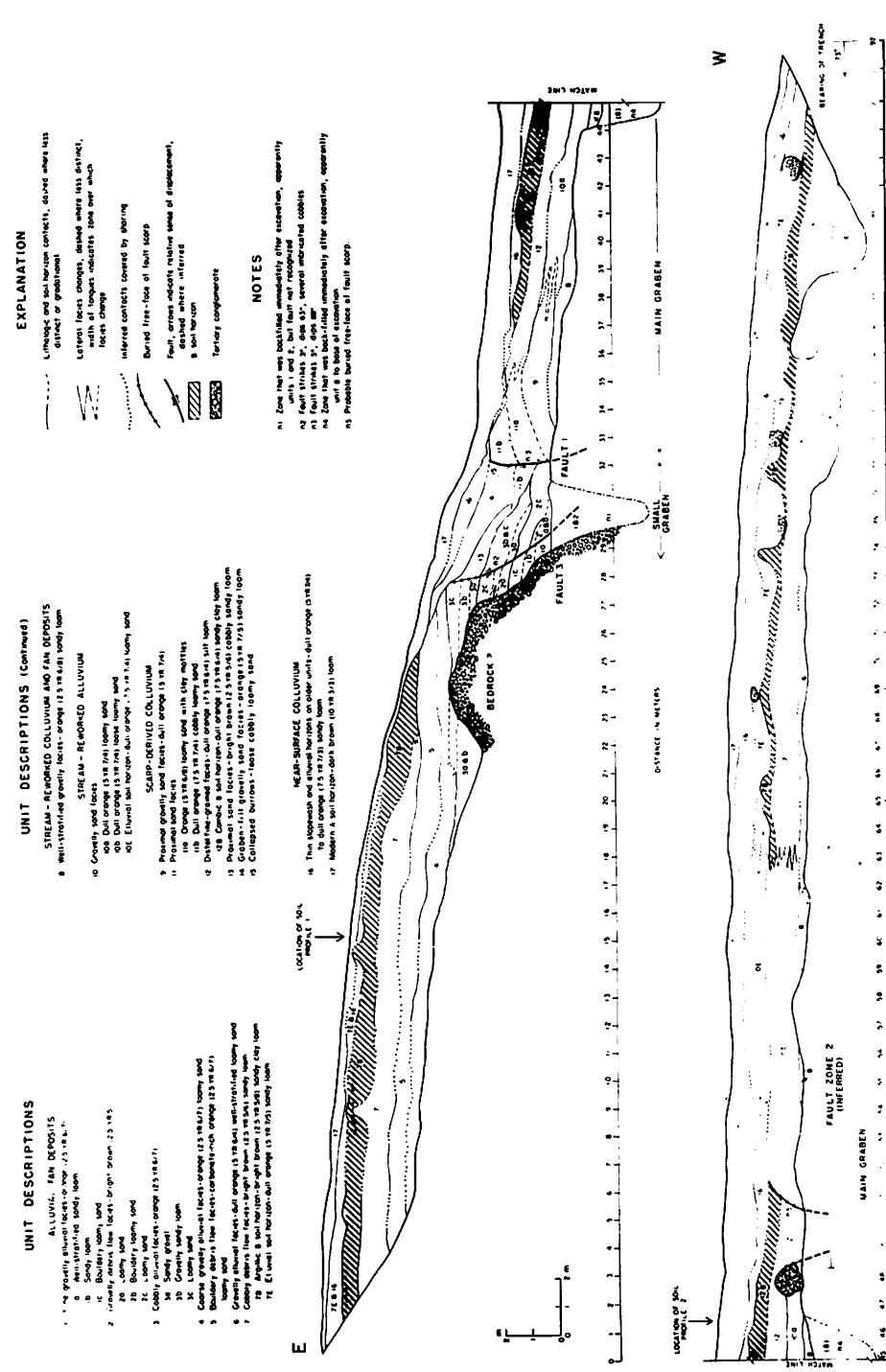

Figure 4. Geologic map of Co-op Creek trench 1 excavated across the 7-m scarp graben (Figs. 1 and 3). Fault 3 was not recognized prior to mapping the trench; it must extend through the excavated but unshored and unmapped lower portion of the trench between stations 29 and 32 (n1).

Table I. Data summary for soil profiles from Co-op Creek trenches. (Leaders (---) indicate no data; tr=trace).

Profile	Horizon[1]	Average depth (cm)	Parent material	Munsell dry color	Estimated percent by volume			Percent by weight[2]			Percent carbonate[3]	Percent organic matter[4]
					Gravel (0.2–8 cm)	Cobbles (8–25 cm)	Boulders (>25 cm)	Sand (2–0.5 mm)	Silt (50–2 μm)	Clay (<2 μm)		
Co-op Creek Trench 1												
1	A1	0- 10	Colluvium	10YR 3/3	10	25	5	45	36	19	0	10.1
	A2	10- 38	--do---------	10YR 3/3	10	25	5	49	33	18	0	3.4
	2E	38- 60	Alluvial fan	5YR 7/5	10	25	5	57	28	15	0	0.3
	2Bt	60-114	--do---------	2.5YR 5/6	10	20	2	52	25	23	0	0.2
	2C	114-149	--do---------	2.5YR 5/6	25	10	0	55	26	19	0	0.3
	2Ckj	149-210	--do---------	2.5YR 5/7	25	10	0	54	28	18	12	0.2
	3Ckj	210-273	--do---------	5YR 6/7	10	5	30	80	14	6	11	0.1
	4Ckj	273-334+	--do---------	5YR 6/7	30	15	0	64	22	14	8	tr
2	A1	0- 26	Colluvium	7.5YR 4/3	5	0	0	--	--	--	--	--
	A2	26- 58	--do---------	7.5YR 4/3	5	0	0	--	--	--	--	--
	A3	58- 80	--do---------	7.5YR 4/3	5	0	0	--	--	--	--	--
	E	80-110	--do---------	7.5YR 5/4	1	0	0	--	--	--	--	--
	2Bw	110-155	--do---------	7.5YR 6/4	1	0	0	--	--	--	--	--
	2C	155-230	--do---------	7.5YR 6/4	1	0	0	--	--	--	--	--
	3C	230-300+	Alluvium	7.5YR 6/4	15	20	5	--	--	--	--	--
Co-op Creek Trench 2												
3	A1	0- 11	Colluvium	7.5YR 5/4	10	0	0	38	40	22	0	7.3
	A2	11- 76	--do---------	7.5YR 5/4	10	0	0	40	38	23	0	2.6
	A3	76-105	--do---------	7.5YR 5/4	10	0	0	40	38	22	0	2.3
	Bw	105-149	--do---------	5YR 6/7	15	5	0	36	42	22	0	0.5
	2CB	149-183	--do---------	5YR 7/3	20	10	0	61	30	9	0	0.2
	2C1	183-204	--do---------	5YR 7/5	20	20	0	64	28	9	0	0.1
	2C2	204-279	--do---------	5YR 7/5	20	20	0	60	28	12	0	0.1
	3C	279-360+	Alluvial fan	2.5YR 5/6	5	10	0	49	29	22	0	0.2

[1]Horizon nomenclature of Guthrie and Witty (1982) and Birkeland (1984).
[2]Particle-size distribution of <2-mm fraction using sieve-pipette methods (for example, Carver, 1971) and Sedigraph for some silt-clay fractions with prior removal of carbonates and organic matter using methods of Jackson (1956).
[3]Percent carbonate by method of Dreimanis (1962).
[4]Percent organic matter by method of Walkley and Black (1934).

west) indicate weak argillic horizons can develop in early Holocene (7000 to 10,000 yr) to late Pleistocene (15,000 to 25,000 yr) deposits.

Strawberry Valley is 1200 m higher than the piedmont along the Wasatch Front, with a 4–5°C MAT (mean annual temperature) (vs. 10°C MAT for the Wasatch Front) and 61 cm MAP (mean annual precipitation) (vs. 43 cm for the Wasatch Front). Higher precipitation in Strawberry Valley should result in more rapid clay translocation, but the dust-influx rate is probably much higher along the Wasatch Front (due to its location on the eastern margin of the Bonneville Basin) than on the Strawberry fans. Considering these factors, we interpret the relatively weak argillic horizon development in profile 1 (considering the amount of clay in the parent material) as indicating that this soil is much younger than Bull Lake deposits elsewhere in the region, but is older than Bonneville-age soils along the Wasatch Front. These age estimates suggest active deposition on the fan surface near the fault scarps probably last took place during pre-Bonneville or Pinedale time (15,000 to 70,000 yr).

More precipitation than is now present may have been required to activate the Strawberry fan surface, which is now inactive (Astin, 1977), although large (>1 m), recurrent displacements on the main trace of the Strawberry fault (for which we have no evidence) (Fig. 3) could have produced the same effect. Temperature estimates for the last glacial period in the region proposed by Pierce (in Porter et al., 1983) suggest higher precipitation rates were not likely until the climatic warming that led to Pinedale deglaciation (about 15,000 to 30,000 yr). Pierce and Scott (1984) inferred that a major episode of gravel deposition took place on alluvial fans in Idaho during Pinedale deglaciation. If we make the same assumption for the Strawberry fans, a best estimate for the age of the sediment on most of the fan surface is roughly 15,000 to 30,000 yr.

The lack of well-developed soil profiles on any of the buried colluvial units exposed in CC-1 suggests that there have been no long periods of scarp stability since they were deposited and thus, that all colluvial sediments are relatively young. The soil on the fine-grained colluvium in the middle of the trench is weakly developed (profile 2, Table I). We interpret the slightly higher clay content of unit 12B relative to unit 12 in this soil to the gradual fining upward of the parent material in this unit rather than to argillic horizon development; if this interpretation is correct, unit 12B is a cambic B horizon.

Age assessment of the colluvial units is also difficult because there are no numerically-dated soils from a similar setting with which to compare them. However, the lack of an argillic horizon in the fine textured colluvium of unit 12 and comparisons with Bonneville-age soils described from fine-grained lake sediments (Shroba, 1980) suggests that profile 2 on the younger colluvium is not significantly older than mid-Holocene.

Sequence of Faulting and Deposition

Based on the lithologies, stratigraphic relationships, and estimated ages of units in CC-1, the following sequence of events is inferred (Figs. 4 and 5):

(1) Units 1 through 6 were deposited successively on the alluvial fan by small braided streams and debris flows prior to 15,000–30,000 yr; there may be unrecognized unconformities between some of the units.

(2) Unit 7 was deposited about 30,000–15,000 years ago, as a debris flow over the entire area. A thin mantle of colluvium was deposited by slopewash processes as soil development on unit 7 began.

(3) One or more faulting events (faulting event a , Fig. 5) offset units 1 through 7 down to the west near station 32 (fault 1). The amount of displacement during this event(s) is unknown because later fluvial erosion in the main graben may have removed some of the upper portion of the down-dropped alluvial fan units and the base of the graben was not exposed. Down-to-the-east antithetic faulting somewhere between stations 48 and 63 (fault zone 2) probably occurred simultaneously, thus forming a graben parallel with the present main scarp.

(4) Intermittent diversion of part of the stream flow in the tributary to Co-op Creek just north of the trench (Fig. 3) took place through the graben, reworking both colluvium in the graben and alluvial fan sediments and depositing them locally as unit 8. During the same period a proximal colluvial wedge (unit 9) was deposited on unit 8 adjacent to the eroded scarp (unit 8 may consist mostly of scarp-derived colluvium east of station 39). This wedge could be a depositional response to renewed displacement on fault 1, but the parallel dip of the indistinct upper and lower contacts of unit 9 suggest it was more likely due to continued erosion of the scarp produced just prior to the deposition of unit 8 (see below). During or following the deposition of unit 9, the tributary of Co-op Creek was diverted intermittently along the graben, reworking the distal part of the wedge to form unit 10a. The genesis of units in the western part of the graben is far from clear, but the gradational facies changes between unit 10b (a graben-filling fluvial deposit) and unit 7, and between units 8 and 6, suggest lateral westward stream erosion of units 6 and 7. We hypothesize that an antithetic fault scarp forming the western edge of the graben (fault zone 2) diverted the stream against the free face of the scarp, obliterating any evidence of a fault. Unit 10E is interpreted as an eluvial horizon developed on unit 10—the equivalent of unit 7E, but both vertical and lateral contacts are very gradational.

(5) Renewed down-to-the-west faulting at station 32 (fault 1; event b, Fig. 5) resulted in a thick colluvial wedge (unit 11). The higher percentage of cobbles in unit 11b than in unit 11a, and blebs of clay which may be fragments from an argillic horizon, suggest that this wedge may

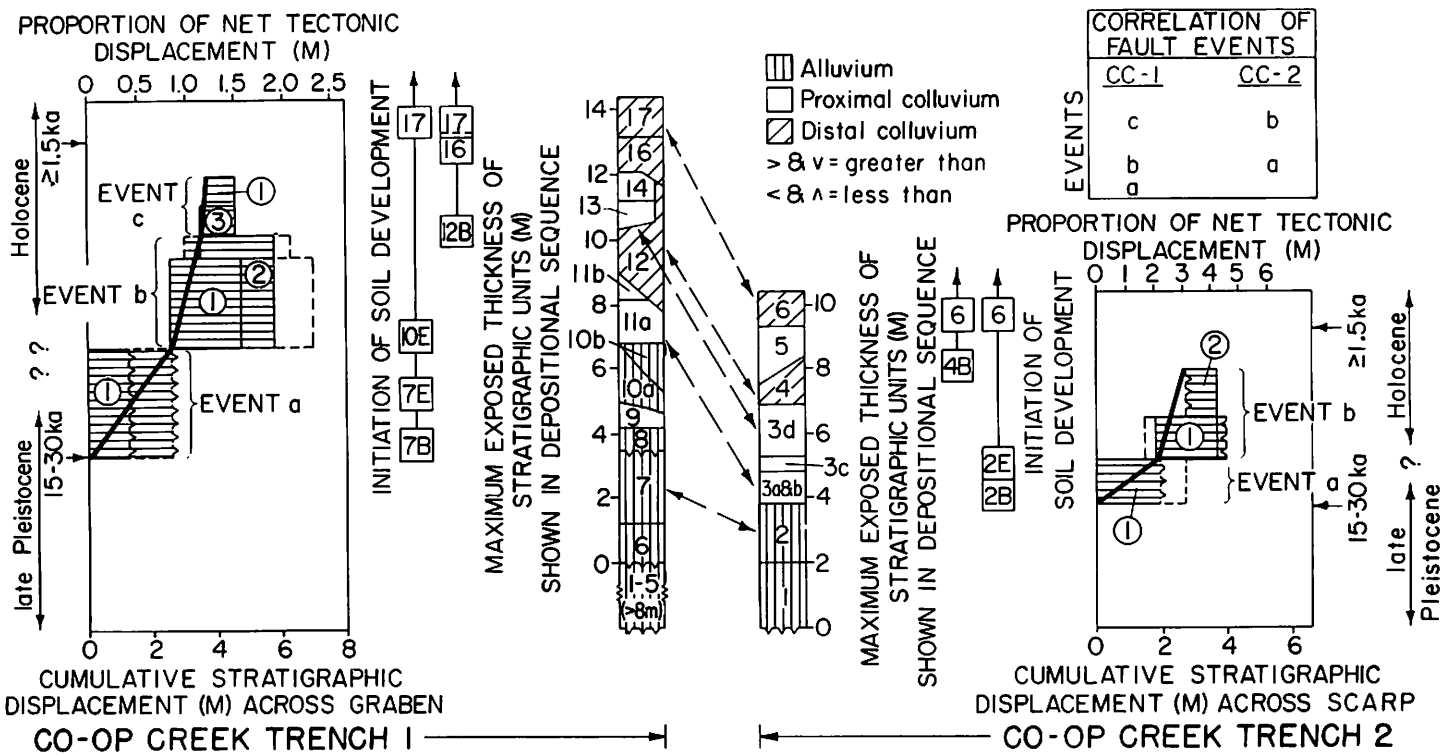

Figure 5. Displacement–time diagrams for Co-op Creek trenches 1 and 2 showing maximum exposed stratigraphic unit thickness (on scaled edge of columns) (ruled pattern indicates genesis), cumulative displacement [both stratigraphic and net vertical tectonic (Swan et al., 1980)], periods during which soil horizons formed (small squares indicate approximate time of initiation of development of soil horizon), and limited time-control points. The height of rectangles in the displacement-time portion of the diagram corresponds with the thickness of units produced as a response to that displacement event. Solid horizontal lines indicate measured stratigraphic displacement (often minimum or maximum values), dashed lines are estimates of displacement for some events based on double the maximum thickness of colluvial wedges, and ruled areas indicate our best displacement estimates considering the geometry of stratigraphic units (these are the values used for cumulative displacement). Circled numbers in displacement rectangles show the fault (zone) (Figs. 4 and 6) where the displacement event occurred. The correlation of stratigraphic units between trenches indicated by the heavy dashed arrows also applies to fault events (lower case letters on diagrams; also see table in upper right corner of Fig.).

reflect the inverted stratigraphy of units exposed in a former free face of units 1–7 at this location. Colluvial units 9 and 11 (and possibly the eastern 6 m of unit 8) were faulted and backtilted on fault 1 during this event, as shown by the eastward dip on the faint unit 9 contacts at station 33. Unit 10 is apparently displaced down to the east about 0.8 to 1.8 m at station 50, with a smaller antithetic displacement at station 49. The sharp contacts between units 10 and 12 at stations 48 and 51 were interpreted as fault-scarp or possibly erosional-scarp free faces which were buried by unit 12 with no subsequent displacement. The interfingering facies relationships of unit 12 (fine, distal colluvium) with unit 11 (proximal scarp-derived colluvium) near station 35 suggest that this second inferred displacement in fault zone 2 was contemporaneous with event b on fault 1. Apparently, the tributary to Co-op Creek cut to below the level of the north end of the graben during this period and no longer flowed parallel to the scarp (Fig. 3).

(6) During the early to mid-Holocene, additional fine colluvium was deposited (with an increasingly finer eolian component in the upper part of unit 12), which filled the small graben at station 49. Soil development continued on units 7 and 10 with the thickening of units 7B, 7E, 10E, and 16 (particularly in areas of gentler slope).

(7) The final surface displacement event was expressed as a down-to-the-west fault of about 1 m displacement at station 29 (event c, fault 3), 3 m east of fault 1. The shear zone is thin (1 to 5 cm wide) and difficult to discern in places because of the lithologic similarity of the alluvial fan units. The down-to-the-east displacement of what we interpret to be the upper part of colluvial wedge 11b shows that a down-to-the-east fault (almost vertical) of about 0.9-m displacement at station 32 (event c; fault 1) formed at about the same position as the previous fault at station 32, but with the opposite sense of displacement. This produced a graben block between 28 and 32 which was tilted westward, apparently with some drag or slumping (10 to 20 cm) of units 11 and 9. Thus, total displacement across the scarp during this event appears to be very small (about 20 cm, Fig. 5). Two units of proximal scarp-derived colluvium were deposited into the graben between faults 1 and 3 immediately after faulting. Unit 13 was derived from the units 3–4 scarp and was then covered by more gradual deposition of material (unit 14) derived from both of the scarps of the small graben and surface colluvium (unit 16) from the E horizon of soils above the main scarp (fault 3). Relationships are obscured at station 32 where loose, brown colluvial material (unit 15) is highly burrowed. While rapid eluviation took place in the sandy colluvium of unit 14, soil development on units 7, 10, and 12 (12B) continued with the thickening of units 7E, 10E, and 16. Soil development continued in the late Holocene with deposition of material making up the present A horizon (unit 17) over the whole trench by slopewash and eolian deposition with a higher deposition rate in the main graben.

Co-op Creek Trench Two

A second trench (CC-2), excavated across the 7-m fault scarp 1.6 km south of CC-1 (Fig. 3), exposed alluvial mud and debris flow sediments (Fig. 6) similar to those in CC-1, except that the sediments were finer grained and the lower half of the upthrown block consisted of clayey silt with very few clasts (unit 1). Auger hole 4 (Fig. 3) shows that sediment similar to unit 1a extends to a depth of 7 m on the downthrown side of the scarp just south of CC-2. CC-2 contains colluvial units very similar to those in CC-1, but unit contacts in the older colluviums are even more gradational and difficult to trace. Subtle lithologic changes within unit 3 suggest it was produced by several colluvial events. Projection of the fan surface across the scarp suggests about 2.6 ± 0.2 m of net vertical tectonic displacement at CC-2.

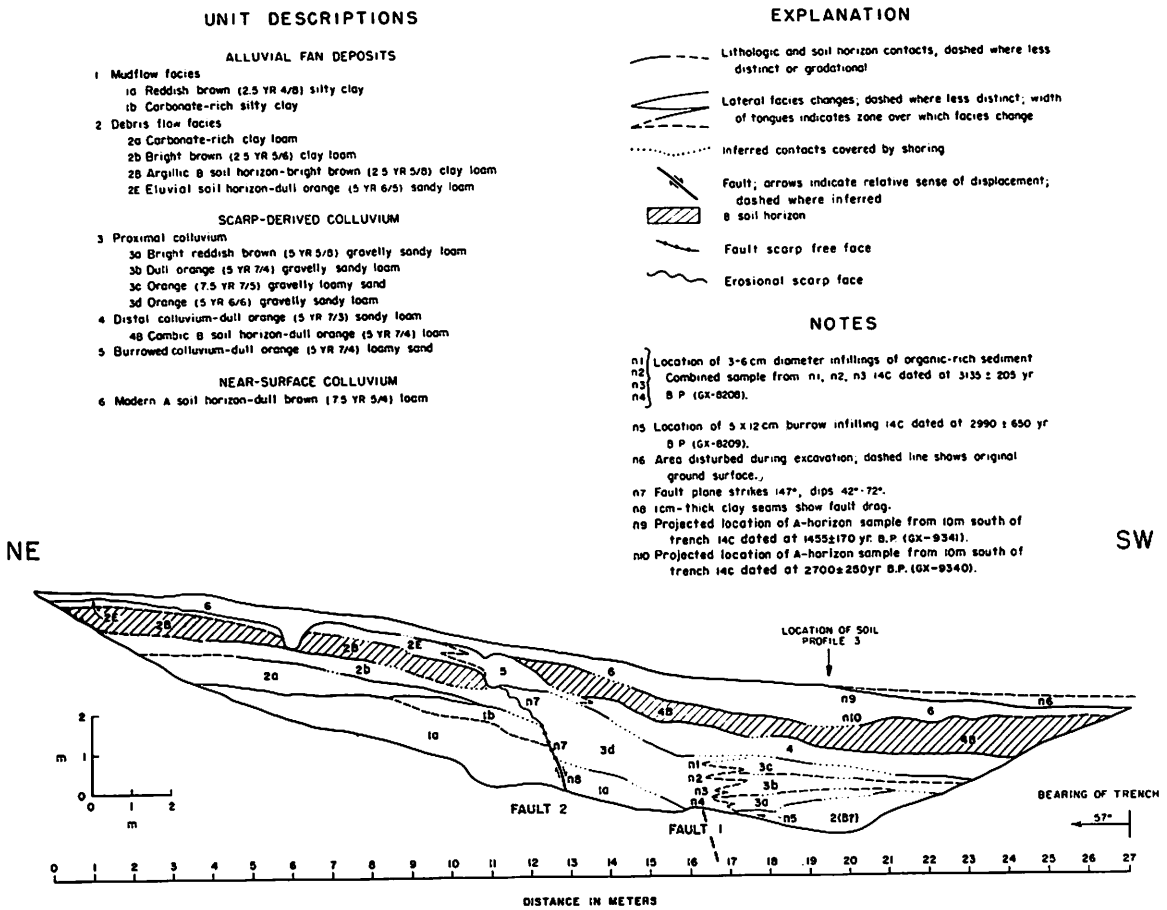

Figure 6. Geologic map of Co-op Creek trench 2 across the 7-m scarp about 1.6 km south of Co-op Creek trench 1 (Figs. 1 and 3). The location of ^{14}C-dated samples (Table II) is also shown. A unit in this trench similar to unit 16 in CC-1 was too thin and discontinuous to map and was therefore included with units 2E, 4B, and 5.

Age of Faulted Deposits

The soil on unit 2 is almost identical to that on unit 7 in CC-1; unit 2B in CC-2 is the time equivalent of unit 7B in CC-1, and unit 2E (with part of unit 5) in CC-2 is the genetic equivalent of units 7E and 16 in CC-1 (Fig. 5). Units 2a and 1b form a carbonate-rich horizon (stage I morphology) which truncates the bedding in the alluvial fan sediments, demonstrating its relationship to the present topography. Unit 4B in soil profile 3 has thin argillans coating clasts and lining pores (Fig. 6), a higher chroma than underlying horizons, but no more clay than overlying horizons (Table 1). This B horizon is lighter with less clay toward fault 2 where the unit 4 colluvium thickens (station 16 and 13) and becomes coarser, but otherwise it is very similar to unit 12B in CC-1. These features indicate unit 4B is a cambic B horizon which developed on distal colluvium as it accumulated. Based on our earlier comparisons, the degree of soil development in unit 4 suggests an early to mid-Holocene age for the colluvium.

Five small areas of organic-rich sediment in CC-2 between stations 16 and 18 (n1 through n4 on Fig. 6) were analyzed for ^{14}C in an attempt to date unit 3. Originally, these organic-rich zones were interpreted as A horizon material incorporated into ground cracks during fault displacement of the colluvium at station 16 (Nelson and Martin, 1982, p. 66). However, soil mean residence ages (Matthews, 1980) of two additional samples from unit 6 (n9 and n10 on Fig. 6) and our previous estimates of the age of colluvial units suggest that all these organic-rich zones are infilled small mammal burrows which have collapsed. Therefore, the burrow infillings, which may be as young as 1500 yr (Table II), are unrelated to faulting and these ages provide only a very minimum age for the most recent fault displacement and resulting colluvial deposition.

Sequence of Faulting and Deposition

The following history is inferred for CC-2 (Figs. 5 and 6):

(1) Units 1 and 2 were deposited as mud and debris flows prior to 15,000–30,000 yr and soil development on unit 2 began.

(2) Movement (event a, Fig. 5) on an inferred fault that was not exposed in CC-2 dropped units 1 and 2 down to the west about 2 m. Unit 2, which overlies unit 1 on the upthrown block, is missing on the upthrown side of inferred fault 1 between stations 13 and 16. Unit 2(B?) in the downthrown block has a clayey matrix like unit 1, but is also cobbly like unit 2; it is most likely the downthrown equivalent of the upper part of unit 2 (either a lateral facies change or 2B, the argillic horizon). Following faulting, colluvium (unit 3a) eroded from unit 2 on the upthrown block was deposited off of a scarp at station 16 which no longer exists.

Table II. Radiocarbon dates for samples from Strawberry Valley.

Depth (m)	^{14}C Laboratory number	Texture of sample material	Sample weight (g)		Estimated carbon (g)[2]	^{14}C date (yr B.P.)	$\delta\ ^{13}C$ (‰)
			Untreated	Clay-silt/ humus concentrate[1]			
Co-op Creek Trench 2							
0.1	GX-9341[3]	Silty sand	3146	280	>1.0	1,455 ± 170	−25.9
1.0	GX-9340	Silty sand	3278	597	>1.0	2,700 ± 250	−25.8
2.5	GX-8208	Silty sand	1500	272	0.065	3,135 ± 205	−29.6
3.5	GX-8209	Sandy silt	2950	591	0.030	2,990 ± 650	−29.0
Indian Creek Core 1							
1.7−2.2	GX-8211	Clayey silt	343	267	>1.0	8,230 ± 190	−27.0
6.6−6.9	GX-8213	Sandy clay	506	199	>1.0	>37,000	−26.7
8.9−9.2	GX-8214	Silty clay	255	167	>1.0	25,840 ± 1,300	−28.6
10.6−10.7	GX-8210	Silt and peat	345	---	>1.0	>37,000	−27.8
Indian Creek Core 2							
1.3−1.7	GX-8212	Silty sand	461	134	>1.0	2,955 ± 145	−26.7
Indian Creek Auger Hole 3							
7.3	Beta-2520	Clayey silt	767	183	0.9	11,290 ± 220	---

[1]Preparation methods of Kihl (1975). Dash indicates preparation not done.
[2]Amount of dated carbon in concentrate estimated by dating laboratory.
[3]This surface horizon sample has an apparent mean residence age (Matthews, 1980) of about 1500 yr. Because the two lower dated samples in trench 2 are burrow infillings derived from similar surface horizons, they may be as young as 1500 yr (3000−1500= 1500 yr).

Apparently, all of unit 2 near the edge of the original scarp was eroded from above unit 1a between stations 13 and 16 before displacement occurred on fault 2. Randomly-oriented fragments of argillic horizon peds in unit 3a show that this unit was partially derived from a unit like unit 2B, while the carbonate coating clasts in unit 3b may reflect erosion of carbonate-rich sediment from unit 1b. Thus, the stratigraphy of the colluvial wedge suggests an inversion of the stratigraphy probably exposed in a scarp free face just east of station 18. Less clay and brighter, more iron-oxidized colors in unit 3c indicate slight reworking of the upper part of the wedge sediments by intermittent flows off the scarp or from one of the small drainages adjacent to the site. Continued soil development on unit 2 thickened units 2E and 2B and carbonate (stage I) continued to accumulate in units 1 and 2.

(3) During the early to mid-Holocene, faulting at station 12 (event b, Fig. 5) displaced unit 1 about 1 m down to the west. The eastward dip of the faint contacts between units 2, 3a, and 3b and the change in slope of the unit 3–unit 4 contact at station 16 suggest slight backtilting of units 3a–3c following deposition. On this basis, we infer roughly 50–80 cm of down-to-the-west concurrent faulting on fault 1. However, prior to this event the upper contact of unit 1a at station 16 must have been at least as high as the contact between units 3b and 3c. Thus, unit 1a was dropped $>$ 80 cm down-to-the-east relative to units 3a–3c during this same event to form a graben. As seems to be the case in CC-1, a new fault forming east of the original fault caused renewed antithetic movement on or near fault 1, deforming the colluvial wedge produced by the first event and probably displacing the upper half of the wedge down-to-the east relative to the lower half. Unit 3d, which rapidly infilled the narrow graben between stations 12 and 17, was derived from material eroded from the main scarp on fault 2 and the antithetic scarp on fault 1 formed in units 3b and 3c, and possibly 3a. It should be emphasized that no discrete shear plane was recognized at the location of fault 1; we infer two displacement events on a fault here entirely from the colluvial stratigraphy and the analogous stratigraphy in CC-1. If our interpretation is correct, about 1.3–2.0 m of down-to-the-west displacement occurred across the 7-m scarp during event b (Fig. 5). Following the deposition of the proximal wedge (unit 3d), units 4 and 5 began accumulating by slopewash and eolian processes. Rodent burrowing is probably the explanation for the step in the base of unit 5 at station 11.

(4) Soil development continued on units 2 and 4, gradually forming a cambic B horizon on unit 4 (4B). Slight scouring by drainage along the scarp may have produced the depression in the unit 4–unit 6 contact at stations 19–20. In the late Holocene, unit 6 was deposited by slopewash and eolian processes. The burrows in units 3d and 2(B?) were dug and infilled during this period, prior to 1500 yr (Table II).

Correlation of Faulting Events and Estimated Recurrence

Correlation of stratigraphic units and faulting events between the two trenches indicates that each site has had a similar history of fault displacement (Fig. 5), but more events are represented in CC-1. Units in CC-1 represent two or, more likely, three fault events, but there is evidence for only two events in CC-2. Because alluvial and colluvial units in both trenches were derived from the faulted alluvial fan sediments and transported short distances, many units of different genesis look similar. Proximal fault-scarp-derived colluvium is particularly difficult to distinguish from the stream-reworked colluvium and alluvial fan sediment into which it grades laterally. Intense rainfall on the alluvial fan may also have resulted in the deposition of units off the fault scarps, which we have interpreted as fault-related colluviums. However, small (< 0.5 m) surface displacement events are difficult to recognize because so little evidence of them is usually preserved (Schwartz and Coppersmith, 1984). Units in the downthrown block correlative with upthrown units were not reached in CC-1, and thus, one or two early fault events may also be unrecognized. For these reasons, our estimate of two to three surface faulting events on the 7-m scarp is probably a minimum value.

Stratigraphic relationships in both trenches suggest stratigraphic displacements of 1 to 2 m for each fault event. Stratigraphic displacements were estimated by measuring the contacts of faulted units, by dividing total displacement by the number of events suggested by colluvial units (e.g., Swan et al., 1980), and by doubling the maximum colluvial wedge thickness (Fig. 5). Models of scarp erosion (e.g., Nash, 1981) show that given sufficient time between fault events for scarps to erode to angles well below the angle of repose, double the wedge thickness is a maximum estimate of stratigraphic displacement. For graben-filling events b and c (Fig. 5) the wedge thickness approaches the scarp height. The displacement rectangles on Figure 5 are arranged to show that the antithetic faulting, which occurred during events b and c, reduced the net displacement for those events. Thus, the diagram shows the cumulative displacement across the area exposed by each trench, and the heavy line running through the rectangles indicates the average slip rate (time scale is non-arithmetic).

Our age estimates, based on soil development and regional correlations of Quaternary deposits, suggest these two to three surface displacement events occurred during the last 15,000 to 30,000 yr, yielding a maximum recurrence interval of 15,000 yr and a minimum recurrence of 5000 yr. These are average values only; all events could be clustered closely in time with the limitation that the last event occurred during the early to mid-Holocene.

Slip Rate Estimates

Our estimates of net vertical tectonic displacement across the 7-m fan scarp, measured from scarp topographic profiles, are much less than the stratigraphic displacements (Fig. 5) because of graben formation and backtilting. These estimates yield average slip rates of 0.04 to 0.17 mm/yr for the 7-m scarp, but it is subsidiary to the main trace of the Strawberry fault. Fault slip almost certainly took place on the 5-m-high scarp west of the trenched scarp, the 2-m-high east-facing scarp east of the trenched scarp, and/or along the main trace of the fault at the fan–bedrock contact during at least some of the events recorded in the trenches (Fig. 3). Deformation which was not expressed as surface rupture may also have occurred across the entire Strawberry fault zone. For these reasons, net vertical tectonic displacement per event and long-term slip rates across the entire fault zone cannot be accurately estimated.

Coring Near Indian Creek

South of the trench sites, Indian Creek flows from the west across a 9-km^2 alluvial plain on the downthrown side of the Strawberry fault into a 175-m-deep stream-cut valley on the upthrown block (Figs. 1 and 7). Detailed mapping of the Tertiary beds near the site and shallow seismic refraction profiling show that the main trace of the fault runs along the west edge of the bedrock spur 120 m west of the main scarp marked by the colluvium–bedrock contact (Fig. 7). The refraction profiling suggests that the fault dips westward about 58° at depth, a dip similar to that measured by Thompson (1971) on the fault in a tunnel north of Strawberry Reservoir. Refraction data also suggest that bedrock is within 4 m of the surface in the stream valley east of the bedrock scarp and greater than 60 m deep, 80 m west of the scarp (Fig. 7). These relationships suggest movement on the Strawberry fault displaced late Quaternary alluvium below the bedrock lip in the stream valley.

Eight-cm diameter push-tube samples of fine grained alluvial sediments were taken inside a hollow-stem auger west of the scarp (core 1) and east of the trace of the scarp (core 2) at the edge of the stream valley to determine the age of the alluvial fill on the alluvial plain and in the stream valley (Figs. 7 and 8). Both cores contain brown to gray-green silty clays to silty sands typical of alluvial plain sediments deposited by a meandering stream, as well as coarse sandy gravels (not sampled) deposited during periods of higher discharge. Thick beds of organic-rich clay in core 1 suggest periods of ponding, but these could be the result of the filling of oxbow lakes as well as more extensive ponding due to damming of the creek by scarps produced during discrete fault events.

During initial investigation of the Indian Creek site, an auger hole (borehole 3, Fig. 7) was drilled about 700 m north of the site of core 1.

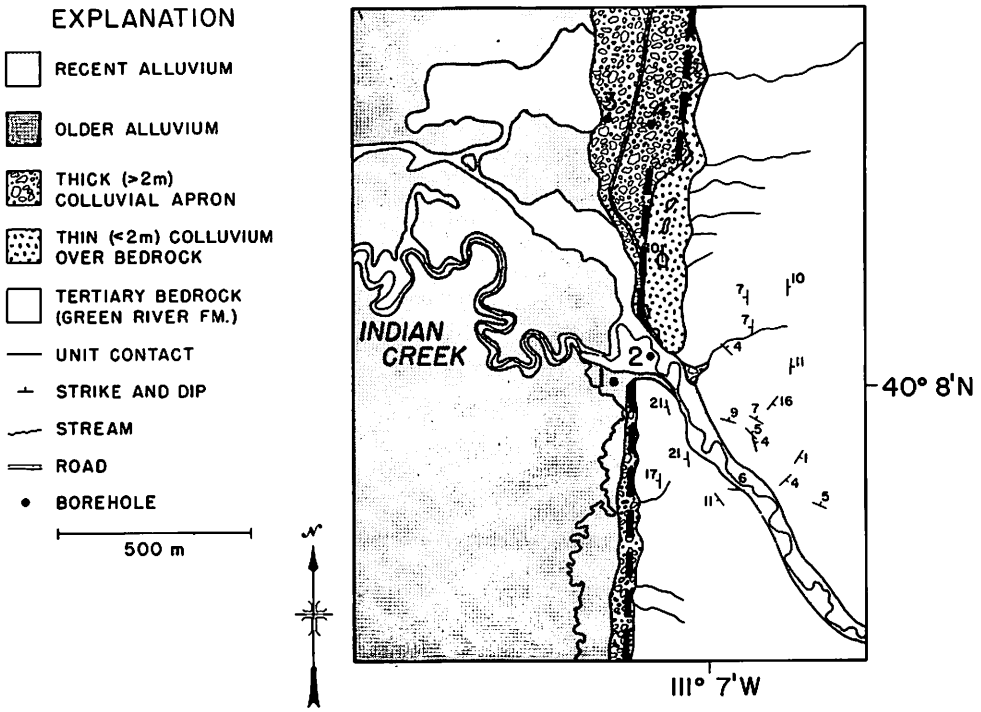

Figure 7. Geologic map of the area where Indian Creek flows across the Strawberry fault scarp (Fig. 1), showing the location of push-tube cores 1 and 2 (Fig. 8) and boreholes 3 and 4. The trace of the fault near the surface (inferred trace shown by heavy dashed line) must be near the east edge of the thick colluvial apron, but the colluvium does not appear to have been faulted. South of borehole 4 the fault may bend or make an en echelon jump about 100 m to the west. Drag occurs within 400 m of the fault, as shown by moderate west dips in the Tertiary bedrock (regional dips are about 10° E-NE). Northeast to northwest-oriented strikes measured along the canyon cut by Indian Creek may be due to the adjustments of large slump blocks.

Similar alluvial plain stream and lake sediments were encountered between 4 and 8 m depth below the distal edge of the fine grained colluvial apron extending out from the main fault scarp. Borehole 4 (Fig. 7) showed > 9 m of fine grained colluvium higher up on the apron.

Radiocarbon Dating of Core Sediments

One sample from core 2 and four from core 1 were analyzed for ^{14}C activity to determine the age of the sediment in each core (Fig. 8). A bulk sediment sample with a 2-cm peat bed was analyzed from near the base of core 1 (10.5 m), but the other samples required concentration of organics in the silt–clay fraction to obtain enough carbon for dating (Table II). Consideration of (1) the hard water effect on the carbon isotopes incorporated in the aquatic organic material, (2) the 11,300 yr radiocarbon age from the base of borehole 3 (700 m to the north), (3) the probable effects of older reworked alluvial organic material and contamination by younger

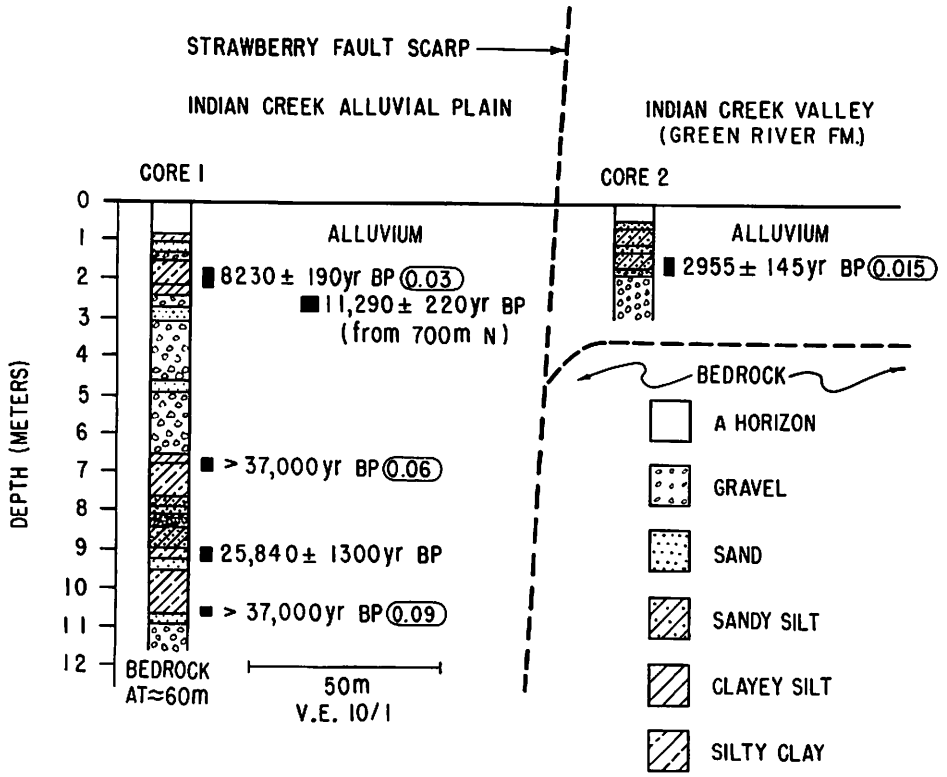

Figure 8. Schematic cross section (vertical exaggeration × 10) showing the relationship of push-tube cores 1 and 2 to the alluvial units adjacent to the scarp in bedrock of the Strawberry fault (Fig. 7). Refraction profiling was used to estimate depth to bedrock and the angle on the fault scarp below the surface of the alluvial plain. The lithology of the cores, radiocarbon dates on organic-rich sediments (including a date from the base of borehole 3 located 700 m north of this cross section), and average aIle/Ile amino acid ratios on gastropods (ovals) are also shown. Samples were not recovered from the thick gravel sections of core 1.

carbon in the dated samples, and (4) the amino acid ratios discussed below, suggests that the 3000 yr age from core 2 is a maximum, but that the 8200 yr age for core 1 is accurate. The three lower ^{14}C dates from core 1 are interpreted as minimum ages. The middle sample (Table II; Fig. 8) was almost certainly contaminated by a small amount (< 3%; Olsson, 1968) of modern carbon giving an apparent finite age to a sample, which based on the ages at 7 m and 10.5 m, is > 37,000 yr. Age and depth data from core 2 and the upper part of core 1 cannot be used to calculate fault displacement rates because about 8000 yr-old sediments on the downthrown side of the fault occur at about the same level as < 3000 yr-old sediments on the upthrown side. In addition, the rate of downcutting of Indian Creek east of the fault, although probably rapid (e.g., Hamblin et al., 1981), is not known. Thus, the minimum ages from the base of core 1 cannot be used to calculate maximum displacement rates.

Amino Acid Age Estimates From Snails in the Cores

In an attempt to obtain finite age estimates from the cores, both terrestrial and freshwater gastropods, suitable for amino acid analysis, were separated from three of the four carbon-14-dated samples from core 1 and from an additional sample from the base of the core (Table III). Only recently have amino acid ratios measured on terrestrial and freshwater gastropods been used in relative dating of Quaternary deposits (Miller et al., 1979, 1982; Rutter et al. 1980; McCoy, 1981; Harmon et al., 1983). Numerical-age estimates are more difficult to obtain because of the large uncertainties in amino acid racemization kinetics and the difficulty in estimating the effective diagenetic temperature history (EDT) of fossils (Miller and Hare, 1980; Wehmiller, 1982). However, if independently dated calibration samples are available from the same region as the samples to be dated, the approximate ages of the undated samples can be estimated.

At Indian Creek, the D-alloisoleucine/L-isoleucine ratio (aIle/Ile) in the total acid hydrolyzate (the primary ratio used in dating) of the gastropod shells (Table III) was used to evaluate the reliability of the radiocarbon dates from core 2 and to calibrate the rate of isoleucine epimerization (racemization) using the gastropod samples from the 8200 yr level in core 1 (methods of Miller and Hare, 1980). Amino acid age calculations using the EDT derived from aIle/Ile ratios in shells from the 8200 yr level in core 1 (Table III) suggest an age of 1200 to 1600 yr (using *Lymnaea* ratios) and 2.0 to 3200 yr (using *Pisidium* ratios) for the 1.5 m level in core 2, which was radiocarbon dated at 3000 yr. Thus, this data suggests that the 3000 yr sample in core 2 may have been contaminated by older carbon and that its age is too uncertain to be of use in estimating an EDT for the site or to be used in calibrating the older samples. The EDT derived from the 8200 yr calibration sample (4.9 ± 1.0°C) at 1.9 m in core 1 is only slightly warmer than the estimated MAT (mean annual temperature) of 4.3 ± 0.5°C (estimated using instrumental data in the region). Miller et al. (1982) found EDTs to be 0.5° to 2°C higher than MATs at a number of sites in the western U.S., and thus, 4.9°C seems a reasonable EDT for the Holocene period (Table III).

Because of the lower temperatures during the Pinedale glaciation, the average EDT experienced by the > 37,000 yr-old gastropods was considerably lower than the Holocene effective temperature. Two paleotemperature models for the last 125,000 yr, using temperature estimates based on the work of McCoy (1981), Pierce (in Porter et al., 1983), and Nelson et al. (1984) allow calculation of approximate age estimates for the gastropods in the cores (Table III) (methods of Miller et al., 1983, and Wehmiller, 1982). Both models assume an average EDT for the period 0 to 11,000 yr of 4.9°C (Table III) and an EDT lowering of 8.5°C for 11,000 to 15,000 yr (McCoy, 1981). Model A then uses 10°C less than MAT for

Table III. D-alloisoleucine/L-isoleucine ratios in the total (free plus peptide-bound) amino acid fraction and calculated temperatures and ages for fossil gastropods from Indian Creek cores, Wasatch County, Utah (SW¼NW¼ sec. 15, T. 4 S., R. 11W.). [(R)=reworked; (PR)=probably reworked; leaders (---) indicate no data].

INSTAAR Laboratory number (Univ. of Colo.)	Depth below surface (m)	Species	Number of shells	Sample weight (mg)	Total aIle/Ile ratio[1]	^{14}C age 10^3 yr	Calculated mean EDT (°C)[2]	Calculated age (10^3 yr) for temperature models[3]	
								Model A	Model B
Core 1									
DAN-125B	1.9	cf. *Lymnaea*	1	8.2	0.030	8.2	4.4	--	--
DAN-125D	1.9	cf. *Lymnaea*	1	4.5	0.034	8.2	5.4	--	--
CAN-125E	1.9	cf. *Lymnaea*	3	8.1	0.126	(R)	---	208*	--
DAN-125J	1.9	*Pisidium*	6	6.0	0.038	8.2	6.9	--	--
DAN-125A	1.9	*Vallonia cyclophorella*	4	2.5	0.030	8.2	4.4	--	--
DAN-125H	1.9	*Vallonia cyclophorella*	4	2.6	0.030	8.2	4.4	--	--
DAN-125G	1.9	*Pupilla muscorum*	4	4.2	0.028	8.2	3.6	--	--
DAN-125C	1.9	*Pupilla muscorum*	3	3.3	0.031	8.2	4.7	--	--
DAN-126A	6.7	*Vallonia cyclophorella*	5	3.0	0.080	(PR)	---	130*	--
DAN-126E	6.7	*Vallonia cyclophorella*	7	4.2	0.065	>37	---	89	94
DAN-126F	6.7	*Vallonia cyclophorella*	3	2.2	0.064	>37	---	86	92
DAN-126G	6.7	*Vallonia cyclophorella*	2	1.5	0.068	>37	---	97	99
DAN-126B	6.7	*Pupilla muscorum*	4½	4.8	0.088	(PR)	---	146*	--
DAN-126C	6.7	*Pupilla muscorum*	4½	5.1	0.067	>37	---	94	97
DAN-126D	6.7	*Pupilla muscorum*	5	7.6	0.067	>37	---	94	97
DAN-128A	7.0	cf. *Lymnaea*	1	6.5	0.101	(R)	---	163*	--
DAN-128B	7.0	*Pupilla muscorum*	½	0.8	0.062	---	---	80	89
DAN-127	9.1	cf. *Lymnaea*	1	1.0	0.115	(R)	---	188*	--
DAN-133A	10.5	*Pisidium*	1	2.0	0.091	---	---	214*	--
DAN-133B	10.5	*Pisidium*	1	2.0	0.098	---	---	233*	--
DAN-133C	10.5	*Vallonia cyclophorella*	3	2.2	0.091	---	---	152*	--

Core 2									
DAN-130A	1.5	cf. *Lymnaea*	½	8.1	0.015	3.0	1.5	--	--
DAN-130B	1.5	cf. *Lymnaea*	½	5.2	0.014	3.0	0.0	--	--
DAN-130C	1.5	cf. *Lymnaea*	1	20.3	0.014	3.0	0.0	--	--
DAN-130D	1.5	*Pisidium*	1	3.8	0.015	3.0	3.5	--	--
DAN-130E	1.5	*Pisidium*	1	2.8	0.017	3.0	2.1	--	--
DAN-130F	1.5	*Pisidium*	1	2.3	0.018	3.0	3.7	--	--
DAN-129	1.6	cf. *Lymnaea*	1	5.1	0.036	(R)	---	10	10

[1]AIle/Ile ratio (peak areas) measured and interpreted by Nelson using methods of Miller and Hare (1980).
[2]Mean effective diagenetic temperature (Wehmiller,1977) calculated using (1) Arrhenius parameters determined for cf. *Lymnaea* by W. D. McCoy (1981), Arrhenius parameters determined by Nelson and others (1984) for *Vallonia* and *Pupilla*, and Arrhenius parameters determined for *Pisidium* by Miller and others (1982); (2) ^{14}C ages; and (3) values of constants in Arrhenius equation (No. 9 in Williams and Smith, 1977).
[3]Age calculated using equation 18 in Williams and Smith (1977) with $K'=0.77$, a modern ratio of 0.014, and two temperature models (discussed in text) with software written by G. H. Miller (Brigham and Miller, 1983). Ages >125,000 yr (indicated by an asterisk) were recalculated using an average EDT for the late Quaternary in this region of 8°C less than present mean annual temperature (Nelson and others, 1984) (for example, Wehmiller, 1982).

15,000 to 125,000 yr while Model B assumes 12°C less than MAT for 15,000 to 75,000 yr and 7°C less than MAT for 75,000 to 125,000 yr. Critical assumptions in applying the models are: (1) the ages of the calibration samples in the region are accurate, (2) linear models of reaction kinetics apply, and (3) estimated differences in MAT at the calibration sites reflect differences in long-term EDTs at the sites (Wehmiller, 1982). Age calculations suggest the shells in core 1 at 6.7 and 7.0 m date from about 80,000 to 100,000 yr and that those at 10.5 m may be 150,000 to 230,000 yr (Table III). About 10 percent of the shells appear reworked. For several reasons (discussed in the literature cited above), these age estimates are more likely to be minimum rather than maximum ages.

Slip Rate Estimates

Using the above age estimates for various levels in the cores, a range of minimum slip rates across the fault can be calculated. At least 8 m of sediment has been displaced below the level of bedrock at the base of the stream channel on the upthrown block (Fig. 8). This is a minimum estimate for the amount of sediment deposited because the rate of bedrock erosion in the channel on the upthrown block is not known. Using our age estimates (Table III), the interval of sediment between the base of the channel at 2.9 m (Fig. 8) and the 7.0-m-level in core 1 was deposited in a total of roughly 70,000 to 90,000 yr, giving a minimum slip rate of 0.04 to 0.06 mm/yr. Using ages and thickness from the 10.5-m depth gives similar rates of 0.03 to 0.05 mm/yr. Because the age of the basal alluvium in the channel on the upthrown block is uncertain and we do not have estimates of channel erosion rates, maximum slip rates cannot be calculated.

We are left with the problems of (1) evaluating the Indian Creek minimum slip rates (if the assumptions of Hamblin and others (1981) are correct actual slip rates may be twice the minimum rates), (2) whether our slip rates derived from the subsidiary 7-m scarp are reasonable estimates for the whole Strawberry fault zone, and (3) whether latest Pleistocene and Holocene (< 30,000 yr) slip rates on the whole fault zone are higher than late Quaternary (< 125,000 yr) rates. If the actual Indian Creek rates are twice our minimum rates (0.03–0.06 mm/yr) and the 7-m scarp rates (0.04–0.17 mm/yr) represent slip on the whole fault zone, then late Quaternary rates along the Strawberry fault are similar. If there is a significant difference in rates along the Strawberry fault, then rates along the northern part of the fault are probably higher than those at Indian Creek, suggesting the fault could be divided into two segments with differing histories. However, whether this postulated difference in rates is a spatial difference along the fault or a temporal difference between latest Pleistocene–Holocene rates and late Quaternary rates cannot be determined from our data.

CONCLUSIONS

Geologic mapping and valley geomorphology suggest Strawberry Valley is a half-graben bounded on the east by the Strawberry normal fault, which may merge with the underlying Strawberry thrust fault (VanArsdale, 1979a). Two trenches across a 7-m-high fault scarp in alluvial fans adjacent to the fault suggest two to three fault events, each of 1 to 2 m stratigraphic displacement, have occurred on the scarp over the last 15,000–30,000 yr, but with smaller net vertical tectonic displacements due to graben formation and backtilting. Age estimates based on soils suggest that the last surface displacement event occurred during the early to mid-Holocene; 1500 yr is a minimum age for this event based on radiocarbon-dated burrow infillings. These displacement and age data suggest recurrence rates on earthquakes large enough to produce recognizable surface displacements on the Strawberry fault (M_s = 6.5–7.0) are in the range of 5000 to 15,000 yr. Latest Pleistocene and Holocene fault slip rates calculated from estimated net tectonic displacement across the 7-m subsidiary scarp in the Strawberry fault zone near Co-op Creek are 0.04 to 0.17 mm/yr, while minimum longer-term late Quaternary rates for the main fault derived from ^{14}C and amino acid dating of alluvial plain cores at Indian Creek are 0.03 to 0.06 mm/yr. Present data prevent us from determining whether these apparent differences in rates are real, either in space or time.

Recurrent late Pleistocene and Holocene displacement on the Strawberry fault shows that the late Quaternary extensional stress regime of the Basin and Range extends at least this far east in central Utah (see also, Martin, 1982), despite the general lack of fault scarps in alluvium and other evidence of recurrent late Quaternary displacement on faults in other back valleys northwest of Strawberry Valley. Our limited slip rate data on the Strawberry fault indicate a latest Pleistocene and Holocene rate at most half, and probably nearly an order of magnitude less than, that for the Wasatch fault (Swan et al., 1980; Schwartz and Coppersmith, 1984). Recurrence rates and the amount of displacement per event are more difficult to estimate, but both are considerably lower than for the Wasatch fault; they are similar to estimates for other faults in the eastern Basin and Range (Wallace, 1984). Whether latest Pleistocene–Holocene slip rates on the Strawberry fault are higher than late Quaternary rates on the fault or than rates on faults in other back valleys or whether our latest Pleistocene–Holocene data represent only a local short-term pulse of activity which reflects a much lower, long-term rate for the eastern Wasatch Mountains (e.g., Wallace, 1984) is unknown. Resolution of these questions will require detailed studies in other back valleys of the eastern Wasatch Mountains.

VanArsdale's mapping of Strawberry Valley was funded in part by the Utah Geological and Mineral Survey and Amoco Production Company. This aspect of the research profitted from conversations with William Hansen, Dan Davis, Charles Hunt, and Laurence Lattman. Trenching and coring along the Strawberry fault by Nelson was part of a larger seismotectonic study for assessment of seismic hazards for Soldier Creek Dam (Nelson and Martin, 1982) supported by the U.S. Bureau of Reclamation. We appreciate the cooperation of the staffs of the Uinta Basin Project Office, Bonneville Construction Office, and Salt Lake City Regional Office, Upper Colorado Region, U.S. Bureau of Reclamation, for providing right-of-way, environmental clearances, and considerable logistical support. We also thank the Strawberry Valley Water Users Association for permission to excavate on their property. Able field assistance was provided by Ed Baltzer, Karen Janowitz, Carol Krinsky, and Becky Stoneman. Ed Baltzer did an aerial photographic study of lineaments for the Strawberry Valley area that included field reconnaisance. Grain size analyses by Rolf Kihl, INSTAAR, University of Colorado, are appreciated. Nelson determined amino acid ratios in the Amino Acid Geochronology Laboratory, INSTAAR, University of Colorado, with the help of Dan Goter, under the direction of Gifford Miller. Discussions with Dean Ostenaa and Tim Sullivan, Seismotectonic Section, USBR, throughout the study were very helpful. The manuscript benefited considerably from initial reviews by Tim Sullivan, Ron Bruhn, William McCoy, Gifford Miller, Dean Ostenaa, Lucy Piety, and especially Mike Machette, Jim McCalpin, and Dave Schwartz.

References

Anderson, R. E. (1979). Quaternary tectonics along the Intermountain Seismic Belt south of Provo, Utah. *Brigham Young University Geology Studies* **25** (1), 1–10.

Arabasz, W. J., Smith, R. B., and Richins, W. D. (1980). Earthquake studies along the Wasatch front, Utah: Network monitoring, seismicity, and seismic hazards. *Seismological Society of American Bulletin* **70**, 1479–1500.

Astin, G. K. (1977). Structure and stratigraphy of the Co-op Creek Quadrangle, Wasatch County, Utah. *Brigham Young University Geology Studies* **24** (1), 13–34.

Birkeland, P. W. (1984). *Soils and Geomorphology*. New York: Oxford University Press, 372 pp.

Bissell, H. J. (1952). Stratigraphy and structure of northeast Strawberry Valley Quadrangle, Utah. *American Association of Petroleum Geologists Bulletin* **36**, 575–634.

Bissell, H. J. (1959). North Strawberry Valley sedimentation and tectonics, in *Guidebook to the geology of the Wasatch and Uinta Mountains transition area*. Intermountain Association Petroleum Geologists, **10**, 159–165.

Brigham, J. K., and Miller, G. H. (1983). Paleotemperature estimates of the Alaskan arctic coastal plain during the last 125,000 years, in *Proceedings of Fourth International Conference on Permafrost*. Washington, D. C.: National Academy Press, 80–85.

Bucknam, R. C., and Anderson, R. E. (1979). Estimation of fault-scarp ages from a scarp-height-slope-angle relationship. *Geology* **7**, 11–14.

Carver, R. E., Ed. (1971). *Procedures in Sedimentary Petrology*. New York: Wiley-Interscience, 653 pp.

Colman, S. M., and Watson, K. (1983). Ages estimated from a diffusion equation model for scarp degradation. *Science* **221**, 263–265.

Crone, A. J., and Harding, S. T. (1984). Relationship of late Quaternary fault scarps to subjacent faults, eastern Great Basin, Utah. *Geology* **12**, 292–295.

Dohrenwend, J. C. (1978). Systematic valley asymmetry in the central California Coast Ranges. *Geological Society of America Bulletin* **89**, 891–900.

Dreimanis, Aleksis (1962). Quantitative gasometric determination of calcite and dolomite by using chittick apparatus. *Journal of Sedimentary Petrology* **32**, 520–529.

Eardley, A. J. (1944). Geology of the north-central Wasatch Mountains, Utah. *Geological Society of America Bulletin* **55**, 819–894.

Gilbert, G. K. (1928). Studies of Basin and Range structure. *U.S. Geological Survey Professional Paper* **153**, 89 pp.

Gile, L. H., Peterson, F. F., and Grossman, R. B. (1966). Morphological and genetic sequences of carbonate accumulation in desert soils. *Soil Science* **101**, 347–360.

Guthrie, R. L., and Witty, J. E. (1982). New designations for soil horizons and layers and the new Soil Survey Manual. *Soil Science Society America Journal* **46**, 443–444.

Hamblin, W. K., Damon, P. E., and Bull, W. B., (1981). Estimates of vertical crustal strain rates along the western margins of the Colorado Plateau. *Geology* **9**, 293–298.

Hanks, T. C., Bucknam, R. C., Lajoie, K. R., and Wallace, R. E. (1984). Modification of wave-cut and faulting-controlled landforms. *Journal of Geophysical Research* **89** (B7), 5771–5790.

Harmon, R. S., Mitterer, R. M., Kriausakul, N., Land, L. S., Schwarcz, H. P., Garrett, P., Larson, G. J., Vacher, H. L., and Rowe, M. (1983). U-series and amino-acid racemization geochronology of Bermuda: implications for eustatic sea-level fluctuations over the past 250,000 years. *Palaeogeography, Palaeoclimatology, Palaeoecology* **44**, 41–70.

Hopkins, D. L., and Bruhn, R. L. (1983). Extensional faulting in the Wasatch Mountains, Utah. *Geological Society of America, Abstracts with Programs* **15** (5), 402.

Jackson, M. L. (1956). *Soil Chemical Analysis, Advanced Course* [unpublished]. Madison: University of Wisconsin, Department of Soil Science, 656 pp.

Kihl, R. (1975). Appendix: Physical preparation of organic matter samples for C14 dating, in Andrews, J. T., Radiocarbon date list II from Cumberland Peninsula, Baffin Island, N.W.T., Canada. *Arctic and Alpine Research* **7**, 90–91.

Madole, R. F. (1976). Glacial geology of the Front Range, Colorado, in Mahaney, W. C., Ed., *Quaternary Stratigraphy of North America*. Stroudsburg, PA: Dowden, Hutchinson, and Ross, 297–318.

Martin, R. A., Jr. (1982). Contemporary seismicity and tectonics of the south flank of the Uinta Mountains, Utah [unpub. M.S. thesis]. Golden, CO: Colorado School of Mines, 109 pp.

Matthews, J. A. (1980). Some problems and implications of ^{14}C dates from a podzol buried beneath an end moraine at Haugabreen, southern Norway. *Geografiska Annaler* **62A**, 182–208.

Mayer, L. (1984). Dating Quaternary fault scarps formed in alluvium using morphologic parameters. *Quaternary Research* **22** (3), 300–313.

McCoy, W. D. (1981). Quaternary aminostratigraphy of the Bonneville and Lahontan basins, western U.S., with paleoclimatic implications [Ph.D. thesis]. Boulder: University of Colorado, 157 pp.

Miller, G. H., and Hare, P. E. (1980). Amino acid geochronology: Integrity of the carbonate matrix and potential of molluscan fossils, in Hare, P. E., Hoering, T. C., and King, K., Jr., Eds., *Biogeochemistry of Amino Acids*. New York: Wiley, 415–443.

Miller, G. H., Nelson, A. R., McCoy, W., and Metcalf, A. L. (1979). Amino acid geochronology utilizing terrestrial gastropods from western U.S. *Geological Society of America, Abstracts with Programs* **11** (6), 280–281.

Miller, G. H., McCoy, W. D., and Nelson, A. R. (1982). Environmental controls in the amino acid racemization rate from continental-interior deposits. *Geological Society of America, Abstracts with Programs* **14** (7), 565.

Miller, G. H., Sejrup, H. P., Mangerud, J., and Anderson, B. (1983). Amino acid ratios in Quaternary molluscs and foraminifera from western Norway: Correlation, geochronology, and paleotemperature estimates. *Boreas* **12**, 107–124.

Nakata, J. K., Wentworth, C. M., and Machette, M. N. (1982). Quaternary fault map of the Basin and Range and Rio Grande Rift provinces, western United States. *U.S. Geological Survey Open-File Report 82-579*, 2 plates, 1:2,500,000 scale maps.

Nash, D. B. (1980). Morphologic dating of degraded normal fault scarps. *Journal of Geology* **88**, 353–360.

Nash, D. B. (1981). Fault: A Fortran program for modeling the degradation of active normal fault scarps. *Computers and Geosciences* **7**, 249–266.

Nelson, A. R., and Krinsky, C. K. (1982). Late Cenozoic history of the upper Weber and Provo Rivers, NE Utah. *Geological Society of America, Abstracts with Programs*, **14** (3), 344.

Nelson, A. R., and Martin, R. A. (1982). Seismotectonic study for Soldier Creek Dam, Central Utah Project: Seismotectonic Report 82-1, Engineering and Research Center, U.S. Bureau of Reclamation, Denver, Colorado, 115 pp.

Nelson, A. R., Madole, R. F., Evanoff, Emmett, Piety, L. A., and Scott, G. R. (1984). Quaternary paleotemperature estimates using amino-acid ratios measured on terrestrial gastropods from fluvial sequences in Colorado: Boulder, Colorado, American Quaternary Association, 8th Biennial meeting, Program and Abstracts, p. 92.

Olsson, I. U. (1968). Modern C^{13} aspects of radiocarbon datings. *Earth Science Reviews* **4**, 203–218.

Pierce, K. L. (1979). History and dynamics of glaciation in the northern Yellowstone National Park area. *U.S. Geological Survey Professional Paper No. 729-F*, 90 pp.

Pierce, K. L., and Scott, W. E. (1984). Pleistocene episodes of alluvial-gravel deposition, southeastern Idaho, in Bonnichsen, B., and Breckenridge, R. M., Eds., Cenozoic geology of Idaho. *Idaho Bureau of Mines and Geology Bulletin* **26**, 685–702.

Porter, S. C., Pierce, K. L., and Hamilton, T. D. (1983). Late Wisconsin mountain glaciation in the western United States, in Wright, H. E., Jr., Late-Quaternary environments of the United States, Porter, S. C., Ed., *The Late Pleistocene*, Vol. 1, Minneapolis, Minnesota: University of Minnesota Press, 71–111.

Royse, F. (1983). Extensional faults and folds in the foreland thrust belt, Utah, Wyoming, Idaho. *Geological Society of America, Abstracts with Programs* **15** (5), 295.

Rutter, N. W., Crawford, R. J., Hamilton, R. (1980). Correlation and relative age dating of Quaternary strata in the continuous permafrost zone of northern Yukon with D/L ratios of aspartic acid of wood, freshwater molluscs, and bone, in Hare, P. E., Hoering, T. C., and King, K., Jr., Eds., *Biogeochemistry of Amino Acids*. New York: Wiley, 463–475.

Schwartz, D. P., and Coppersmith, K. J. (1984). Fault behavior and characteristic earthquakes: examples from the Wasatch and San Andreas fault zones. *Journal of Geophysical Research* **89** (B7), 5681–5698.

Shroba, R. R. (1980). Influence of parent material, climate, and time on soils formed in Bonneville-shoreline and younger deposits near Salt Lake City and Ogden, Utah. *Geological Society of America, Abstracts with Programs* **12** (6), 304.

Shroba, R. R. (1982). Soil B-horizon properties as age indicators for late Quaternary deposits along the Wasatch Front, northcentral Utah. *Geological Society of America, Abstracts with Programs* **14** (4), 233.

Shroba, R. R., and Birkeland, P. W. (1983). Trends in late-Quaternary soil development in the Rocky Mountains and Sierra Nevada of the western United States, in Wright, H. E., Jr., Ed., *Late-Quaternary environments the United States*, Porter, S. C., Ed., *The late Pleistocene*, Vol. 1. Minneapolis, Minnesota: University of Minnesota Press, 145–156.

Shuey, R. T., Shellinger, D. K., Johnson, E. G., and Alley, L. B. (1973), Aeromagnetics and the transition between the Colorado Plateau and Basin and Range provinces. *Geology* **1**, 107–110.

Smith, R. B., and Bruhn, R. L. (1984). Intraplate extensional tectonics of the eastern Basin and Range: Inferences on structural style from seismic reflection data, regional tectonics, and thermal-mechanical models of brittle-ductile deformation. *Journal of Geophysical Research* **89** (B7), 5733–5762.

Sullivan, J. T., and Nelson, A. R. (1983). Late Cenozoic faulting in Heber and Keetley valleys, northeastern Utah, in Crone, A. J., Ed., Paleoseismicity along the Wasatch front and adjacent areas, central Utah, in *Geologic excursions in neotectonics and engineering geology in Utah*, Geological Society of America, Fieldtrip guidebook for Rocky Mountain and Cordilleran Section Meeting—Part IV: Utah Geologic and Mineral Survey Special Studies **62**, 55–61.

Swan, F. H., III, Schwartz, D. P., and Cluff, L. S. (1980). Recurrence of moderate to large magnitude earthquakes produced by surface faulting on the Wasatch fault zone, Utah. *Bulletin Seismological Society of America* **70**, (5), 1431–1462.

Thompson, F. (1971). Construction Geologic Report, Water Hollow Tunnel [unpublished]: Salt Lake City, Utah, *U.S. Bureau of Reclamation, Report No. G-275*, 36 pp.

Threet, R. L. (1959). Geomorphology of the Wasatch-Uinta Mountains Junction, in Guidebook to the Geology of the Wasatch and Uinta Mountains Transition Area. *Intermountain Association of Petroleum Geologists* **10**, 24–33.

VanArsdale, R. B. (1979a). Geology of Strawberry Valley and regional implications [Ph.D. thesis]: Salt Lake City: University of Utah, 65 pp.

VanArsdale, R. B. (1979b). Geometry and most recent movement along Strawberry normal fault, Wasatch County, Utah. *Geological Society of America, Abstracts with Programs* **11** (7), 531–532.

Walkley, A., and Black, I. A. (1934). An examination of the Degtjareff method for determining soil organic matter, and a proposed modification of the chromic acid titration method. *Soil Science* **34**, 29–38.

Wallace, R. E. (1977). Profile and ages of young fault scarps, north-central Nevada. *Geological Society of America Bulletin* **88** 1267–1281.

Wallace, R. E. (1984). Patterns and timing of late Quaternary faulting in the Great Basin Province and relation to some regional tectonic features. *Journal of Geophysical Research* **89** (B7), 5763–5769.

Wehmiller, J. F. (1977). Amino acid studies of the Del Mar, California midden site: apparent rate constants, ground temperature models, and chronological implications. *Earth and Planetary Science Letters* **37**, 184–196.

Wehmiller, J. F. (1982). A review of amino acid racemization studies in Quaternary mollusks: stratigraphic and chronologic applications in coastal and interglacial sites, Pacific and Atlantic coasts United States, United Kingdom, Baffin Island, and Tropical Islands. *Quaternary Science Reviews* **1**, 82–120.

Williams, K. M., and Smith, G. G. (1977). A critical evaluation of the application of amino acid racemization to geochronology and geothermometry. *Origins of Life* **8**, 91–144.

Zandt, G., and Owens, T. J. (1980). Crustal flexure associated with normal faulting and implications for seismicity along the Wasatch Front, Utah. *Seismological Society of America Bulletin* **70**, 1501–1520.

Zoback, M. L. (1983). Structure and Cenozoic tectonism along the Wasatch fault zone, Utah, in Miller, D. M., Todd, V. R., and Howard, K. A., Eds., Tectonic and stratigraphic studies in the eastern Great Basin. *Geological Society of America Memoir* 157, 3–29.

Origin of the Yaracuy Basin, Boconó-Morón Fault System, Venezuela

Carlos Schubert

Centro de Ecología, I. V. I. C., Apartado 1827 Caracas 1010A, Venezuela

The Yaracuy basin is a tectonic depression within an en echelon stepover in the Boconó-Morón-El Pilar fault system. This basin is interpreted as a pull-apart basin formed by right-lateral offset along this fault system; basin formation began as a releasing bend along the system and, with increasing offset, it developed into a rhomboidal basin between en echelon faults. The right-lateral offset necessary for the formation of the basin and its present dimensions is 50 to 60 km; this figure is consistent with estimates of a total late Tertiary–Quaternary right-lateral offset of 100 to 125 km along the Boconó-Morón-El Pilar fault system, which is part of the Caribbean–South American plate boundary.

La cuenca de Yaracuy es una depresión tectónica dentro de un salto en echelon en el sistema de fallas de Boconó-Morón-El Pilar. Se interpreta a esta cuenca como una cuenca de tracción formada por desplazamiento rumbo-deslizante hacia la derecha a lo largo de este sistema; la formación de la cuenca comenzó como una curvatura de alivio a lo largo del sistema y, con un desplazamiento progresivamente mayor, se convirtió en una cuenca romboidal entre fallas en echelon. El desplazamiento rumbo-deslizante hacia la derecha necesario para la formación de la cuenca en sus dimensiones actuales es de 50 a 60 km; esto es consistente con una estimación del desplazamiento rumbo-deslizante hacia la derecha total durante el Terciario tardío–Cuaternario de 100 a 125 km, a lo largo del sistema de fallas de Boconó-Morón-El Pilar, el cual forma parte del límite entre las placas de América del Sur y del Caribe.

INTRODUCTION

In the past decade, formation of sedimentary basins along strike-slip zones has received much attention (Crowell, 1974a, b; Ballance and Reading, 1980). Basins often form in places where strike-slip faults bend, converge, or diverge. Depending on the sense of the displacement (right- or left-lateral) and the sense of the discontinuity (right- or left-stepping), a basin is formed by extension or a thrust-bounded uplift is formed by compression. Basins originated in this manner were first named pull-apart basins by Burchfiel and Steward (1966). Since then, about 60 Quaternary pull-apart basins have been suggested around the world. Extensive reviews on the origin and evolution of pull-apart basins were published by Aydin and Nur (1982), Mann et al. (1983), and Bahat (1983).

Neotectonics: An International Journal of Crustal Dynamics, Vol. 1, 39-50 (1986)
© 1986 John Wiley & Sons, Inc. CCC 0884-8157/86/010039-12$04.00

The southern boundary of the Caribbean Sea is a transform plate boundary between the Lesser Antilles and western South America subduction zones (Molnar and Sykes, 1969). The existence of large strike-slip fault zones in northern Venezuela supports this interpretation (Bucher, 1952; Rod, 1956; Schubert, 1981). These fault zones are superimposed on various pre-Quaternary (especially early Tertiary) tectonic provinces (Fig. 1): the late Cretaceous–Eocene Caribbean province, with large southward nappes along sub-horizontal surfaces (Bellizzia, 1972; Stephan et al., 1980), and the Andean province which, in its youngest (post-Eocene) phase, consists mainly of horsts, grabens, and faulted crustal blocks (Shagam, 1975). The fact that the strike-slip fault zones cross and offset these contrasting tectonic provinces is important evidence of the comparatively young age of these displacements (late Tertiary?–Quatarnary), which may have taken advantage of previous local zones of weakness, and that large displacements of the order of several hundreds of kilometers cannot be expected along them.

Several pull-apart basins have been detected and partially described along the Boconó-Morón-El Pilar fault system (Schubert, 1984). The principal ones are the La González, Yaracuy, Valencia, and Cariaco basins (Fig. 1). In this report, I describe and postulate an origin for the Yaracuy basin (Figs. 1 and 2), at the northeastern end of the Boconó fault zone, concerning which little has been published.

GEOLOGIC SETTING

Figure 1 schematically represents the principal Late Cenozoic tectonic features of northern Venezuela. The western Caribbean nappes were thrust to the south over the northeastern end of the Andes in post-Eocene and pre-Oligocene–Miocene time (Beck, 1977); the central Caribbean nappes were thrust over the Guayana Shield in the Eocene. The Boconó fault zone apparently offsets the frontal thrust of these nappes in a right-lateral sense by approximately 70 km (Stephan et al., 1980). The possible eastward extension of the Oca fault zone has been detected by marine geophysical studies (see the review by Schubert and Krause, 1984). This fault zone is thought to be less active at present than both the Boconó and Morón fault zones; offset Holocene beach ridges suggest that it is active (Cluff and Hansen, 1969). As they reach the Caribbean Sea, the Boconó and Oca fault zones are parallel and, eastwards, they form a complex zone of diverging and converging faults in the Venezuelan continental borderland and the Coastal Range (Morón fault zone; Schubert and Krause, 1984). To the east, there is a right en echelon stepover, and the zone continues as the El Pilar fault zone. In the stepover zone, the Cariaco pull-apart basin was formed in the Late Tertiary(?)–Quaternary, which contains over 1 km of sediments (Schubert, 1982a). These sediments are mostly Quaternary in age, as shown by

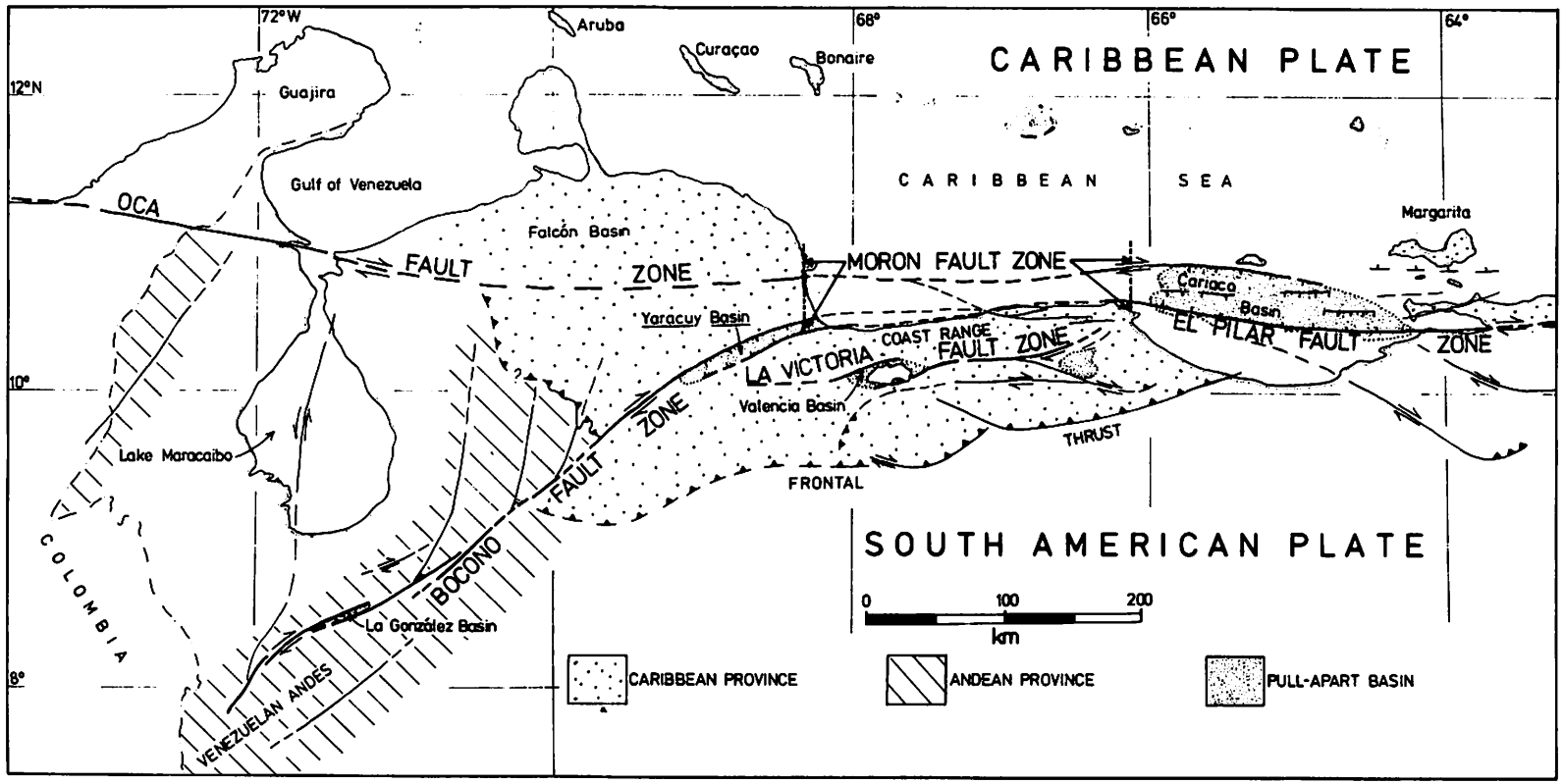

Figure 1. Principal Late Conozoic tectonic features of northern Venezuela (modified after Schubert, 1981 and 1984). For location see Figure 4.

sedimentation rates and paleontologic analyses of a core obtained during leg 15, locality 147, of the Deep Sea Drilling Project (Saunders et al., 1973). Model studies of pull-apart basin formation (Rodgers, 1980) suggest that Cariaco basin is the result of a right-lateral offset of 25 km (minimum) and less than 100 km (maximum), along the Morón-El Pilar fault system, Assuming that the length of a pull-apart basin is approximately equal to the strike-slip offset necessary to produce it (Aydin and Nur, 1982) suggests a maximum right-lateral offset of 125 km along the Morón-El Pilar fault system. All of these faults form the Bocono-Moron-El Pilar fault system, which extends from the Colombia–Venezuela border to Trinidad (Schubert, 1981).

The geologic and neotectonic characteristics of the Boconó-Morón-El Pilar fault system have been described by Rod (1956), Rod et al. (1958), Schubert (1979, 1982a, b), and Schubert and Krause (1984). In particular, the Boconó fault zone represents an active zone, characterized by a well-defined neotectonic morphology, typical of strike-slip faults (Fig. 2). Right-lateral offset along this fault zone has been estimated as 70 km (apparent offset of frontal thrust; middle Tertiary?), 20 to 30 km (apparent offset of Mesozoic rocks; Fig. 3), more than 1 km (Pleistocene alluvium), and between 0.06 and 0.1 km (Late Pleistocene lateral moraines) (Schubert, 1982b).

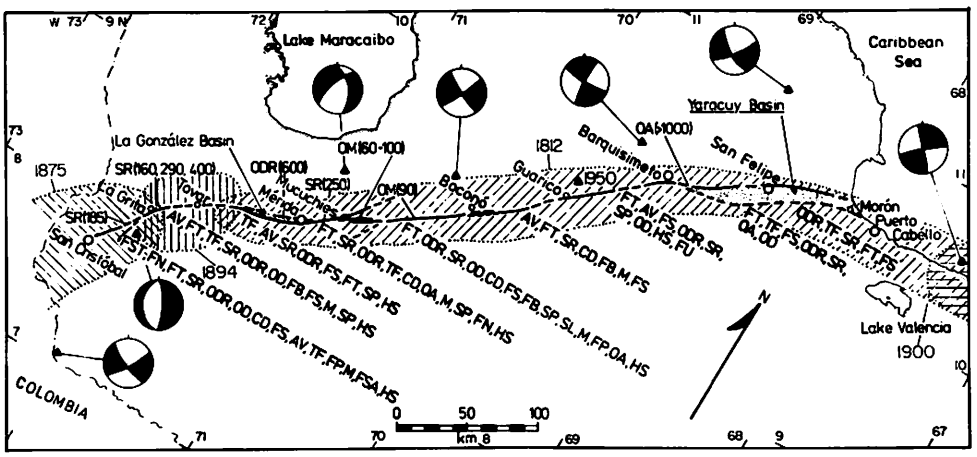

Figure 2. Neotectonic morphology of the Boconó fault (for location see Figure 4). Shaded areas represent pull-apart basins. Letters represent neotectonic features (in order of decreasing frequency from left to right) found in each of the fault segments between the shown localities. The symbols associated with numbers represent neotectonic features with measured right-lateral offset in meters. Symbols: AV: aligned valley; CD: closed depression; FB: fault bog; FN: fault notch; FP: fault plane; FS: fault scarp; FSA: fault saddle; FST: fault step; FT: fault trench; FU: fumarole; HS: hot spring; M: mylonite, cataclastic rock, fault gouge; OA: offset alluvium; OD; open depression; ODR: offset drainage; OM: offset moraine; SL: slickensides; SP: sag pond; SR: shutterridge; TF: triangular facet. Estimated rupture zones for some major earthquakes are shown (after Kelleher et al., 1973) and focal mechanisms of some recent earthquakes (after Molnar and Sykes, 1969; Dewey, 1972; and Pennington, 1981). Shaded quadrants represent compressional seismic wave arrivals and triangles represent epicenters.

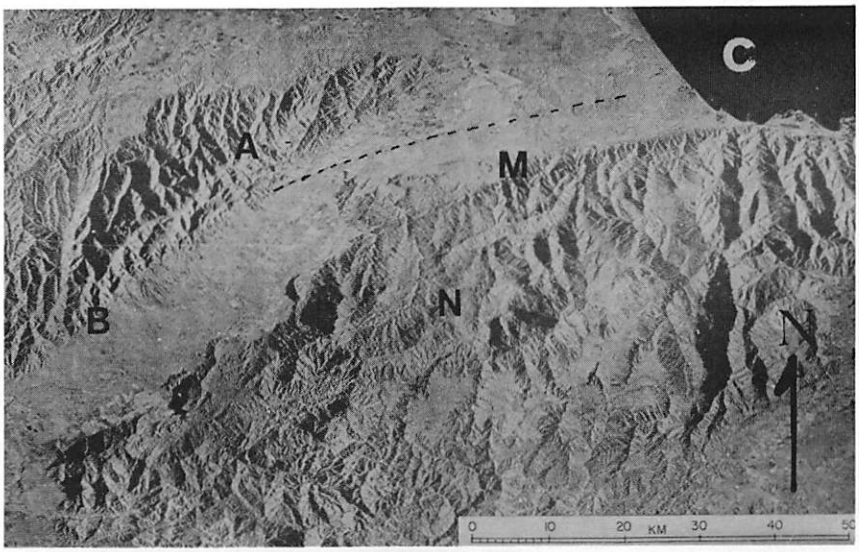

Figure 3. Side-looking radar image of the Yaracuy pull-apart basin (Y). The Boconó fault (B) bounds the basin to the northwest and offsets large alluvial cones in a right-lateral sense. The Morón fault (M) bounds the basin to the southeast. C: Caribbean Sea; N: Nírgua massif; A: Sierra de Aroa. The broken line shows the fault scarp of the Boconó fault across the Yaracuy river coastal plain.

THE YARACUY BASIN

The Yaracuy basin is located in the central-western region of Venezuela (Fig. 1) and traverses the State of Yaracuy in an east-northeast direction (Zambrano, 1976). It occupies an area of approximately 2600 km^2 and is drained by the Urachiche and Yaracuy rivers (Fig. 3 and 4); to the northwest and southeast, the basin is bounded by the Sierra de Aroa (1800 mm elevation) and the Nírgua massif (1360 m elevation), respectively. To the southwest, the basin extends towards the Turbio river valley in the Barquisimeto and the Yaritagua depressions, from which it is separated by a shallow watershed (280 m above sea level); to the northeast, the basin extends to the Caribbean Sea. The first suggestion that the Yaracuy basin is structurally controlled was by Sievers (1888, p. 57).

The geology of the State of Yaracuy was described in detail by Bellizzia and Rodríguez (1976). Three Mesozoic metamorphic rock units crop out in the Sierra de Aroa: (1) the Yaritagua Complex (Jurassic?), which consists of porphyroblastic gneiss, quartz-mica-feldspar schist, amphibolite, and local granitic bodies; (2) the Nírgua Formation (Jurassic?), which consists of crystalline limestone, marble, quartz-mica, graphitic schist, amphibolite, and local bodies of eclogite, quartzite, and gypsum; and (3) the Aroa Formation (Jurassic?–Cretaceous), which consists of calcareous-graphitic schist, metaconglomerate, and metasandstone. Along the southwestern slope of the Sierra de Aroa, the

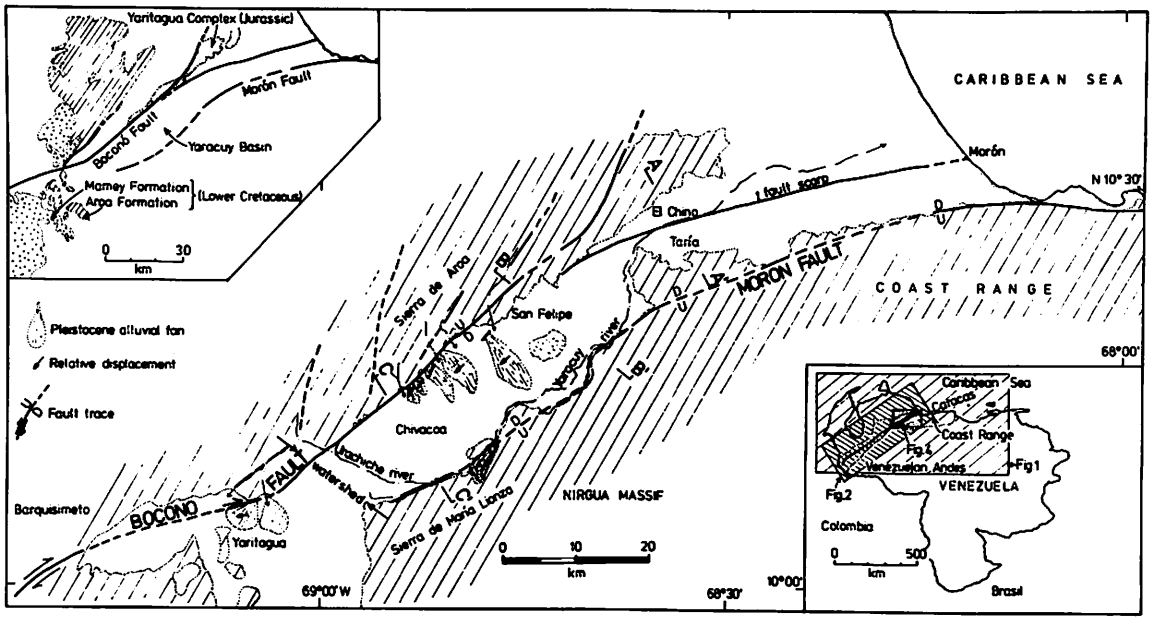

Figure 4. Tectonic-geomorphologic map of the Yaracuy basin, showing the bounding faults and some offset sedimentary features (D: down-faulted; U: up-faulted). The upper left inset shows the distribution of the Mamey and Aroa Formations, and of the Yaritagua Complex, which suggests right-lateral offset by the Boconó fault.

following stratigraphic units crop out (Dirección de Geología, 1970): (1) the Mamey Formation (Cretaceous), which consists of quartz-sericitic schist, metaconglomerate, limestone, metasandstone, and phyllite; and (2) the Barquisimeto Formation (Cretaceous), which consists of slate, siltstone, marl, chert, and limestone.

The same Mesozoic metamorphic rock units described above crop out in the Nírgua massif, in addition to the Las Brisas Formation (Jurassic?), which consists of quartz-mica-feldspar-graphitic schist, amphibolic gneiss, amphibolite, quartzite, and metaconglomerate. Along the northern slope of this massif, the Maporita Formation (Miocene–Pliocene) crops out, which consists of sandstone, siltstone, shale, clay, and marl.

The contacts among all of these stratigraphic units are frequently faulted. The La Victoria fault zone, identified in the central valley of the Coastal Range (Fig. 1), displaces rocks of the Nírgua massif (Las Brisas Formation) in an apparent right-lateral sense (Bellizzia and Rodríguez, 1968). The distribution of the Mamey and Aroa Formations, and the Yaritagua Complex, in the Sierra de Aroa (Fig. 4) suggest that the Boconó fault has apparently offset them by 18 and 35 km, respectively, in a right-lateral sense.

EVIDENCE FOR PLEISTOCENE OFFSETS

The southeastern slope of the Sierra de Aroa and the northwestern slope of the Nirgua massif are linear and very steep (Figs. 3 and 4); along them is numerous evidence of recent faulting: triangular facets, offset drainages, shutterridges, fault trenches, exposed fault planes with slickensides, offset alluvium, and fault depressions. All of these features suggest that the Yaracuy basin is bounded to the northwest and southeast by two important faults, along which the most evident (but not necessarily the most important) offset is normal, forming a tectonic depression. Along the northwestern slope (Boconó fault), an alluvial cone north of Yaritagua is offset in a right-lateral sense by at least 1 km. Along the same fault to the northeast, there are several alluvial cones that form basinward-dipping terraces (Figs. 3 and 4); these cones have no present-day connection with rivers or creeks from the Sierra de Aroa (from which they were obviously derived), and this suggests that they have been offset by the Boconó and associated faults. This offset is at least 1 km, judging from the location of the nearest stream which could have originated the cone. The age of these alluvial deposits has not been established. During the Late Pleistocene glaciation, the climate of northern Venezuela was more arid than at present (demonstrated by palynological studies in the Lake Valencia basin, about 50 km southeast of the Yaracuy basin; Salgado-Labouriau, 1980) and large amounts of alluvium were deposted in the Venezuelan Andes and the Coastal Range (Garner, 1959; Schubert, 1985; Schubert and Valastro, 1980); in contrast, little alluvium is being deposited at present. Therefore, a Pleistocene age (probably Late Pleistocene) can be postulated for the offset alluvium. This suggests a Late Pleistocene–Holocene offset rate of the order of a millimeter per year along the Bocono fault.

The two faults that bound the Yaracuy basin are the Boconó and Morón faults (Schubert, 1982b; Schubert and Krause, 1984). The active trace of the Boconó fault is observed northeastward along the southeast slope of the Sierra de Aroa until San Felipe; from there, it turns slightly eastward forming a scarp of several meters height (north side down), which crosses the Yaracuy river coastal plain (Figs. 3 and 4), reaching the Caribbean Sea near Morón. The Morón fault forms a prominent scarp along the Coastal Range; westward, this scarp turns to the southwest and borders the Nírgua massif until the Sierra de María Lionza. From there to the southwest it loses its geomorphic identity.

Three cross sections through the Yaracuy basin are shown in Figure 5, from the northeast end (A–A′) to the southwest (C–C′). These sections show the slope (in %) of the different segments (slopes of the bonding ranges and basin floor). From these sections, it is evident that the basin floor is lower to the southeast; this asymmetry increases to the southwest, until it forms the watershed between the Turbio river

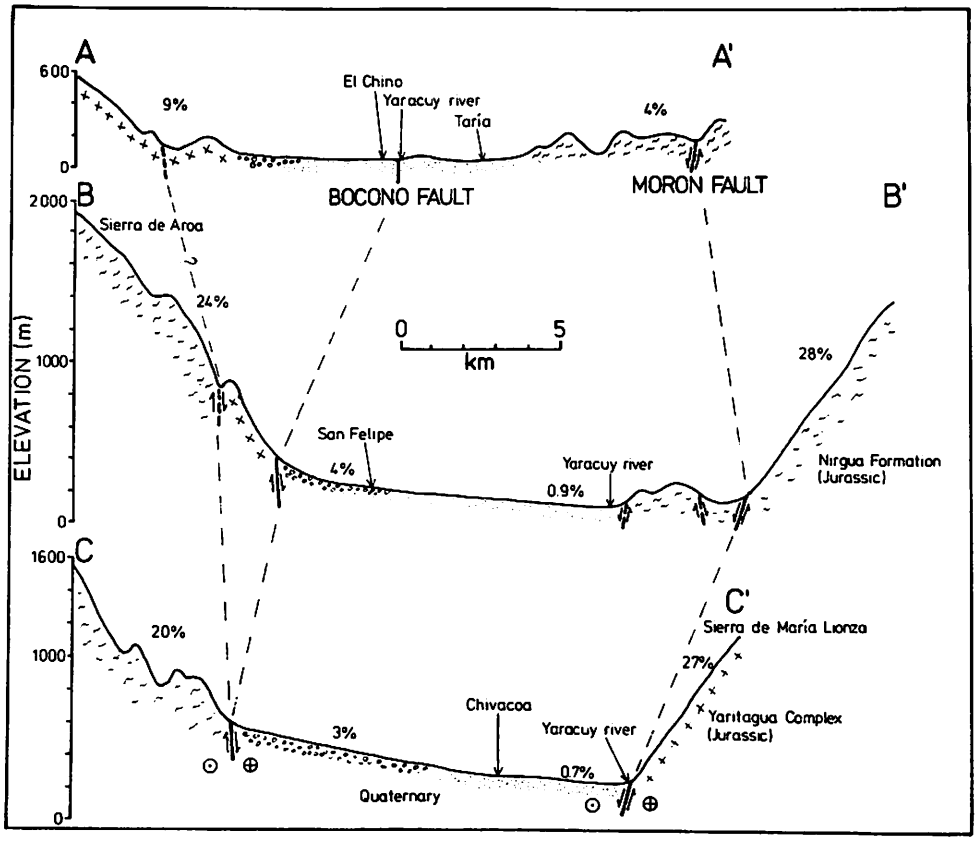

Figure 5. Cross sections of the Yaracuy basin (for location see Figure 4), showing the average slopes (in %) of different sectors and the location of the principal faults. Note the progressively greater asymmetry of the basin floor from A–A′ to C–C′. Normal offset along faults is represented by arrows; strike-slip offset is represented by a circle (with dot: out of page; with cross: into the page).

(Barquisimeto depression) and the Yaracuy river basin. The existence of this asymmetry is supported by gravimetric data (Bellizzia and Rodríguez, 1976), which suggest that the maximum thickness of sediments in the Yaracuy basin is approximately 600 m, and is located along the southeastern border. The watershed between the Yaracuy basin and the Barquisimeto depression could be a consequence of the left curvature of the Boconó fault north of Yaritagua; this small curvature would produce a local compressional zone, which could cause slight uplift in the area.

ORIGIN OF THE YARACUY BASIN

Molnar and Sykes (1969) suggested that the relative displacement of the Caribbean plate with respect to the South American plate is to the east. Aggarwal (1983) suggested that this displacement is part of a

rotation of South America around a pole located aproximately at 4.5°S and 67°5.W. This implies that the displacement along this plate boundary varies in orientation, becoming more southward to the west; this is also suggested by the orientation of the major faults within the plate boundary. Therefore, it may be expected that, if the Boconó-Morón-El Pilar fault system is an active expression of this boundary, offset along the Boconó fault is not in an east–west sense, but west–southwest.

In this manner, a model for the Yaracuy basin formation, as well as other basins in the fault system, can be constructed, based on the orientation of the Boconó and Morón faults, and the sense of offset along them. Figure 6 shows this model in schematic form. Assuming that the surficial trace of the Boconó-Morón fault system has maintained its shape during at least the Quaternary, one can reconstruct the opening of a pull-apart basin along a releasing bend in the system. With a right-lateral offset of 10 km, a small basin (proto-Yaracuy basin) begins to form. The second basin corresponds to the tectonic depression north of the central Venezuelan coast. As offset increases, the dimensions of the pull-apart basin increase, until, when right-lateral offset is 40 km, the pull-apart basin opens eastward toward the Caribbean Sea. With an offset of 50 to 60 km, the dimensions of the basin are similar to the present-day dimensions.

In the model of pull-apart basin formation of Mann et al. (1983), the rhomboidal Yaracuy basin would correspond to the advanced stage. According to this model, pull-apart basins initiate at releasing bends and subsequently develop into spindle-shaped, S-shaped, and rhomboidal basins. In the final stage, the releasing bend is converted into an en echelon discontinuity along the fault zone.

Another theoretical model of pull-apart basin formation (Rodgers, 1980) utilizes total displacement along the master faults, en echelon separation, and fault-end superposition, in the calculation of the basin formation along strike-slip fault zones. This model uses basin dimensions to calculate total offset along the fault zone necessary to produce the pull-apart basin. Using Rodgers' model, the dimensions of the Yaracuy basin suggest a right-lateral offset along the Boconó-Moron fault system of 6 to 16 km (Schubert, 1984). According to the relationship derived by Aydin and Nur (1982), that the length of a pull-apart basin is approximately equal to the strike-slip offset necessary to produce it, the right-lateral offset along the Boconó-Moron fault system can be estimated as approximately 75 km, a result which is much closer to the estimate based on my model. In the application of models of pull-apart basin formation to estimations of strike-slip offset, it is important to note that basin depth and length are often difficult dimensions to measure (Aydin and Nur, 1982). In this case, basin length is equal to the dimension of the basin along the sides bounded by the faults. In addition, the tectonic environment of the Yaracuy basin is not a simple environment

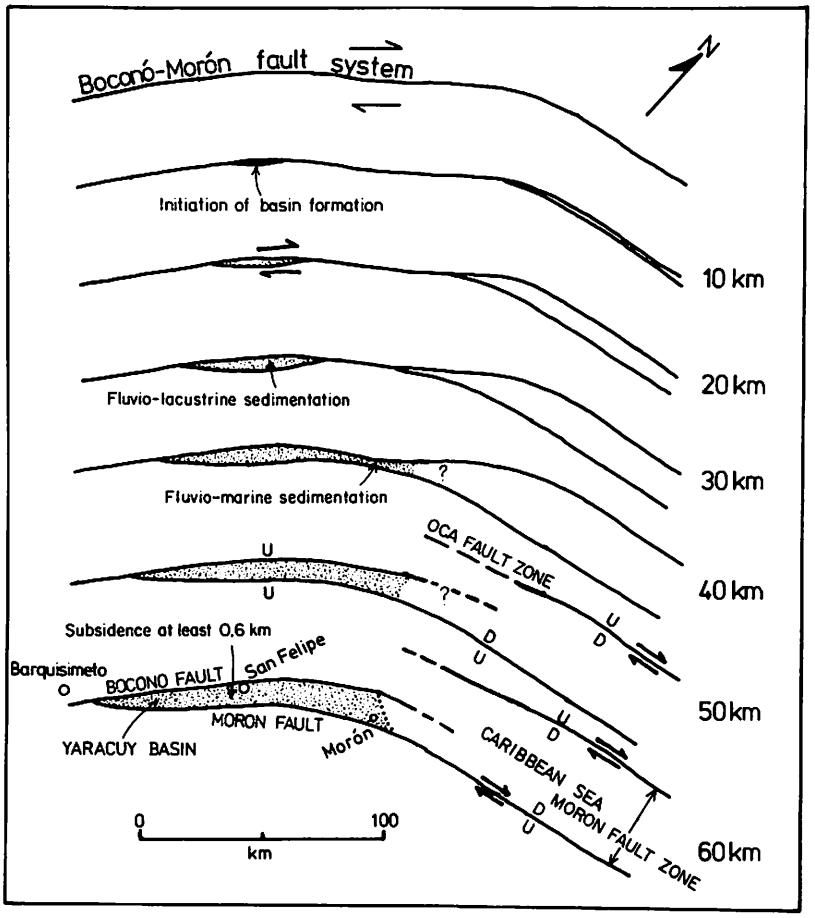

Figure 6. Schematic model of the formation of the Yaracuy basin. Beginning with a single trace of the Boconó-Morón fault system, the opening of the Yaracuy pull-apart basin is shown as right-lateral offset increased. When this offset was approximately 40 km, the basin opened to the Caribbean Sea. Present-day morphology and dimensions of the basin are achieved with an offset of 50 to 60 km.

of two en echelon faults, but is a complex environment, with a curved fault interacting with other faults (Oca, El Pilar). Previous to the events described here,the faults probably had different orientations and/or offsets, and may have belonged to different tectonic environments. The Yaracuy basin is open to the Caribbean Sea and, therefore, forms part of a complex continental and marine system.

The age of the Yaracuy basin cannot be established with certainty, due to lack of cores through its sedimentary fill. However, comparing this pull-apart basin with others along the Boconó-Morón-El Pilar fault system (Cariaco basin) and the La Victoria fault zone (Valencia basin; Schubert, 1980), suggests that it is a Late Tertiary (maximum)–Quaternary basin. The young geologic age of the strike-slip displacement along this fault system (late Tertiary) supports this conclusion.

I thank the Dirección de Cartografía Nacional (Caracas) for authorization to publish the side-looking radar image of Figure 3 (communication 4141-0316 of 17 October, 1983). Paul Mann, Kevin Biddle, and Nick Christie-Blick reviewed and significantly improved the manuscript; however, they do not necessarily agree with my conclusions.

References

Aggarwal, Y. (1983). Present-day boundary and the motion of the Caribbean plate relative to South America. *Programa y Resumenes, 10th Caribbean Geological Conference* (Cartagena), **16**.

Aydin, A., and Nur, A (1982). Evolution of pull-apart basins and their scale independence. *Tectonics* **1**, 91–105.

Bahat, D. (1983). New aspects of rhomb structures. *Journal of Structural Geology* **5**, 591–601.

Ballance, P. F., and Reading, A. G. (1980). Sedimentation in oblique-slip mobile zones. *Internatinal Association of Sedimentologists* Sp. Pub. **4**, 265 pp.

Beck, C. (1977). Geología de la faja piemontina y del frente de montaña en el noreste del Estado Guárico. *Mem. 5. Congreso Geológico Venezolano* **2**, 759–788.

Bellizzia, A. (1972). Sistema montañoso del Caribe, borde sur de la place del Caribe ¿Es una cordillera alóctona? *Trans. 6th Caribbean Geological Conference* (Caracas), 247–258.

Bellizzia, A., and Rodríguez, D. (1968). Consideraciones sobre la estratigrafía de los Estodos Lara, Yaracuy, Cojedes y Carabobo. *Boletin de Geologia* (Venezuela) **9** (18), 515–563.

Bellizzia, A., and Rodríguez, D. (1976). Geología del Estado Yaracuy. *Boletín de Geología* (Venezuela) Pub. Esp. **5**, **6**, 3317–3415.

Bucher, W. H. (1952). Geologic structure and orogenis history of Venezuela. *Geological Society of America* Memoir 49, 1–113.

Burchfield, B. C., and Stewart, J. H. (1966). "Pull-apart" origin of the central segment of Death Valley, California. *Geological Society of America Bull.* **76**, 439–442.

Cluff, L. S., and Hansen, W. R. (1969). Seismicity and seismic geology of northwestern Venezuela. Unpub. Report, *Compania Shell de Venezuela*, Caracas.

Dewey, J. W. (1972). Seismicity and tectonics of western Venezuela. *Bull. Seismological Society of America* **62**, 1711–1751.

Dirección de Geología (1970). Léxico estratigráfico de Venezuela (second edition). *Ministerio de Minas e Hidrocarburos*, Caracus, 756 pp.

Garner, H. F. (1959). Stratigraphic-sedimentary significance of contemporary climate and relief in four regions of the Andes mountains. *Geological Society of America Bull.* **70**, 1327–1368.

Kelleher, J., Sykes, L., and Oliver, J. (1973). Possible criteria for predicting earthquake locations and their application to major plate boundaries of the Pacific and the Caribbean. *Journal of Geophysical Reseach* **78**, 2547–2585.

Mann, P., Hempton, M. R., Bradley, D. C., and Burke, K. (1983). Development of pull-apart basins. *Journal of Geology* **91**, 529–554.

Molnar, P. and Sykes, L. R. (1969). Tectonics of Caribbean and Middle America regions from focal mechanisms and seismicity. *Geological Society of America Bull.* **80**, 1639–1684.

Pennington, W. D. (1981). Subduction of the eastern Panama basin and seismotectonics of northwestern South America. *Journal of Geophysical Research* **86**, 10753–10770.

Rod, E. (1956). Strike-slip faults of northern Venezuela. *American Association of Petroleum Geologists Bull.* **40**, 457–476.

Rod, E., Jefferson, C. von der Osten, E., Mullen, R., and Graves, G. (1958). Determination of the Boconó fault. *Asociación Venezolana de Geología, Minería y Petróleo Bol. Inform.* **1**, 69–100.

Rodgers, D. A. (1980). Analysis of pull-part basin development produced by en echelon strike-slip faults, in Ballance, P. F., and Reading, H. G., Eds., Sedimentation in oblique-slip mobile zones. *International Association of Sedimentologists* Sp. Pub. 4, 27–41.

Salgado-Labouriau, M. L. (1980). A pollen diagram of the Pleistocene-Holocene boundary of Lake Valencia, Venezuela. *Reviews in Palaeobotany and Palynology* **30**, 297–312.

Saunders, J., Edgar, N. T., and Donnelly, T. W. (1973). Cruise synthesis, in Edgar, N. T., and Saunders, J. B., Eds., *Initial Reports of the Deep Sea Drilling Project* **15**, 1077–1111.

Schubert, C. (1979). El Pilar fault zone, northeastern Venezuela: brief review. *Tectonophysics* **52**, 447–455.

Schubert, C. (1980). Contribution to the paleolimnology of Lake Valencia, Venezuela. *Catena* **7**, 275–298.

Schubert, C. (1981). Are the Venezuelan fault systems part of the southern Caribbean plate boundary? *Geologische Rundschau* **70**, 542–551.

Schubert, C. (1982a). Origin of Cariaco basin, southern Caribbean Sea. *Marine Geology* **42**, 345–360.

Schubert, C. (1982b). Neotectonics of Boconó fault, western Venezuela. *Tectonophysics* **85**, 205–220.

Schubert C. (1984). Basin formation along the Boconó-Morón-El Pilar fault system, Venezuela. *Journal of Geophysical Research* **89**, 5711–5718.

Schubert, C. (1985). Aluviones colgantes en la Cordillera de la Costa: indicio de aridez durante el Cuaternario Tardío. *Acta Científica Venezolana* **36**, 201–202.

Schubert, C., and Krause, F. F. (1984). Morón fault zone, north-central Venezuelan borderland: identification, definition, and neotectonic character. *Marine Geophysical Researchers* **6**, 257–273.

Schubert, C., and Valastro, S. (1980). Quaternary Esnujaque Formation, Venezuelan Andes: preliminary alluvial chronology in a tropical mountain range. *Zeitschrift der Deutschen Geologischen Gesellschaft* **131**, 927–947.

Shagam, R. (1975). The northern termination of the Andes, in Nairn, A. E. M., and Stehli, F. G., Eds., *The ocean basins and margins III, The Gulf of Mexico and the Caribbean.* New York: Plenum Press, 325–420.

Sievers, W. (1888). Die Cordillere von Mérida nebst Bemerkungen ueber das karibische Gebirge. *Geographische Abhandlungen (Penck)* **3**, 1–238.

Stephan, J. F., Beck, C., Bellizzia, A., and Blanchet, R. (1980). La chaîne caraïbe du Pacifique a l'Atlantique. *Memoirs Bureau de Recherche Géoloqique et Minière* No. **115**, 38–59.

Zambrano, A. (1976). Estudio fisiográfico regional de las cencas Yaracuy-Aroa, Estado Yaracuy. *Boletín de Geología* (Venezuela) Pub. Esp. 7, **2**, 849–878.

Determination of the Land Uplift from Old Water Marks and Tide Gauge Data at Ratan and Lövgrundet/Björn, Sweden

Lars E. Sjöberg

The University of Uppsala, Institute of Geophysics, Dept. of Geodesy, Hällby, S-755 90 Uppsala, Sweden, and National Land Survey, S-801 12 Gävle, Sweden

Old water marks (the oldest from 1731) are combined with more recent tide gauge data at Ratan and Lövgrundet/Björn in Sweden in an analysis of the land uplift. The study shows that the hypothesis of a significant change of the uplift rate at the beginning of this century cannot be verified. Furthermore, the tide gauge data does not support a decrease of the uplift rate.

1. INTRODUCTION

The relative changes of the water levels in Fennoscandia have been recognized and studied by geoscientists for the last three centuries. At the beginning, the phenomenon was generally thought of as sinking water level. For example, in 1719 Swedenborg suggested that the water level changes were global, as a consequence of retarding earth rotation. In 1743 A. Celsius published the first direct measurements and calculations of the water level changes. He found that Rike Nils' seal stone outside Gävle (mentioned already in a taxation letter in 1583) had elevated eight feet in 168 years (or approximatly 1.5 cm/yr). Celsius also ordered the first water mark in Sweden (at Lövgrundet, 1731) for later registration of the water level decreases. However, all hypotheses on the origin of the level changes were so far based on a non-dynamic earth.

The first ideas of something that may be characterized as an isostatic theory for the Fennoscandian phenomenon, ideas admitting elastic deformation of the earth's crust due to mass motion (or, for example, water masses), were published by E.O. Runeberg (1765, 1769), and much later by Playfair (1802). Although the hypotheses had changed from sinking water levels to land uplift, no one had so far come up with a convincing theory.

In 1882 T.F. Jamieson was the first to develop a theory of glacial depression and rebound of Fennoscandia. The glacial-isostatic model of the uplift process still prevails among geophysicists, but recently new

Neotectonics: An International Journal of Crustal Dynamics, Vol. 1, 51-59 (1986)
© 1986 John Wiley & Sons, Inc. CCC 0884-8157/86/010051-09$04.00

hypotheses on tectonic movements have been put forward (Mörner, 1977; 1979; 1981).

In this study, old water mark data at two locations in Sweden and more recent tide gauge (mareograph) data from stations nearby will be used to analyze the ongoing uplift process.

2. THE DATA SETS

The old water mark data to be used in this study are taken from the compilation by Bergsten (1954). They are given in Table I for the sites Ratan [latitude (φ) = 64°0′] and Lövgrundet (φ = 60°45′). As is shown, there are eight observations from 1749 to 1946 at Ratan and 16 observations from 1731 to 1946 at Lövgrundet. These data will be analyzed together with nearby tide gauge data at Ratan [φ = 63°59′, longitude (λ) = 20°54′] and Björn (φ = 60°38′, λ = 17°58′). See Figure 1. The initial year for the continuous mareograph recordings is in both cases 1892. The data are given in the form of yearly mean values of the water level at the stations up until 1981 at Ratan and until 1975 at Björn.

Table I. Old water level marks at Ratan and Lövgrundet (from a compilation by Bergsten, 1954).

Site	Year	Height of mark above MW in cm	Visitor
Ratan	1749	0	Chydenius
	1785	50.5	Schultén
	1795	74	Wallman
	1819	77	Hällström
	1822	74	Bruncroma
	1846	83	Unknown
	1869	126	Holmström
	1946	190	Bergsten
Lövgrundet	1731	0	Rudman
	1785	72	Schultén
	1796	64	Robsahm
	1811	72	Unknown
	1820	74	Bruncroma
	1831	74	Forsman
	1834	86	Lyell
	1839	93	Almlöf
	1847	101	Erdman
	1855	109	Unknown
	1866	107	Selkirk
	1869	105	Holmström
	1870	117	Arwidsson
	1922	136	Unknown
	1931	140	Unknown
	1946	162	Lindström

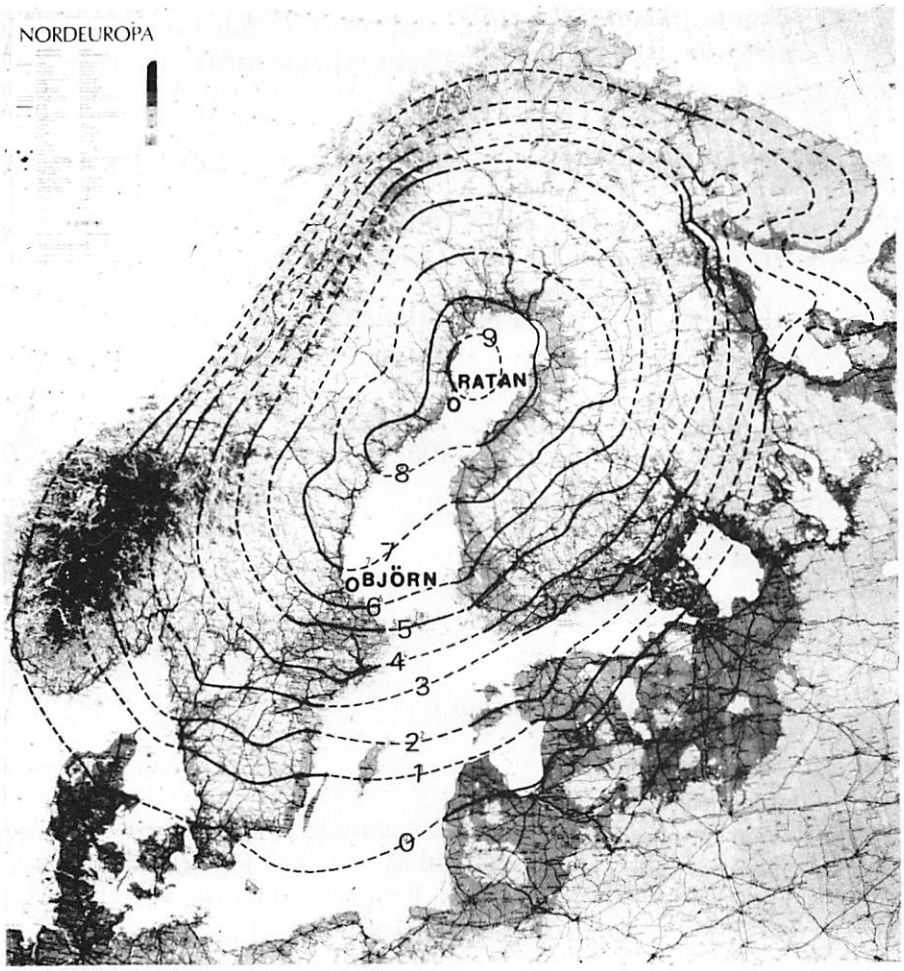

Figure 1. Observed land uplift if Fennoscandia (mm/year). Compilation by Ekman (1984).

3. LINEAR REGRESSION MODELS

According to the analyses by Mörner (1977, 1979), the exponential glacial readjustment of the crust died out some 2000–3000 years BP, and the origin of the present uplift is still unknown. Furthermore, "because the data from old water marks along the coast of Norrland seem to agree with the geological data, there may have been a change of the reference level along the Norrland coast at about 1900 AD" (Mörner, 1981). Mörner (1981) proposes that apparent shifts in the rate of rotation of the earth, changes in the geomagnetic field, and a change in seismic energy release at about 1900–1910 are related to a change in the rate of the Fennoscandian uplift. This hypothesis will not be tested by the data given in the previous section.

We assume that the land uplift at a site is constant, but changes between the years 1905–1906. (The year is not critical.) Then we get the observation equations

$$x_1 + x_3 (t_i - t_{1905}) = \ell_i - \epsilon_i \text{ for tide gauge data before 1906}$$

$$x_2 + x_3 (t_i - t_{1905}) = \ell_i - \epsilon_i \text{ for water mark data before 1906}$$

$$x_1 + x_4 (t_i - t_{1905}) = \ell_i - \epsilon_i \text{ for tide gauge data after 1905}$$

$$x_2 + x_4 (t_i - t_{1905}) = \ell_i - \epsilon_i \text{ for water mark data after 1905}$$

where

x_1 = tide gauge water level at 1905

x_2 = old water mark level at 1905

x_3 = uplift rate prior to 1906

x_4 = uplift rate after 1905

l_i = water level observation

ϵ_i = random error of observation l_i

t_i = year l_i observed

The random observation errors were assumed to be uncorrelated with the *a priori* variances $s_1^2 = 1$ cm^2 and $s_2^2 = 8$ cm^2 for mareograph data and old water mark data respectively. From the above observation equations (now written in matrix notations; n = no. of observations):

$$\underset{(n,4)}{A}\ \underset{(4,1)}{X} = \underset{(n,1)}{L} - \underset{(n,1)}{\epsilon} \quad ; \quad E\{\epsilon\epsilon^T\} = Q \tag{1}$$

where the covariance matrix Q was estimated by

$$\hat{Q} = s_1^2 \begin{pmatrix} I_1 & \\ & 0 \end{pmatrix} + s_2^2 \begin{pmatrix} 0 & \\ & I_2 \end{pmatrix}, \tag{2}$$

I_1 and I_2 being unit matrices of dimensions equal to the number of tide gauge data and old water mark data, respectively. Normal equations were formed and solved for $\hat{X}$ ($P = \hat{Q}^{-1}$)

$$A^T P A \hat{X} = A^T P L \rightarrow \hat{X} = (A^T P A)^{-1} A^T P L \tag{3}$$

and finally the residuals

$$\hat{\epsilon} = L - A\hat{X} \tag{4}$$

were determined. As the weight relation between mareograph data and old water mark data might play an essential role in the result of the test we decided to improve the weight relation by determining new variance components s_1^2 and s_2^2 from the residual by (see Förstner, 1979; and Sjöberg, 1983):

$$s_i^2 = \hat{\epsilon}_i^T \hat{\epsilon}_i / \{n_i - \mathrm{tr}(A_i^0)\}, \; i = 1,2 \tag{5}$$

where

$\hat{\epsilon}_1$ = residuals of the n_1 tide gauge data

$\hat{\epsilon}_2$ = residuals of the n_2 old water mark data

A_1^0 and A_2^0 are the symmetric $(n_1 \times n_1)-$ and $(n_2 \times n_2)-$ matrices given by

$$A^0 = \begin{bmatrix} A_1^0 & A_{12}^0 \\ (A_{12}^0)^T & A_2^0 \end{bmatrix}$$

$$A^0 = A(A^T P A)^{-1} A^T P$$

The procedure (1)–(5) was then iterated until the ratio of any of the estimated variance components in two successive steps was within 1%. In all computations this limit was reached within two iterations. The result of the computations is given in Table II.

The maximum measuring residual $|\hat{\epsilon}_i / S_i|$ was 2.34 for Ratan and 2.58 for Lövgrundet/Björn. These values are far less than the critical value $\tau_{5\%} \approx 3.38$ for possible outliers within the data (see Pope, 1975; and Lund, 1975). Thus there is no reason to believe that the data are contaminated by gross errors. Table II clearly shows that there is no significant difference between the rates of uplift prior to and after 1905/1906. Thus from this analysis there is no reason to believe that the uplift rate changed about 1900–1910.

4. SECOND ORDER ADJUSTMENT MODEL

If the present land uplift is caused by a glacial readjustment there should be an opportunity to study it in the old water mark and tide gauge data. A simple study of this type was carried out by Bergsten (1954), but the analysis was neither based on the least squares method, nor was it completed with any tests of significance of estimated parameters.

First we will use the following model to analyse old water mark data only:

$$x_1 + x_2 \, \delta t_i + x_3 \, \delta t_i^2 = \ell_i - \epsilon \; ; \quad i = 1,2, \ldots, n_2 \tag{6}$$

Table II. Result of least squares adjustment.

Site	<n>	x_1: tide gauge level at 1905 (cm)	x_2: old water mark level at 1905 (cm)	x_3: uplift rate prior to 1906 (cm/y)	x_4: uplift rate after 1905 (cm/y)	x_3-x_4 (mm/y)	cm s_1	s_2
Ratan	98	378.61 ± 1.10	153.33 ± 8.50	0.90 ± 0.09	0.85 ± 0.03	0.5±1.0	6.1	12.3
Lövgrundet/ Björn	100	378.83 ± 1.02	133.36 ± 3.83	0.67 ± 0.05	0.61 ± 0.03	0.6±0.6	5.6	9.0

$n = n_1 + n_2$ = no. of observations. s_1 = standard deviation of mareograph data. s_2 = standard deviation of old water mark data.

where

$$\delta t_i = t_i - t_{1900}$$

and

$$E\{\epsilon_1^2\} = S_2^2$$

The result of these computations is given in Table III.

Obviously the decrease of the land uplift is significant at Lövgrundet but not at Ratan. The reason for this negative result at Ratan could be that there are too few and not very reliable observations (cf. s_2 of Table II). A more conclusive answer to whether the present uplift rate is attenuating or not should be obtained by combining the old water mark data and the tide gauge data at each site. For the mareograph data we therefore add the observation equations

$$x_0 + x_2\,\delta t_i + x_3\,\delta t_i^2 = \ell_i - \epsilon_i \;;\quad i = 1,2,\ldots,n_1 \tag{7}$$

with

$$E\{\epsilon_i^2\} = s_1^2$$

to those provided by (6). Again the variance components s_1^2 and s_2^2 were determined iteratively (cf. the previous section). The result of the computations are given in Table IV.

Again, the result is that the uplift attenuation at Ratan is not significant. At Lövgrundet/Björn the ratio (x_3/s_{x3}) has decreased from 5 to 1.67, but x_3 is still significant at the 5% risk level, because $t_{0.95}(96) = 1.661$. Apparently there is no support for the land uplift model (6) + (7) in the mareograph data. The standard deviation (s_1) for these data does not differ between this model and the linear model of section 3, while the standard deviation for old water mark data (s_2) decreases when passing from the linear to the second order model.

5. CONCLUSIONS

Our analyses of old water mark data and the tide gauge data at two locations in Sweden have revealed:

(a) that there is no significant change of the uplift rate before or after the beginning of this century, and

(b) that the tide gauge data does not support the hypothesis of a decreasing uplift rate.

Table III. Result of least squares adjustment by formula (6) for old water mark data. n_2 = no. of observations.

Site	n_2	x_1 (cm)	x_2 (mm/y)	x_3 (mm/y^2)
Ratan	8	148.80 ± 1.80	8.67 ± 0.35	−0.003 ± 0.003
Lövgrundet	16	129.38 ± 1.07	5.49 ± 0.25	−0.010 ± 0.002

Although the combination of the two data sets shows a significant decreasing uplift rate at one location (Lövgrundet/Björn), future tide gauge data are needed to settle the question of whether or not the uplift is retarding. In this context, a reduction for the variation of mean sea level is needed. Unless this effect is taken into account, an apparent decrease of land uplift may very well be due to an increasing mean sea level caused by melting polar ice caps and thermal expansion of ocean masses.

Table IV. Result of least squares adjustment with formulas (6) and (7).

Site	x_0 (cm)	x_1 (cm)	x_2(mm/y)	x_3 (mm/y^2)	s_1 (cm)	s_2 (cm)
Ratan	374.04 ± 1.07	147.99 ± 6.72	8.69 ± 0.33	−0.0023 − 0.0040	6.1	12.2
Lövgrundet/	375.63 ± 0.98	130.27 ± 2.87	6.32 ± 0.22	−0.0040 − 0.0024	5.6	8.5

Most of this study was carried out during the author's visit at the Stuttgart University, Department of Geodesy, as a fellow of the Alexander von Humbold Stiftung. The stimulating discussions with the host, Professor E.W. Grafarend and Mr M. Ekman, are cordially acknowledged. The work was also supported by grants from the Swedish Natural Science Research Council (NFR) under Project No. G-GU 4071-101.

References

Bergsten, F. (1954). The land uplift in Sweden from the evidence of the old water marks. *Geografiska Annaler*, Häfte **1-2**, 81−111.

Celsius, A. (1743). Anmärkningar om vatnets förminskande så i Östersjön som Vesterhafvet. Kungl. Vet. Akad. Handlingar.

Ekman, M. (1984). Gaussian and mean curvatures of earth tides and postglacial land uplift, and their effects on earthquakes. The University of Uppsala, Uppsala (Dissertation).

Förstner, W. (1979). Konvergenzbeschleunigung bei der a posteriori Varianzschätzung. *ZfV, 104* 4, 149−156.

Jamieson, T. F. (1882). On the oscillation of land in Glacial period. *Geol. Magazine*, London.

Lund, R. E. (1975). Tables for an approximate test for outliers in linear models. *Technometrics* **17**, 473−476.

Mörner, N. -A. (1977). Past and present uplift in Sweden; glacial isostacy, tectonism and bedrock influence. *Geol. Fören. i Stockholm Förhandl.* **99** 48−54.

Mörner, N. -A. (1979). Earth movements in Sweden 20,000 BP to 20,000 AP. *Geol. Fören. i Stockholm Förhandl.* **100**, 279−286.

Mörner, N. -A. (1981). Crustal movements and geodynamics in Fennoscandia. *Tectonophysics* **71**, 241−251.

Playfair, J. (1802). Illustrations to the Huttonian theory of the earth. Edinburgh.

Pope, A. J. (1975). The statistics of residuals and the detection of outliers. Report to the IUGG XVI General Assembly, Grenoble.

Runeberg, E. O. (1765). Om några förändringar på jordytan i allmänhet och under de kalla climat i synnerhet. Kungl. Vet. Akad. Handlingar.

Runeberg, E. O. (1769). Forklaring på några omständigheter rörande frågan om vattuminskningen. Kungl. Vet. Akad. Handlingar.

Sjöberg, L. E. (1983). Non-negative variance component estimation in linear adjustment models. Submitted to *Manuscripta Geodaetica*.

Secular Crustal Strain in Eastern Taiwan and its Neotectonic Implication

Hiroshi Sato and Masahiro Kosuga
Faculty of Science, Hirosaki University, Japan
Hwa Chu Sheu
Ta-Han Junior College of Engineering and Business, Taiwan

Secular horizontal strain of the crust in eastern Taiwan is investigated based on retriangulation data. The strain along the Longitudinal Valley, a probable plate boundary of the Philippine Sea and the Eurasian plate, is compressive, with a large rate of 2 to 3 microstrains per year, and the maximum compression axis intersects the valley with an angle of about 60°. This suggests that the valley is not a place of pure collision, and that the relative movement of the plates has a left-lateral component there. The strain pattern in northeastern Taiwan shows a marked contrast to that along the valley. The predominant strain is extensional in a direction parallel to the plate boundary extending from the coast of Taiwan to the end of the Ryukyu arc.

Le champ d'effort de la terre dans l'est du Taiwan est obtenu par les données de la re-triangulation. L'effort le long de la Vallée Longitudinal, l'endroit de la borne du plates de la Phillipine Sea et d'Eurasia, est compresseur avec la vitesse de 2 à 3 micro-effort par l'an et l'axe compresseur entrecoupe la vallée avec l'angle environ 60°. Le fait montre que la vallée n'est pas l'endoit de la collision simple des plates. Le long de la vallée, Il'y a un composant du mouvement relatif des plates, lateral à gauche. Le champ d'effort dans le nord-est du Taiwan mettre en contraste avec celui du long de la vallée. L'effort prédominant celui-ci est prolongement dans la direction parallere à la borne des plates de la côte du Taiwan au bout d'arc de Ryukyu.

INTRODUCTION

Taiwan is a part of the Ryukyu-Taiwan-Luzon-Philippine island arc system (Fig. 1). The region from the junction between the Ryukyu arc and Taiwan to the northern part of the Luzon trench is the most complex part of the Philippine Sea-Eurasian plate boundary (Seno and Kurita, 1978). The Ryukyu trench changes its trend and disappears in the vicinity of Taiwan. To the south of Taiwan, it appears that the Luzon trench is west-facing. Hence, Taiwan occupies a gap in a long subduction boundary (Wu, 1978), and the eastern part of Taiwan is believed to be a collision boundary between the Philippine Sea and the Eurasian plates.

Neotectonics: An International Journal of Crustal Dynamics, Vol. 1, 61–74 (1986)
© 1986 John Wiley & Sons, Inc. CCC 0884-8157/86/010061-14$04.00

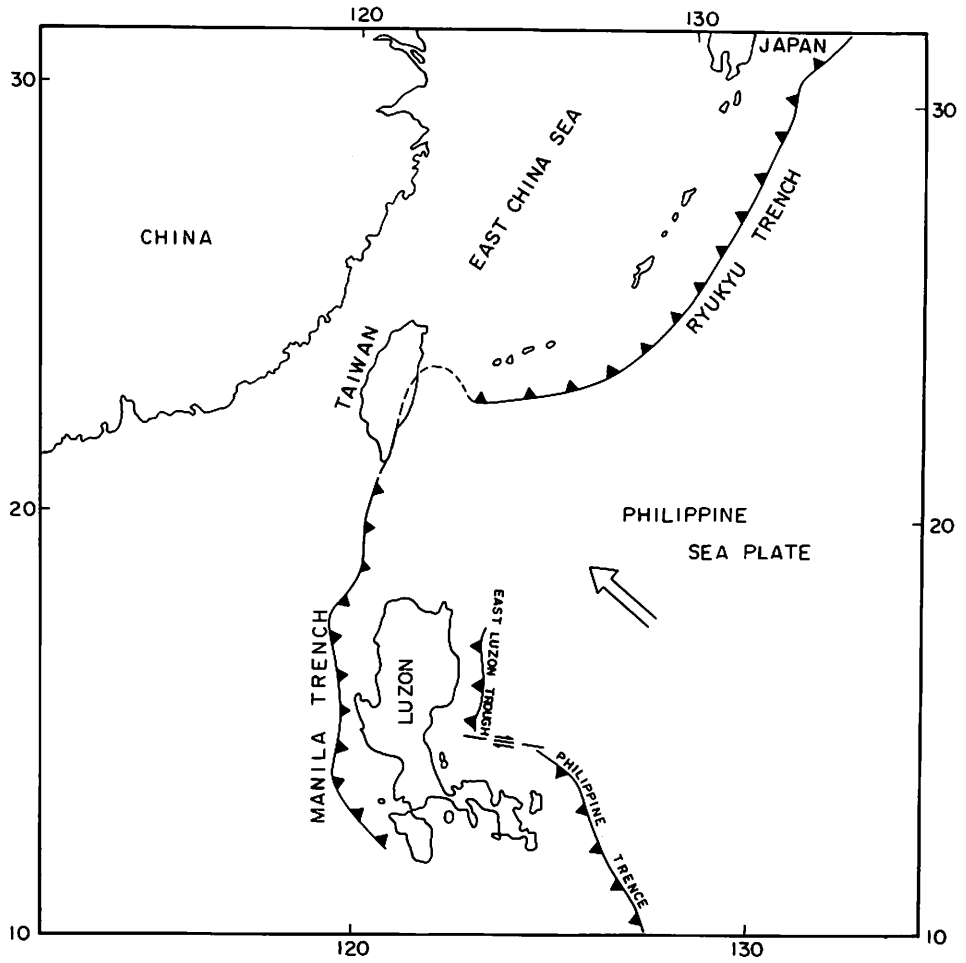

Figure 1. Location of Taiwan in the Ryukyu-Taiwan-Luzon-Philippine island arc chain. The white arrow indicates the direction of relative motion between the Philippine Sea and the Eurasian plates (after Seno, 1977).

The anomalous nature of the neotectonics of Taiwan and its vicinity has been noticed by many seismologists and geologists, and there are many works discussing the tectonics of Taiwan (e.g., Chai, 1972; Biq, 1971, 1972; Karig, 1973; Seno and Kurita, 1978; Wu, 1978; Lin and Tsai, 1981). Most of these works, however, treat seismicity patterns and focal mechanisms of earthquakes with respect to geomorphic features and geological structures. There are only a few papers which discuss the present state of crustal movement in the area, although it is important to understand the tectonics of such a complex area. In this paper, we present secular horizontal strain of the crust in the eastern part of Taiwan and interpret it in terms of tectonic structure of this region.

OUTLINE OF TECTONICS IN THE EASTERN PART OF TAIWAN

Taiwan represents a unique situation in the island arc chain from Ryukyu to the Philippines. As shown in Figure 1, Taiwan lies in a gap in the arc chain. Whereas the tectonics of the adjacent areas of Ryukyu and Luzon are interpreted in terms of subduction of the lithosphere, Taiwan is characterized by a collision of plates. The Longitudinal Valley of eastern Taiwan is believed to represent a part of the colliding boundary between the Philippine Sea plate and the Eurasian plate (e.g., Biq, 1974; Wu, 1978; Lin and Tsai, 1981).

The Longitudinal Valley (Fig. 2) from Taitung at its southern end to Hualien, is the most important structural line in Taiwan; it has a length of about 150 km and a width of 5 to 7 km (Fig. 3). From the bathymetry, the valley extends across the sea floor from Haulien to the north for a distance of tens of kilometers. The valley is bounded on its western and eastern sides by two high-angle reverse faults. On the eastern side of the valley, the Coastal Range trends parallel to it, and the lofty and massive Central Range is on the western side (Fig. 3). The stratigraphy of the Coastal Range is composed of Neogene and Miocene rocks; the Central Range is of Paleogene strata; the basement of both are metamorphics from Paleozoic to Mesozoic age (Hsu, 1976; Wu, 1978). With regard to crustal structure in this area, it is reported from seismic data that the main part of the island has a velocity structure very similar to that of

Figure 2. The Longitudinal Valley of eastern Taiwan, looking to the north from the site labeled "P" in Figure 3.

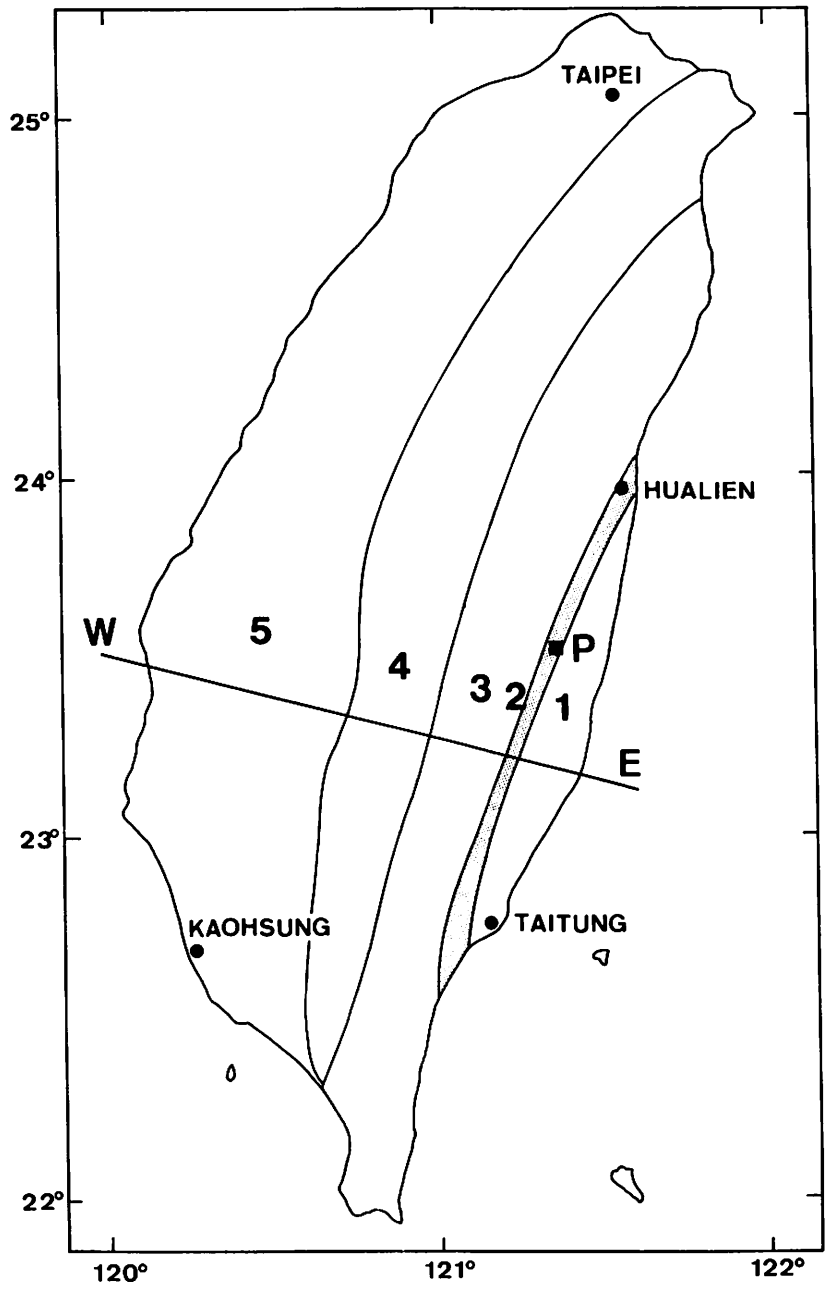

Figure 3. Physiographic provinces of Taiwan (after Wu, 1978). 1: Coastal Range; 2: Longitudinal Valley (shaded area); 3: E. Central range; 4: W. Central range; 5: foothills and coastal plain. The straight line labeled "E" and "W" indicates the position of the profile in Fig. 4. See the caption for Figure 2 for the square labeled "P."

continental crust, while the structure beneath the Coastal Range has characteristics of oceanic crust or of a transition layer (Wu, 1978). Figure 4 shows a terrain profile perpendicular to the valley in mid-Taiwan. Figure 5 shows a Bouguer gravity anomaly compiled from the report of Tomoda and Fujimoto (1982). A sharp positive gradient from the Coastal Range to the east, off the coast of Taiwan is remarkable, and this belt of high gradient stretches to the Ryukyu trench. In general, however, the main part of Taiwan island has a negative Bouguer anomaly.

All of the data presented here suggest that the Longitudinal Valley marks the boundary of the Philippine Sea plate and the Continental plate.

SECULAR HORIZONTAL STRAIN OF EASTERN TAIWAN

The first order triangulation net of Taiwan had been established during the period from 1917 to 1921, and retriangulation of the net was made from 1976 to 1979. We have been able to calculate the secular strain during the past several tens of years from the results of those triangulations. There is, however, a problem in the difference between the reference system of the new and the old triangulations. The old

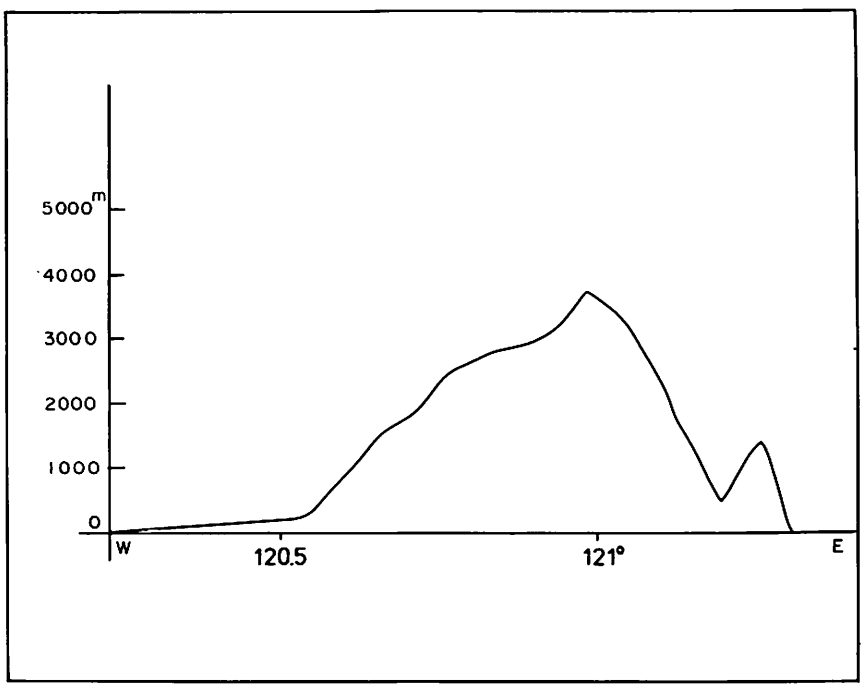

Figure 4. Topographic terrain profile in mid-Taiwan. Vertical exaggeration is 10 × horizontal scale.

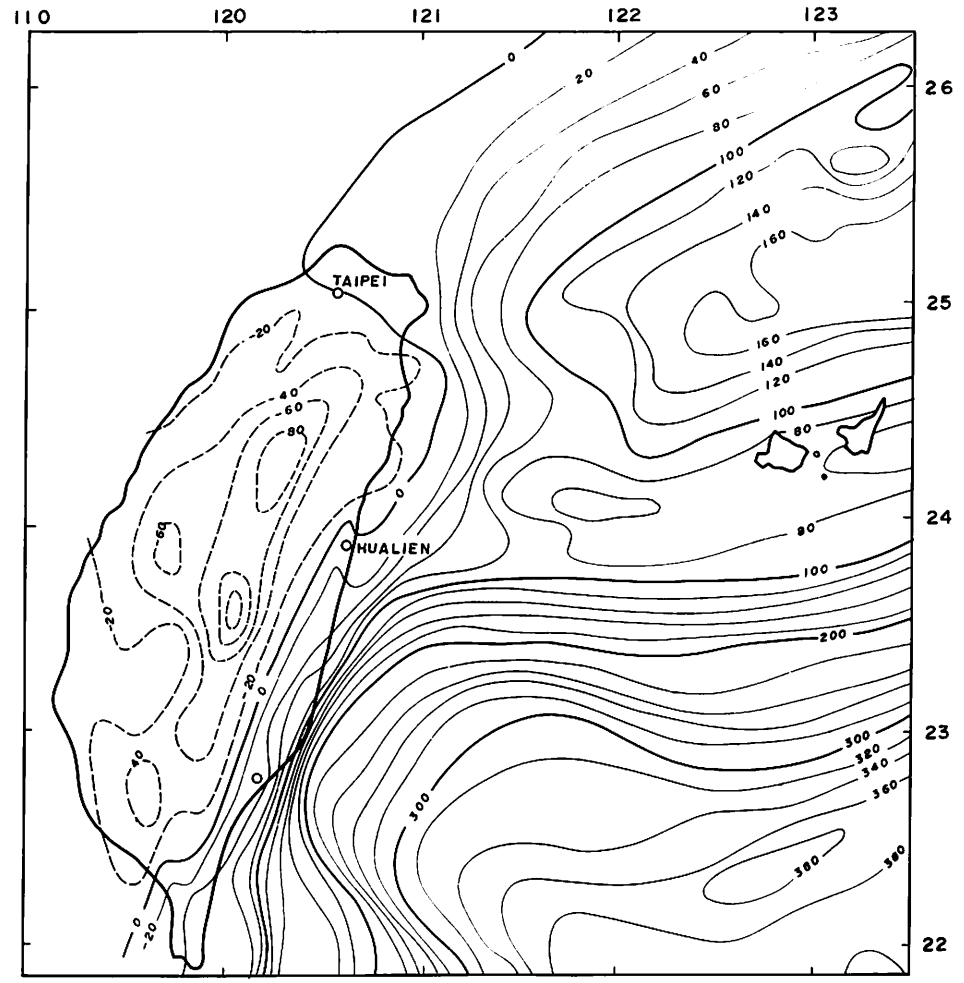

Figure 5. Bouguer gravity anomaly in the vicinity of Taiwan, compiled after Tomoda and Fujimoto (1982). Units are milligals.

triangulations in Taiwan were carried out by the Japanese Military Land Survey. At that time, coordinates of triangulation points were calculated using the Bessel ellipsoid as the reference ellipsoid. At the new survey made by the Chinese government, the reference ellipsoid was changed to the International ellipsoid, adopted by IAG in 1967. The difference in the scale of the reference ellipsoids results in a slight shift of the coordinates of the triangulation points. In order to avoid this effect, we calculated the side-length changes of triangles between the old and the new surveys by using the following differential formula of geodetic lines:

$$ds = -M_2 \cos \alpha_{21} d\varphi_2 - M_1 \cos \alpha_{12} d\varphi_1 - N_2 \cos \varphi_2 \sin \alpha_{21} (d\lambda_2 - d\lambda_1)$$

where $d\varphi$ and $d\lambda$ are the differences in latitude and longitude between the new and the old survey; M, N, and α are the radius of curvature of the meridian, that of the prime vertical, and the azimuth of the geodetic line; subscript 1 and 2 refer to the both ends of the side.

Linear strain E in the direction of azimuth α is obtained by dividing ds by the side-length s, and is expressed in terms of strain components E_x, E_y, and γ_{xy} as follows:

$$E = E_x\cos^2\alpha + \gamma_{xy}\cos\alpha\sin\alpha + E_y\sin^2\alpha$$

If we get the strain components from the linear strain of three sides of a triangle, the principal strain and its direction are deduced by the following formulas:

$$E_1 = \tfrac{1}{2}(E_x + E_y) + \tfrac{1}{2}\sqrt{(E_x - E_y)^2 + \gamma_{xy}^2}$$

$$E_2 = \tfrac{1}{2}(E_x + E_y) - \tfrac{1}{2}\sqrt{(E_x - E_y)^2 + \gamma_{xy}^2}$$

$$\tan 2\theta = \gamma_{xy}/(E_x - E_y)$$

where θ is the direction of the maximum strain measured counterclockwise from the X axis. Figure 6 represents the triangles used for strain calculation in the triangulation net of eastern Taiwan. Side lengths of these triangles are about 20 km on average, except those containing Lanhsu and Lutao islands. The obtained secular strain elements are given in Table I. The annual rate of principal strains are illustrated in Figure 7. During the period under investigation, there occurred two large earthquakes of M = 7.3 and M = 7.1, which might affect the strain field near the epicenters shown in Figure 6.

DISCUSSION AND CONCLUSION

The most remarkable feature of strain distribution in eastern Taiwan is that the pattern of strain in the area north of Hualien, at the northern end of the Longitudinal Valley, shows a striking contrast to that of the area along the valley. Whereas the strains of the triangles crossing the valley are compressive with the rate of 2 to 3 microstrains per year (except that of triangle 18 affected by the earthquake of 1951), those of the area north of Hualien are extensional with a comparatively small rate. The extensional strain field in this area is consistent with seismic data; focal mechanism solutions of earthquakes occurring in this area are normal fault type with a tension axis of nearly E–W direction (Wu, 1978). Along the valley, the direction of maximum compression trends about N40°W, intersecting the valley at a 60° angle. If the displacement of the Coastal Range is perpendicular to the valley, the

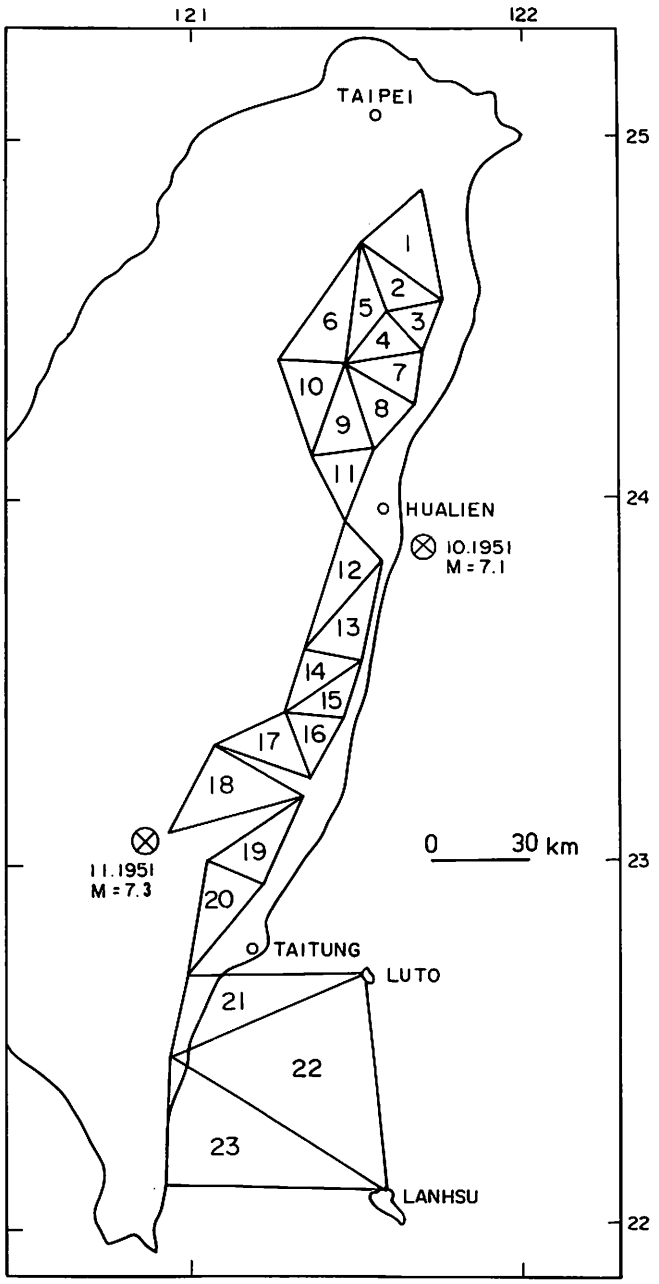

Figure 6. First order triangulation net of eastern Taiwan used in the present calculation of strain. Numbers of triangles correspond to those in Table I. Circles with crosses indicate the locations of large earthquakes that occurred in this area during the period from 1920 to 1980.

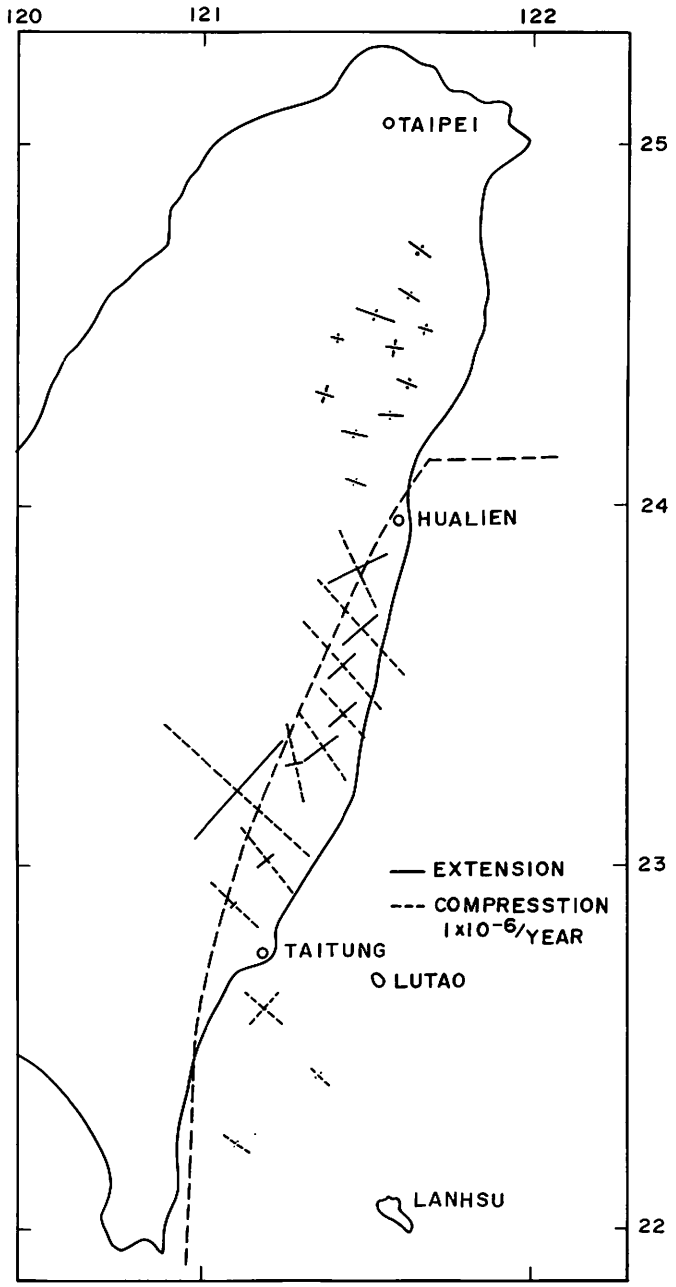

Figure 7. Annual rate of horizontal strain in eastern Taiwan. The length of bars in the legend corresponds to a strain rate of 1 microstrain per year. Dashed line shows estimated plate boundary between the Philippine Sea and the Eurasian plates.

Table I. Secular horizontal strain in eastern Taiwan during the period from 1917 to 1921, and from 1976 to 1979.

Triangle	E_1	E_2	Direction of E_2
1	47.304	− 19.899	N 37.6° E
2	45.528	− 11.026	N 30.9° E
3	27.347	− 16.710	N 10.8° E
4	35.070	− 27.564	N 9.1° E
5	75.210	− 21.597	N 20.6° E
6	26.310	− 19.020	N 8.0° W
7	43.497	− 25.464	N 18.9° E
8	51.909	− 0.175	N 4.0° E
9	47.340	− 7.140	N 11.3° E
10	33.570	− 30.030	N 17.0° E
11	50.670	− 5.219	N 16.2° E
12	125.832	−151.512	N 26.4° W
13	83.910	−222.522	N 42.4° W
14	74.814	−213.588	N 42.6° W
15	71.748	−114.732	N 39.6° W
16	78.984	−149.940	N 36.5° W
17	30.063	−148.490	N 12.7° W
18	232.848	−349.878	N 47.9° W
19	40.524	−148.422	N 38.7° W
20	10.872	−123.918	N 47.4° W
21	− 75.132	− 90.444	N 48.6° W
22	− 15.162	− 59.850	N 48.2° W
23	− 10.452	− 58.836	N 55.6° W

Unit: 10^{-6}.

principal axis must be perpendicular to the valley. When it is parallel to the valley, the axis intersects the valley at a 45° angle. In general, the direction of relative movement of plates and axis of principal strain have the following relation (Shimazaki and Nakamura, 1981):

$$(1 + \delta)\tan \varphi = 1/\tan 2\theta$$

where φ and θ are the angles of displacement and strain axis measured counterclockwise from the plate boundary, and δ denotes Poisson's ratio. In our case, since θ is 60°, we have $\varphi = 65°$, assuming $\delta = 0.25$. This means that the relative movement of the Coastal Range with respect to the plate boundary has a left-lateral component (Fig. 8). The rate of left-lateral displacement is estimated to be 2.5 cm per year, assuming a strain rate of 3 microstrains per year and an average side length of 20 km. Therefore, the Longitudinal Valley is not a site of pure collision, for it has a component of transform faulting. Hsu (1976) argued in favor of neotectonic movements in this region by suggesting left-lateral movement of the Coastal Range Fault that bounds the eastern side of the valley. The present result supports his conclusion.

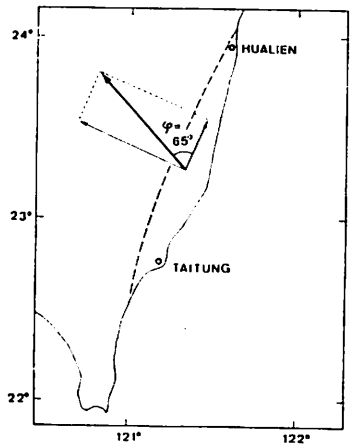

Figure 8. Direction of horizontal displacement (thick arrow) of the Coastal Range relative to the Longitudinal Valley (dashed line). φ denotes the angle between the displacement vector and the valley.

Figure 9 represents distributions of earthquakes in and around Taiwan based on data of the Institute of Earth Sciences in Taipei. It is clear that deeper earthquakes take place under northeastern Taiwan and offshore than under the remainder of the island. The isodepth contours of deep focus earthquakes have an east–west trend. Considering these facts, left-lateral movement of the Coastal Range together with neighboring sea floor, possibly results in subduction of the Philippine Sea plate off the coast of northeastern Taiwan, forming a north dipping Benioff zone from the end of the Ryukyu arc to the coast of Taiwan. The Benioff zone dips 45° and reaches to a depth of 130 km (Tsai et al., 1977). If we assume the lithosphere is 50 km thick and a northward convergence rate of 2.5 cm per year, the age of the initiation of the subduction is estimated at about 4 m.y.a., Pliocene in age.

The east–west trending extensional strain pattern in northeastern Taiwan should relate to relative plate motion along the plate boundary that extends from the coast of northeastern Taiwan to the end of the Ryukyu arc. From the kinematics of the Philippine Sea plate, a right-lateral movement is expected along this boundary. It is quite probable that this right-lateral movement produces a strain field whose extensional axis is parallel to the plate boundary in the study area. Figure 10 shows bathymetry in the vicinity of Taiwan, in which a sharp east–west trending scarp of the sea floor is remarkable. The direction of the extension axis in northeastern Taiwan is roughly coincident to that of the scarp. This scarp may represent the plate boundary in this area. Actually, evidence of right-lateral movement was found in the shallow sediments along the scarp (Wegeman et al., 1970). This fact supports our views on the strain pattern in northeastern Taiwan, although further study is needed to confirm this.

The strain rate deduced from the triangles crossing the Longitudinal Valley is strikingly large as compared with those of other orogenic zones, such as Japan. The strain rate obtained from geodetic data in

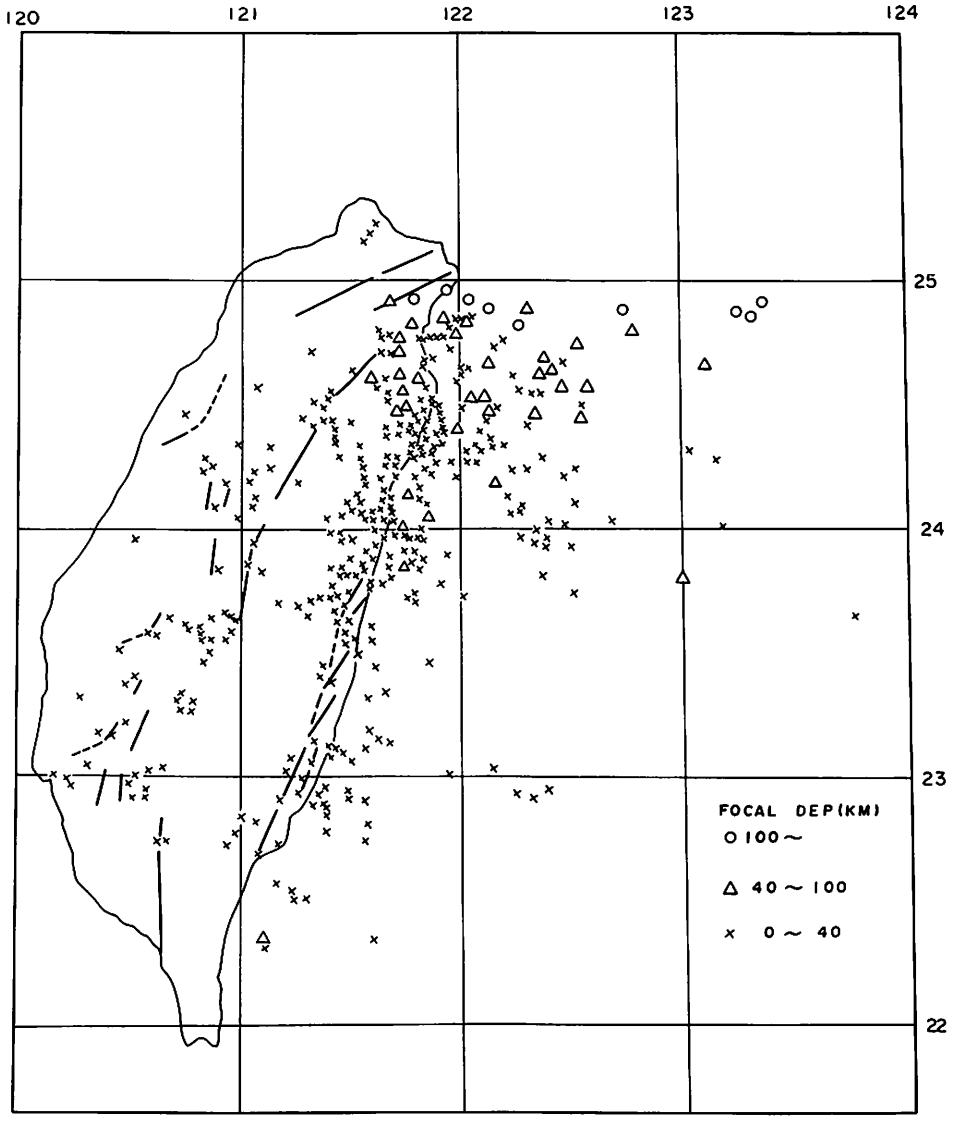

Figure 9. Distributions of small and micro earthquakes in and around Taiwan during the period from July to September, 1975, based on the data of the Institute of Earth Sciences, Taipei.

Japan is on the order of 0.2 to 0.3 microstrain per year (Sato, 1974). This is one order of magnitude smaller than we have calculated along the valley. Seno (1977) determined the rotation vectors for the Philippine Sea plate relative to adjacent major plates. His model gives a convergence rate of 8 cm per year at the plate boundary near Taiwan. A simple calculation shows that nearly two-thirds of this convergence rate is consumed in the narrow zone about 20 km wide along the Longitudinal Valley, which causes active orogenic movement in the eastern part of Taiwan.

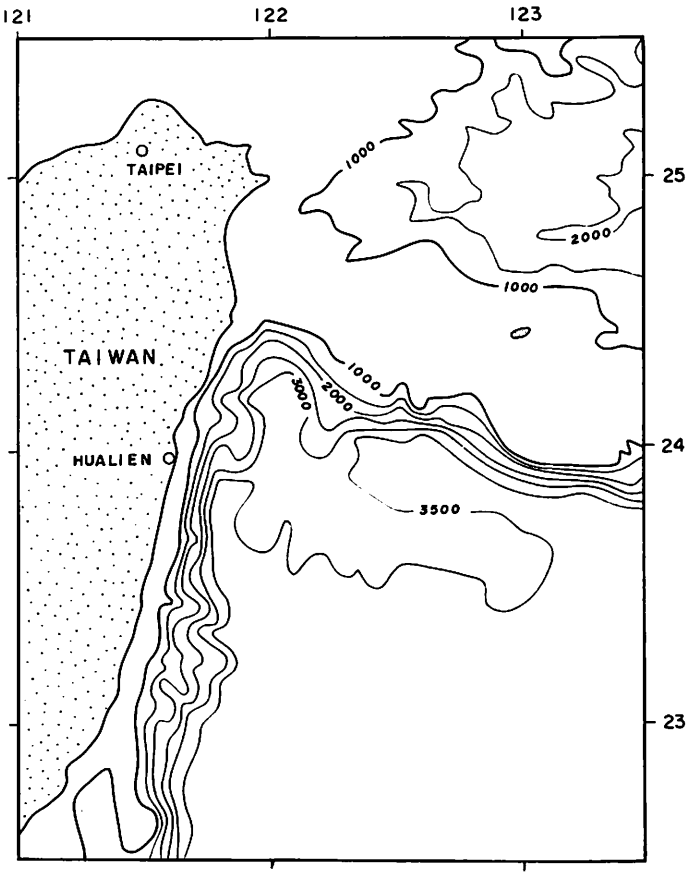

Figure 10. Bathymetric features in the vicinity of Taiwan, based on the map of the Hydrographic Department of Japan.

Horizontal movements of the Coastal Range were discussed by Chen (1974). However, the results were obtained from the retriangulation of a local third order net near Hualien. It seems that his results contain (1) coseismic movement due to the earthquake of 1951 near Hualien, and (2) apparent shifts of triangulation points resulting from the change in the reference system. The present study has clarified the secular strain during the past several tens of years in eastern Taiwan. This may give a clue to understanding the interesting and complex features of neotectonics in Taiwan and its vicinity.

The authors wish to thank Prof. A. Takagi for his encouragement throughout this study. Comments of Dr. T. Seno on the tectonics of Taiwan were helpful.

References

Biq, C. C. (1971). Some aspects of post-orogenic block tectonics in Taiwan, Recent Crustal Movements. *R. Soc. N. Z. Bull.* **9**, 19–24.

Biq, C. C. (1972). Transcurrent buckling, transform faulting and transpression: Their relevance in eastern Taiwan kinematics. *Petrol. Geol. Taiwan* **10**, 1–10.

Biq, C. C. (1974). Metallogeny in Taiwan; a plate-tectonic approach. *Bull. Geol. Surv. Taiwan* **24**, 139–156.

Chai, B. H. T. (1972). Structure and tectonic evolution of Taiwan. *Am. J. Sci.* **272**, 389–422.

Chen, C. Y. (1974). Verification of the north-northeastward movement of the Coastal Range, eastern Taiwan, by retriangulation. *Bull. Geol. Surv. Taiwan* **24**, 119–124.

Hsu, T. L. (1976). Neotectonics of the Longitudinal Valley, eastern Taiwan. *Bull. Geol. Surv. Taiwan* **25**, 53–63.

Karig, D. E. (1973). Plate convergence between the Philippines and the Ryukyu Islands. *Marine Geology* **14**, 153–168.

Lin, M. T., and Tsai, Y. B. (1981). Seismotectonics in Taiwan-Luzon area. *Bull. Inst. Earth Sci. Academia Sinica* **1**, 51–82.

Sato, H. (1974). A study of horizontal movement of the earth crust associated with destructive earthquakes in Japan. *Bull. Geogr. Surv. Inst. Japan* **19**, 89–130.

Seno, T. (1977). The instantaneous rotation vector of the Philippine Sea plate relative to the Eurasian plate. *Tectonophysics* **42**, 209–226.

Seno, T., and Kurita, K. (1978). Focal mechanisms and tectonics in the Taiwan-Philippine region. *J. Phys. Earth* **26** (Suppl.), S249–S263.

Shimazaki, K., and Nakamura, K. (1981). Quantitative relation between orientation of plate convergence and principal strain axis in the overriding plate. *J. Geod. Soc. Japan* **27**, 329–332.

Tomoda, Y., and Fujimoto, H. (1982). Maps of gravity anomalies and bottom topography in the western Pacific. *Bull. Ocean Res. Inst. Univ. Tokyo* **14**, 1–158.

Tsai, Y. B., Teng, T. L., Chiu, J. M., and Liu, H. L. (1977). Tectonic implications of the seismicity in the Taiwan region. *Mem. Gol. Soc. China* **2**, 13–41.

Wegeman, J. M., Hilde, T. W. C., and Emery, K. O. (1970). Structural framework of the East China Sea and Yellow Sea. *Am. Assoc. Petrol. Geol. Bull.* **54**, 1641–1643.

Wu, F. T. (1978). Recent tectonics of Taiwan. *J. Phys. Earth* **26** (Suppl.), S265–S299.

Possible Differential Uplift of New River Terraces in Southwestern Virginia

Hugh H. Mills

Department of Earth Sciences, Tennessee Technological University, Cookeville, Tennessee 38505

High terraces along streams in the Valley and Ridge province commonly rest on carbonate bedrock, solution of which obliterates their original form. Although correlation of individual terraces under such circumstances is not possible, the preferred elevations of terraces in a given area can be determined statistically. A 100-m grid is superimposed over maps of alluvium-covered areas and the elevation of each grid point above modern river level (AMRL) then calculated. The frequency distribution of these point elevations is then inspected for modes that show preferred elevations. This procedure was applied to terraces in two quadrangles along the New River in southwestern Virginia. The Radford North quadrangle shows a bimodal frequency distribution, with alluvial deposits abundant at 0–12 m AMRL and 30–49 m, and sparse at 12–30 m. The point-elevation frequency distribution for the Pearisburg quadrangle is also bimodal, but the higher mode is centered at 67 m AMRL, 27 m above that of the Radford North quadrangle. The most reasonable explanation for this difference is differential uplift of the Pearisburg area relative to the Radford North area. Based on estimated maximum and minimum ages of the undated high terraces, the average differential uplift rate is between 30 and 200 mm/1000 yr. Such uplift is consistent with probable movements on faults associated with the Giles County seismic zone.

INTRODUCTION

Documenting the displacement or disturbance of surficial sediments, particularly alluvial sediments, plays an important role in neotectonic studies. In contrast to many other parts of the United States, however, little effort has been made to use alluvial deposits in the unglaciated Appalachians for this purpose. In large part, this neglect undoubtedly arises from the fact that stream terraces in this region are poorly suited for chronological study. Datable materials are present only in the lowest terraces. Most terraces are unpaired and discontinuous, making downstream correlation difficult. In the Valley and Ridge province this problem is exacerbated by the carbonate bedrock that commonly underlies the terraces. The karst topography developed by solution of this rock type obscures the treads and risers of higher terraces, replacing them with an irregular, hilly terrain veneered with alluvium and reworked alluvium. Although these difficulties obviously prohibit

Neotectonics: An International Journal of Crustal Dynamics, Vol. 1, 75–86 (1986)
© 1986 John Wiley & Sons, Inc. CCC 0884-8157/86/010075-12$04.00

the preciseness of terrace studies in other regions, I shall nevertheless attempt to show that, under certain circumstances, information useful to neotectonic studies can be obtained from high terraces in the Valley and Ridge province.

PHYSICAL SETTING

The present study concerns a 100-km reach of the New River between Claytor Lake dam in the Radford South U.S. Geological Survey 7½′ quadrangle and the West Virginia border in the Peterstown quadrangle, located mainly within the Valley and Ridge province of southwest Virginia (Fig. 1). Of primary importance are the New River deposits in the Radford North and Pearisburg quadrangles, and the brief review of bedrock geology below therefore concentrates on these quadrangles. Structurally, the study area can be divided into two areas north and south of the Pulaski fault, which runs southeast of and parallel to Brush Mountain (Fig. 1). South of this fault, geologic units are exposed in a complex of imbricate thrust sheets. Physiographically, this area corresponds to the Great Valley. In the Radford North quadrangle, terraces are underlain mainly by the Elbrook Formation (Middle and Upper Cambrian), consisting chiefly of dolomite with lesser amounts of limestone. Also present is the Knox Group (Upper Cambrian), mainly dolomitic in composition.

The study area north of the Pulaski fault consists largely of the Narrows fault block, bounded on the south by the northeastern-trending Saltville fault located just south of Buckeye-Spruce Run Mountain, and on the north by the northeast trending Narrows fault, running just north of the town of Narrows (Fig. 1). This fault block is characterized by a series of northeast-trending plunging anticlines and synclines composed of bedrock units ranging in age from Early Cambrian to Middle Devonian. Between Buckeye-Spruce Run Mountain and Pearisburg, the New River flows across a broad valley, elongate to the northeast and flanked on the northeast, northwest, and southwest by mountains attaining elevations of 1200 m or more. In the Pearisburg quadrangle, the upper Knox Group (Lower Ordovician), consisting of dolomite and limestone, and Middle Ordovician limestones comprise the bedrock beneath the New River terraces.

PROCEDURE

All deposits of the New River between Claytor Lake dam and the West Virginia border were mapped, utilizing soils maps compiled by U. S. Soil Conservation Service survey teams in Pulaski, Montgomery, and Giles counties (unpublished data). Information was transferred from aerial-photograph field sheets to 1:24,000-scale topographic maps. Soil

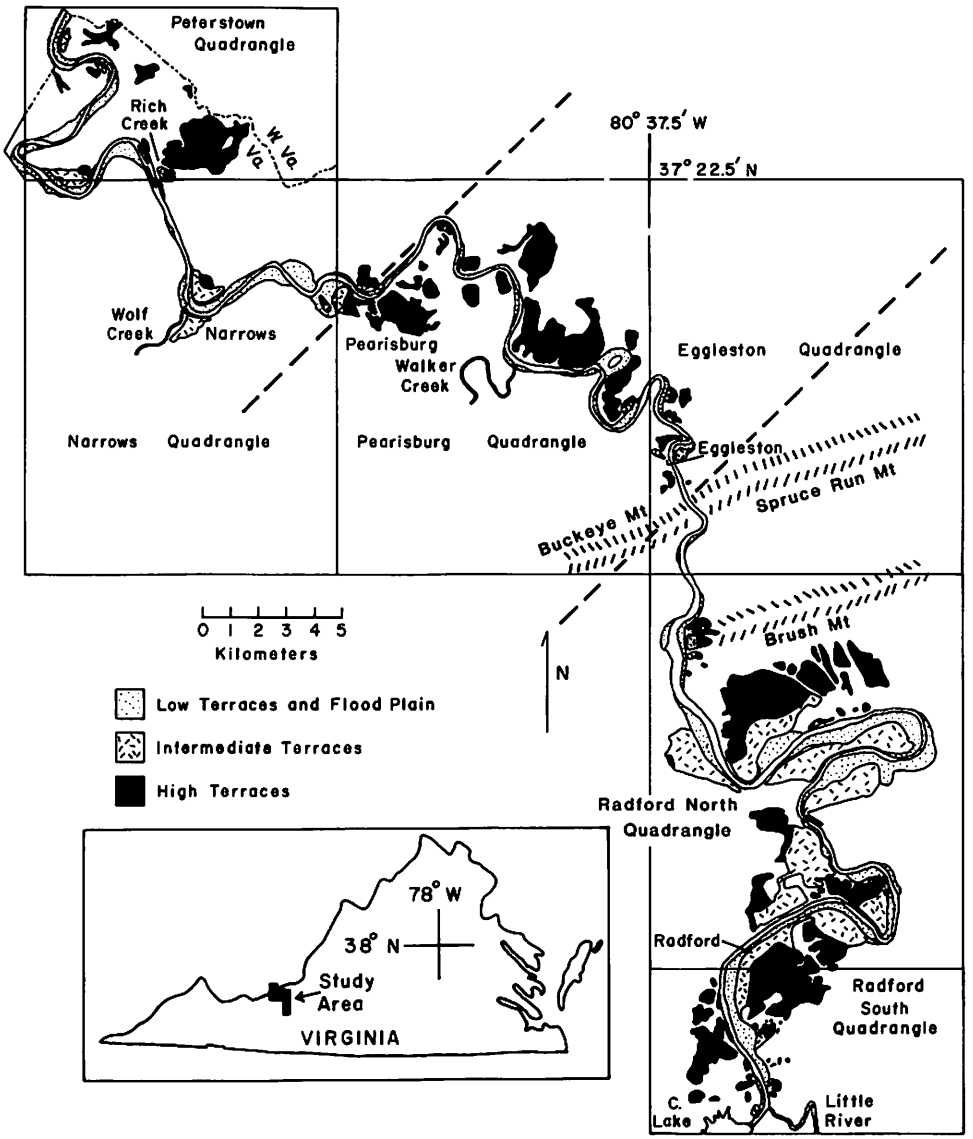

Figure 1. Overlay showing terraces of the New River between Claytor Lake dam and the West Virginia boundary. Low terraces are those less than 25 m above the modern river level, intermediate terraces are those 25–50 m above, and high terraces are those greater than 50 m above. Dashed lines show approximate boundaries of central part of Giles County seismic zone, as indicated by data from Munsey and Bollinger (1985, Fig. 7).

series defined as forming on New River alluvium could be transferred with confidence. Other series, however, were defined simply as forming on alluvial parent material, so that it was necessary to field check all such areas in order to determine whether the alluvium was that of the New River or not, (New River alluvium is readily identified by the presence of abundant vein-quartz and metaquartzite cobbles, which are

sparse in tributary streams north of Little River (Fig. 1). Still other series were defined as forming on either alluvium or colluvium, thus requiring similar field checking. About six weeks of field work was involved.

In order to determine whether low terraces of the New River (which have not yet been subjected to significant solution of their bedrock substrate) could be correlated over long distances, topographic profiles were surveyed across terrace sequences at 36 locations between Radford and the West Virginia border. Topographic profiles were of little use for the higher alluvial deposits, where the irregularity of surfaces makes the term "terrace" almost a misnomer. Observation showed, however, that such deposits are more plentiful at certain elevations above the modern river level (AMRL) than at other elevations. To determine accurately these preferred elevations, the following procedure was used. A 100-m grid was superimposed on 1:24,000-scale maps of all areas covered with New River alluvium, and the elevation of each grid point above the nearest reach of the New River determined to the nearest contour interval (20 ft or 6.1 m). Points falling on steep, obviously erosional slopes were not counted, and points falling on sinkholes were assigned the elevation of the sinkhole rim. The percentage of total terrace area for each 20-ft (6.1-m) interval was then calculated and the results plotted as a histogram. Separate analyses were made for both the Radford North and Pearisburg quadrangles.

An effort was also made to measure the weathering intensity of terrace sediments as a function of elevation AMRL, in order to determine whether the degree of weathering increases steadily with increasing elevation or whether there are discontinuities suggesting gaps in the ages of the deposits. To do this, at 35 will drain sites on flat or gently sloping terrace surfaces in the Radford North and Eggleston quadrangles, sediment samples were taken from the B2 horizon by means of an auger. Site elevations ranged from 1.1 m to 85.4 m AMRL, and properties measured included Munsell color, percent sand, silt, and clay in the less-than-2-mm fraction, and percent heavy minerals by weight. In addition, grain counts of both light and heavy minerals were made for each sample. The details of this weathering study are discussed elsewhere (Mills and Wagner, 1985).

RESULTS

The results of mapping are shown in Figure 1. Low terraces (including flood plains) are defined as those less than 25 m AMRL, intermediate terraces as those between 25 m and 50 m, and high terraces as those greater than 50 m. The break at 25 m appears to have an objective basis, as explained below, whereas that at 50 m is more arbitrary.

A plot of the 36 topographic profiles surveyed across low terrace

sequences produced the results intuitively expected. Not only is there no consistency in the elevation of terraces from site to site, but there is not even consistency in the number of terraces, the number ranging from one to four. In an additional effort to find consistent levels, a plot was made of the elevation of the terraces shown by each topographic profile against distance downstream, similar to the approach of Hack (1965, Fig. 32). This effort also failed. As a broad generalization, it appears that there is a surface at 2–3 m AMRL and another at 4–8 m. Exceptions are so numerous, however, that this generalization probably has little value.

Although the quest for consistent individual terrace levels thus was unsuccessful, the terrace point-elevation frequency distribution for Radford North and Pearisburg quadrangles produced interesting results (Fig. 2). Other things being equal, one might expect a plot of terrace area against elevation AMRL to be a monotonically decreasing curve, for if equal areas of flood plain were originally formed at all previous river elevations, such a curve would simply reflect the greater erosion (and thus decreased extent) of higher terraces. Although both curves in Figure 2 show such a tendency at their high ends, for lower elevations the picture is much different. Both histograms show a mode in the 0–40 ft (0–12.2 m) elevation range, then a low corresponding to elevations with relatively few terraces, and then a second mode at a higher elevation. Presumably the modes reflect elevations (and therefore times) at which

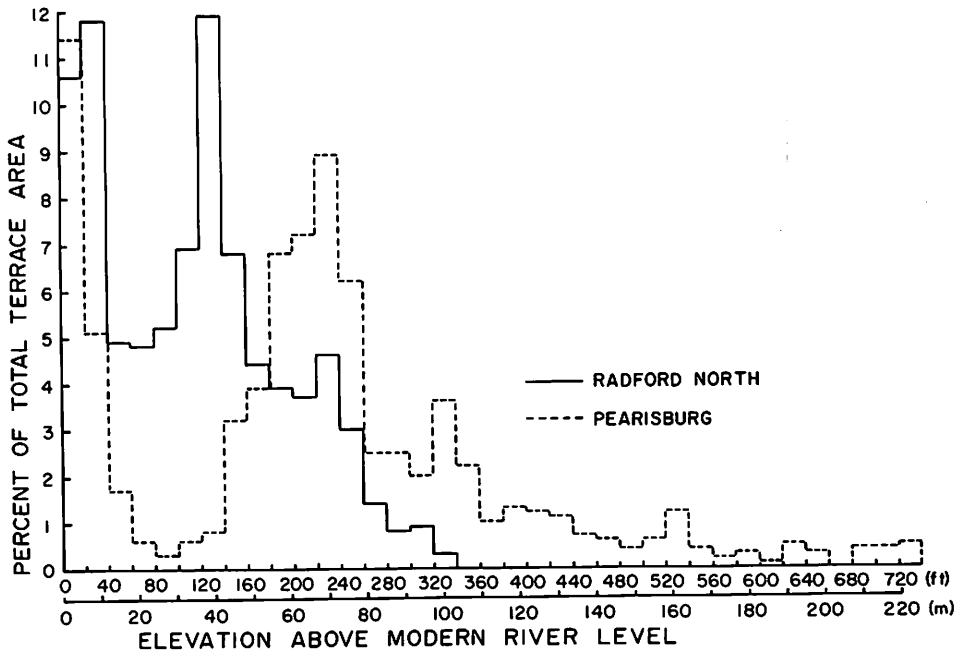

Figure 2. Terrace-elevation frequency distribution for Radford North and Pearisburg quadrangles. The manner in which these distributions were obtained is described in text.

lateral cutting was dominant, whereas the low between the modes reflects a time during which rapid downcutting took place.

Figure 2 also shows that the terrace point-elevation distributions in the two quadrangles differ in several ways. First, in the Radford North quadrangle, the higher mode occurs between 100–160 ft (30–49 m) AMRL, being centered at 130 ft (40 m), in the intermediate-terrace range. In the Pearisburg quadrangle, however, the higher mode occurs between 180–260 ft (55–79 m), being centered to about 220 ft (67 m), in the high-terrace range. Second, the low between the modes is much more pronounced in the Pearisburg quadrangle. Third, whereas the highest elevation of terrace alluvium in the Radford North quadrangle is 330 ft (101 m), in the Pearisburg quadrangle it is 730 ft (223 m), more than twice as high. A fourth difference, not shown in Figure 2, is the ratio of the total terrace area to the total area of the modern river channel. This ratio may be considered as an index of terrace "abundance" in a given area. In the Radford North quadrangle this ratio is 7.1, vs. 5.1 in the Pearisburg quadrangle.

As terraces in both areas overlie carbonate bedrock showing much local variation in structure, a difference in bedrock does not seem to be a likely explanation of the above differences. A difference in topography, however, may account for some of the differences. Local relief along the New River is higher in the Pearisburg quadrangle than in the Radford North quadrangle, owing to the proximity of the former to higher mountains. This difference may explain why terrace remnants occur at much higher elevations in the Pearisburg quadrangle and perhaps also why terraces are less abundant. It does not account, however, for the difference in elevations of the higher modes in Figure 2, nor for the paucity of low and intermediate terraces in the Pearisburg quadrangle.

The sediment-weathering studies in the Radford North quadrangle indicate that the two modes in this quadrangle, at least, are not merely statistical artifacts. As shown by Mills and Wagner (1985), the weathering intensities of sediments at elevations corresponding to the two modes differ greatly. Although the weathering indices generally show a correlation with elevation, there is not simply a steady increase in degree of weathering but rather a pronounced increase between sites lower than 25 m AMRL and those higher. This suggests that the higher terrace mode represents a time during which stream downcutting was slow. This interval was followed by a relatively recent interval of rapid downcutting. It is of interest that the correlation coefficients between weathering indices and elevation are somewhat greater for the low-terrace sites than for the high-terrace sites. Apparently even the lowest of the high-terrace sites are so intensely weathered that additional time, represented by the higher high-terrace sites, increases the weathering indices only slightly.

DISCUSSION

Implications for History of the New River

One possible criticism of this study is that mapping in an area where "terraces" consist of patches of alluvium on the tops and sides of hills, where much alluvium has been reworked during solutional lowering of the land surface, and where alluvium at the highest elevations gradually merges with residuum, is inherently too subjective to be reliable. However, I have compared my terrace maps of Radford North and Pearisburg quadrangles with those by Bartholomew and Schultz (unpublished data), and while details differ, it is obvious that terrace point-elevation frequency distributions determined from their maps would be very similar to mine.

With this assurance, plus that supplied by the weathering studies, the point-elevation distributions suggest a major change in the regime of the New River in this area. Confining attention to the Radford North quadrangle for the moment, the frequency distributions mode centered at 40 m AMRL apparently represents a period of time during which the river approached grade and had relatively broad flood plains. When the river reached about 25–30 m AMRL, however, it began cutting down rapidly, forming only narrow flood plains and thus leaving terraces that were few and narrow. The lower mode in Figure 2 may indicate that downcutting has stopped or slackened during the river's more recent history. However, it may be that there is always a mode at the lowest elevation, regardless of the river's activity, for a large proportion of flood plains and near-flood plain terraces probably are destroyed soon after the stream cuts down to a lower level.

Whether this major change in regime had a tectonic or climatic cause is presently unknown. The date at which downcutting began likewise is unknown, but some considerations suggest probable maximum and minimum ages for the change. Houser (1981) estimated ages of terraces by applying a regional erosion rate of 40 mm/1000 yr, estimated by Hack (1980). An elevation of 25–30 m AMRL would thus correspond to an age of 625,000–750,000 yr, perhaps corresponding to the onset of mid-Quaternary climatic cooling about 700,000 yr BP (e.g., Peterson and Lohmann, 1982), although solution undoubtedly has lowered the terraces from their original elevations. (Houser, 1981, has suggested that older surfaces on carbonate bedrock have been lowered one third of their original elevation AMRL. However, her inference seems rather tenuous, based as it was on zircon/tourmaline ratios in only four samples. Therefore, I shall use uncorrected present elevations, with the understanding that original elevations probably were somewhat higher).

The above age estimates, however, seem an order of magnitude too great for the degree of weathering displayed by the sediments of the

lower terraces. Alluvial deposits at an elevation of 20 m AMRL, for example, should be 500,000 yr old according to the above reasoning, and yet a comparison of their degree of weathering with that of dated glacial deposits in the Northwest and Midwest indicates that they could not possibly be older than Wisconsinan. Using an age of 70,000 yr BP for deposits at 20 m produces a minimum downcutting rate of 286 mm/1000 yr, which would give the break at 25–30 m AMRL an age of 87,500–105,000 yr BP. If correct, this would suggest that the break may have been related to the onset of Wisconsinan cooling and subsequent downcutting, perhaps caused by the greater discharge resulting from decreased evaporation and consequent increased runoff. Supporting this interpretation is the fact that stream downcutting much in excess of 40 mm/1000 yr, at least during the Wisconsinan, has been demonstrated elsewhere in the Appalachians. For example, Delcourt's (1980 and pers. commun., 1982) terrace 2 on the Little Tennessee River is 27,595 radiocarbon years old and it as high as 8 m AMRL; this represents a downcutting rate of 290 mm/1000 yr. In this regard it is important to note that Hack's (1980) estimate of a regional erosion rate for the Appalachians of 40 mm/1000 yr is based on modern river loads and on very long-term erosion estimates, such as Mathews (1975) estimates for the Cenozoic rate derived from sediment volumes on the Atlantic continental shelf. Although such estimates may be accurate for the time intervals they apply to, they by no means prohibit much greater rates over certain relatively short intervals of geologic history, such as Quaternary glaciations. In addition, for intervals of 100, 000 yr or so, a stream can cut down at a rate faster than that at which the landscape as a whole is being lowered; that this has happened in the study area is suggested by the incised nature of the New River valley at many locations.

From the above considerations, the age of initiation of the downcutting could range from less than 100,000 yr to more than 1,000,000 yr (taking solutional lowering into account). An age closer to the former seems more likely, however.

Neotectonic Implications

The most intriguing finding of the study is the difference between the terrace point-elevation frequency distributions in the Pearisburg and Radford North quadrangles, particularly the difference in elevation of their upper modes. The upper mode in the Pearisburg quadrangle (67 m AMRL) is 27 m higher than in the Radford North quadrangle (40 m AMRL). A crucial question is whether these two modes are correlative. Unfortunately, no absolute dating technique appears to be applicable to these sediments, and, as mentioned earlier, weathering of the higher terraces is so advanced that commonly there is little difference in weathering indices between sites several tens of meters apart in elevation.

However, it seems likely that when lateral cutting was dominant in one quadrangle, it was also dominant in the other. If the higher modes do correlate even approximately, clearly more downcutting has occurred in the Pearisburg quadrangle. One possible explanation for this finding is that the difference in elevation modes is only apparent, the terraces in the Radford North quadrangle having been lowered more rapidly by solution than those in the Pearisburg quadrangle. This explanation seems unlikely, however, for the bedrock underlying the two areas seems equally subject to solution. Another possibility is that the New River has increased its gradient during the interval of downcutting, thereby incising to a greater depth downstream. But this would require that the present gradient be several times that of the former. In addition, no downstream increase in elevation of terrace remnants is seen *within* either the Radford North or Pearisburg quadrangles; the difference is seen only *between* the two quadrangles.

The best possible explanation seems to be differential uplift or tilting, with the Pearisburg area having been uplifted 27 m relative to the Radford North area. Using the erosion rates estimated for the Radford North quadrangle earlier, it is possible to make rough estimates of the differential uplift rate. If the conservative erosion rate of 40 mm/1000 yr is used, then the 40 m-high terraces in the Radford North quadrangle are 1,000,000 yr old, and the presumably correlative 67 m-high terraces in the Pearisburg quadrangle of equal age. A differential uplift of 27 m in 1,000,000 yr averages 27 mm/1000 yr. On the other hand, if the erosion rate of 286 mm/1000 yr is used, then the terraces are only about 140,000 yr old. A differential uplift of 27 m in 140,000 yr averages 193 mm/1000 yr. Based on considerations discussed earlier, the differential uplift rate probably is closer to 193 m/1000 yr than to 27 mm/1000 yr.

Uplift of the Pearisburg area relative to the Radford North area is consistent with what is known of the local neotectonics. The Pearisburg area is a known seismic zone, apparently having been the epicenter of the second largest known earthquake in the Southeast (modified Mercalli intensity, VIII; body wave magnitude = 5.8), which occurred on May 31, 1897 (Bollinger and Wheeler, 1982, 1983). The monitoring of earthquakes with a seismograph network during the past few years has allowed this zone to be well defined. It is about 40 km long, 10 km wide, and is oriented approximately northeast–southwest (Fig. 1). The depth distribution of foci define a tabular zone extending from a depth of 5 to 25 km and dipping nearly vertically to the northwest. The zone lies in the basement rocks beneath the Appalachian overthrust belt and may represent the reactivation of an extension fault formed during the opening of the Iapetus Ocean. Recent microearthquakes exhibit predominantly strike-slip motion. However, the motions of older, much larger earthquakes are unknown. Orientation of the seismic zone and principal-

stress estimates from focal-mechanism studies indicate that reverse motion is also quite possible (Munsey and Bollinger, 1985; Bollinger, pers. commun., 1985). Such motion would uplift the northwest relative to the southeast, a sense of movement in agreement with the greater elevation AMRL of terraces in the Pearisburg quadrangle relative to those in the Radford North quadrangle.

What effect this hypothesized faulting has had on the ground surface is unknown. No rupture of the ground surface during the 1897 earthquake was reported or has been found. In addition, there is no known surface offset that could be attributed to slip accumulation by repeated activity in the seismic zone. I suggest that the apparent differential uplift of terraces in the Pearisburg area may record this slip accumulation, or at least part of it. Bollinger and Wheeler (1982) noted that it is not clear how fault slip would be transmitted through several kilometers of overlying complexly layered and faulted sedimentary rocks, and conceivably the slip might even be dissipated within this rock mass. Anther possibility might be that uplift could be transmitted through the sedimentary cover without the propagation of any major faults to the surface. The resulting gentle monocline might produce tilting over a horizontal distance of several kilometers or more, rather than abrupt uplift along a fault line. Because of the complex structure in this area, such uplift might be impossible to detect by a study of bedrock structure and stratigraphy. The terraces, however, because they were formed essentially on a plane dipping slightly downstream, provide a near-horizontal datum plane to indicate this vertical motion, despite their partial destruction by solution. Unfortunately, as Figure 1 shows, New River deposits between the southeastern Pearisburg quadrangle and the northwestern Radford quadrangle are almost nonexistent, making it difficult to use this method to determine where uplift or tilting is concentrated.

Future work on the possible uplift of alluvial terraces in this area should attempt to confirm the correlation between the terraces at 67 m AMRL in the Pearisburg quadrangle and those at 40 m in the Radford North quadrangle. New dating techniques should be investigated for this purpose; thermoluminescence dating (Wintle and Huntley,1982) is one possibility. Even if the utilized techniques give only relative-age dates they might allow correlation to be established. Another approach is to concentrate on low terraces where organic material is available for radiocarbon dating. However, trenching in the area (Mills, 1985) shows that organic material is preserved below the water table only, thus limiting this approach to terraces within a few meters AMRL. Such terraces may be too young to reflect differential uplift between the two quadrangles, especially given the scatter commonly observed in terrace elevations. It would also be desirable to look for uplifted terraces along

other streams in the Pearisburg area. Unfortunately, no other streams cut across the seismic zone at a high angle to it. One is essentially limited to tributaries of the New River, which are oriented within 20° to the seismic zone axis. However, those tributaries that join the New River where uplift is greater should have cut down more (at least in their downstream reaches), and thus their terraces should be higher than terraces of a comparable age located southeast of the uplifted area. Preservation of terraces along the narrow tributary valleys commonly is poorer than along the New River, but careful study of extant remnants might allow determination of any difference between the two areas.

SUMMARY AND CONCLUSIONS

The point-elevation frequency distributions show that there are preferred elevations for terraces in the study area. In the Radford North quadrangle these elevations are 0–12 m and 30–49 m AMRL, with the interval 12–30 m having few terraces. Corresponding to the upper part of the latter interval there is a pronounced increase in weathering intensity at about 25 m AMRL. Thus both topographic and weathering discontinuities seem to indicate an interval of relative stability during which lateral stream erosion was prominent, followed by an interval of downcutting. As terraces below 25 m AMRL seem to be no older than Wisconsinan based on their degree of weathering, a downcutting rate of almost 300 mm/1000 yr is indicated for this time interval, nearly an order of magnitude greater than the regional erosion rate.

The upper point-elevation frequency distribution mode in the Pearisburg quadrangle is about 27 m higher than that in the Radford North quadrangle. If the upper modes in the two areas are correlative, downcutting must have been greater and more rapid in the Pearisburg quadrangle. The most reasonable explanation for the greater downcutting is differential uplift of the Pearisburg area relative to the Radford North Area. Based on the ages and erosion rates estimated for the Radford quadrangle, the rate of differential uplift has averaged as much as 200 mm/1000 yr. This hypothesized uplift is consistent with what is known of the local neotectonics. The orientation of the Giles County seismic zone and principal-stress estimates from focal-mechanism studies indicate that faulting may uplift the Pearisburg area relative to the Radford area. The estimated differential uplift rate provides what is probably a minimum estimate of slip rate on the faults, as only part of the total fault movement may be transmitted through the sedimentary cover. Future research should attempt to confirm correlation between the terraces corresponding to the upper frequency-distribution modes in the two quadrangles.

During the course of this investigation, the author benefitted greatly from discussions with G. A. Bollinger, P. A. Delcourt, W. G. Harris, Brenda Houser, J. L. Howard, W. D. Lowry, R. C. McDowell, W. L. Newell, and R. L. Wheeler. The U.S. Geological Survey supported the study.

References

Bollinger, G. A., and Wheeler, R. L. (1982). The Giles County, Virginia, seismogenic zone—Seismological results and geological interpretations. U.S. Geological Survey Open-file Report 82-585, 136 pp.

Bollinger, G. A., and Wheeler, R. L. (1983). The Giles County, Virginia, seismic zone. *Science* **219**, 1063–1065.

Delcourt, P. A. (1980). Quaternary alluvial terraces of the Little Tennessee River valley, east Tennessee, in Chapman, Jefferson, Ed., *The 1979 archaeological and geological investigations in the Tellico Reservoir.* University of Tennessee Department of Anthropology Report of Investigations 29, 110–121, 175–212.

Hack, J. T. (1965). Geomorphology of the Shenandoah Valley, Virginia and West Virginia, and origin of the residual ore deposits. U.S. Geological Survey Professional Paper 484, 84 pp.

Hack, J. T. (1980). Rock control and tectonism—their importance in shaping the Appalachians: U.S. Geological Survey Professional Paper 1126-B, 17 pp.

Houser, B. (1981). Erosional history of the New River, southern Appalachians, Virginia. U.S. Geological Survey Open-File Report 81-771, 225 pp.

Mathews, W. H. (1975). Cenozoic erosion and erosion surfaces of eastern North America. *American Journal of Science* **275**, 818–824.

Mills. H. H. (1985). Descriptions of trenches dug in New River terraces between Radford and Pearisburg, June, 1981. U.S. Geological Survey Open-File Report 85-474, 67 pp.

Mills, H. H., and Wagner, J. R. (1985). Long-term change in regime of New River indicated by vertical variation in extent and weathering intensity of alluvium. *Journal of Geology* **93**, 131–142.

Munsey, J. W., and Bollinger, G. A. (1985). Focal mechanism analyses for Virginia earthquakes. *Bulletin of the Seismological Society of America*, in press.

Peterson, L. C., and Lohmann, G. P. (1982). Major change in Atlantic deep and bottom waters 700,000 yr ago: Benthonic foraminiferal evidence from the South Atlantic *Quaternary Research* 17, 26–38.

Wintle, A. G., and Huntley, D. J. (1982). Thermoluminescence dating of sediments. *Quaternary Science Reviews* **1**, 31–53.

Neotectonic Movements on a Passive Continental Margin: Salvador Region, Brazil

Louis Martin and Jean-Marie Flexor

Mission ORSTOM-CNPq-Observatório Nacional, Rua General Bruce 586, Rio de Janeiro, Brazil

Abilio C. S. P. Bittencourt and Jose M. L. Dominguez

Programa de Pesquisa e Pós-Graduação em Geofísica e Instituto de Geociências, Universidade da Bahia, Salvador, Brazil

In some restricted sectors of the Brazilian coast, it has been possible to demonstrate the role played by the vertical tectonic movements in shifting Quaternary shorelines. Within Todos os Santos Bay, State of Bahia, located in the Reconcavo graben, vertical movements of faulted blocks produced shifted Holocene shorelines. This neotectonism is related to the reactivation, during the Quaternary, of faults bounding the several crustal blocks which form the sedimentary basin. These deformations are not uniform throughout the basin.

INTRODUCTION

The interest of Brazilian specialists in seismological and neotectonic research in coastal areas was inhibited for a long-time, because the continental margins of Atlantic type were generally assumed to be very stable regions. Nevertheless, from the sixteenth century until the present days, earthquakes have been recorded in different parts of Brazil.

Up until now, structural features indicating neotectonic activities along the Brazilian continental margin and adjacent emerged portions have scarcely and only locally been recognized. Ponte (1969), in the Alagoas-Sergipe basin, and Almeida (1969), Bjornberg et al. (1972), Fulfaro and Ponçano (1974), Hasui et al. (1978), and Asmus and Ferrari (1978), in a narrow emerged portion of southeastern Brazil, presented the most convincing evidence of neotectonic activities.

In the State of Bahia, Sampaio (1916, 1919, and 1920) and Branner (1920) reported some earthquakes during the first two decades of this century in the Reconcavo basin, graben generated during the separation of the African and South American continents (Fig. 1). According to these authors, some witnesses revealed that these seismic events can be considered to have been "very strong." Branner (1920) even presents an isoseismic contour map based on these data.

Neotectonics: An International Journal of Crustal Dynamics, Vol. 1, 87–103 (1986)
© 1986 John Wiley & Sons, Inc. CCC 0884-8157/86/010087-17$04.00

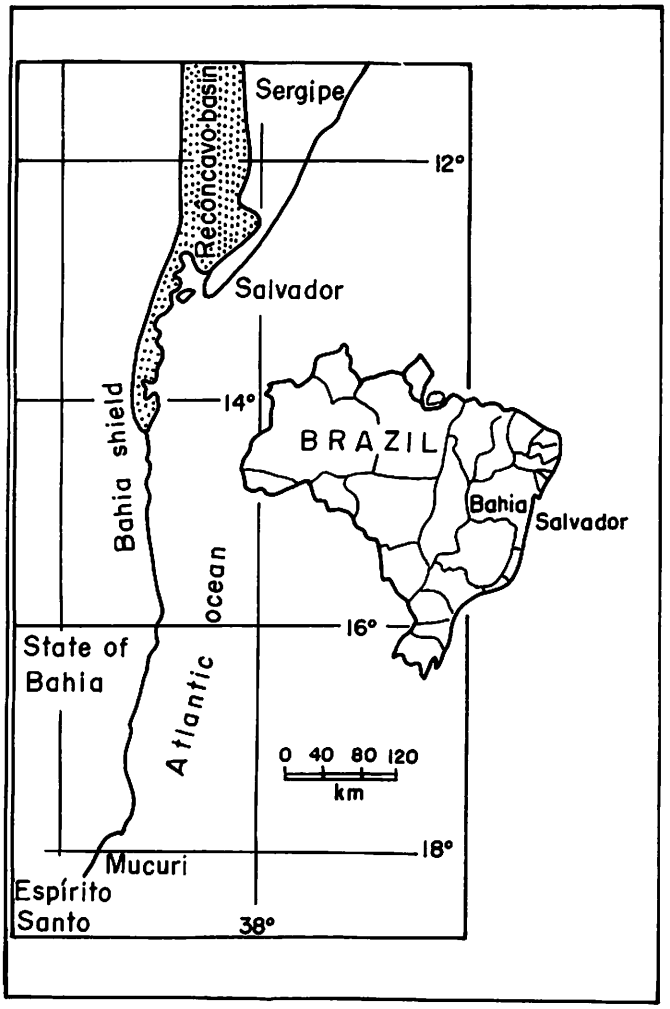

Figure 1. Location map of the study area.

Other authors, considering different kinds of evidence, believe in neotectonic activities in this area (King, 1956; Putzer, 1959; Grabert, 1960; Tricart and Cardoso da Silva, 1968; Suguio and Martin, 1976; Pedreira, 1976; Inda and Barbosa, 1978; Bittencourt et al., 1979; Haberhlenger, 1979; Martin et al., 1980; Fernandes Filho et al., 1982).

The main objective of this paper will be to recognize and try to interpret some geomorphologic and geologic evidence indicative of neotectonic activities in the part of the State of Bahia located between 12°30′ and 13°51′ S that contains the southern extremity of the Reconcavo basin (Fig. 1). This area has been selected because of the above-mentioned reports of seismic activity and because we have reasonable

litho- and chronostratigraphic knowledge of the Quaternary marine sediments overlying the Reconcavo basin Cretaceous deposits (Bittencourt et al., 1979, and Martin et al., 1980).

HISTORICAL GEOLOGY OUTLINE

The studies area belongs to the Eastern Bahia shield, part of the São Francisco craton. The Eastern Bahia shield is a crustal zone deformed during the geodynamic event that occurred toward the end of the Lower Proterozoic, between 1.9 and 2.1 b.y.a. (Transamazonic Regional Deformation) (Inda and Barbosa, 1978).

No record of geological events has remained from the Precambrian to the beginning of the Jurassic. A huge depression, known today as the "Afro-Brazilian depression," formed at the end of the Jurassic, in the present coastal area, and then began to be filled in by essentially continental deposits. This Jurassic basin was affected by deformational movements, as is evident from gravity faults and gently dipping anticlinal folds. When, at the onset of the Early Cretaceous, these movements started to exceed plasticity limits, the structural highs began to evolve into a system of marginal faults marking the borders of the Reconcavo basin. To the east, the system includes the Salvador fault, with a total slip of 4000 m, and to the west the Maragogipe fault, with a total slip of 300 m (Fig. 1) (Asmus and Ponte, 1973; Asmus and Porto, 1980; Fernandes Filho et al., 1982).

In the meantime, during the Early Cretaceous, the basin substrate began to subside, forming a rift valley. Invasion by the sea resulted in sedimentation of deep water deposits and marginal deltas. After a period of inactivity, another sequence of tectonic movements began, this time more vigorous and extensive. The end of the Cretaceous was characterized by progressively diminishing tectonic activity, by loss of its identity and integration into the shield. Some restricted records from northeast Salvador indicate that a brief marine incursion took place in the Reconcavo basin during the Miocene (Ghignone, 1978). The Pliocene is represented by alluvial fan-type continental deposits consisting of sandy and clayey sediments with variegated color. In the State of Bahia they are known as the Barreiras Formation. Two generations of sandy marine terraces related to two distinct transgressive episodes (Bittencourt et al., 1979) have been recognized along the Bahia coastline during the Quaternary. Coral samples from the basal portion of the older terrace have been dated to ca. 120,000 years B.P. (Bernat et al., 1982, and Martin et al., 1982), suggesting that it is of Pleistocene age. At that time sea level was about 8 ± 2 m above the present level (Martin et al., 1980). The more recent terraces are Holocene in age and related to the end of the last great transgression, which crossed the present sea level at about 7000

years B.P. (Martin et al., 1979). During the maximum, about 5100 years B.P., relative sea level was about 4.8 ± 0.5 m above the present level.

The evidence discussed herein shows that some sectors of the Mesozoic graben exhibited differential structural evolution during the Quaternary.

EVIDENCE OF QUATERNARY TECTONISM

Geomorphologic Evidence

Geomorphologic evidence confirms Quaternary tectonism in different parts of the studied region. One of the most remarkable physiographic features within the region is the Todos os Santos bay (Fig. 2). As the bay is situated entirely on the Mesozoic sedimentary rocks of the Reconcavo basin, enclosed by crystalline rocks, its orgin could be explained by differential erosion. Moreover, a detailed study of the hydrographic net shows that its drainage toward the bay is embryonal. In fact, the water separation line is situated 1 to 2 km from the margins. This situation, according to Tricart and Cardoso da Silva (1968), indicates that differential erosion is negligible and of very recent origin. This idea was also held by King (1956), Howard (1962), and Bittencourt et al. (1976). As it is, the bay shows some geomorphologic characteristics of a submerged area, in that it has many islands, indented margins, and several estuaries. The Todos os Santos bay was probably formed by differential subsidence of a series of faulted blocks.

Two other equally remarkable geomorphologic indicators are the Salvador and Maragogipe faults (Fig. 2). The Salvador fault exhibits features of recent movements within the sector between Porto da Barra and Lobato (Fig. 2). In this region the Precambrian crystalline rocks form cliffs at the coast whereas the northeastern portion of the fault is covered by Pliocene sediments of the Barreiras Formation and seems to have been inactive during the Quaternary. On the other hand, the greater part of the Maragogipe in the study area shows indications of recent reactivation. In the portions from the northern extremity of the Iguape bay to Jequiriça river, and from Valença to Igrapiuna, the Precambrian highlands form an extensive, more than 100 m-high, fault scarp. Some rivers did not have enough time to carve down their valleys and flow into Todos os Santos bay as water falls. Elsewhere, the portion of the sedimentary basin at the foot of the fault scarp is depressed and occupied by small bays or tidal creeks, as for example in the Iguape bay area and between Valença and Itubera. Taken together, this evidence suggests that Maragogipe fault is still active and causing subsidence of the areas mentioned.

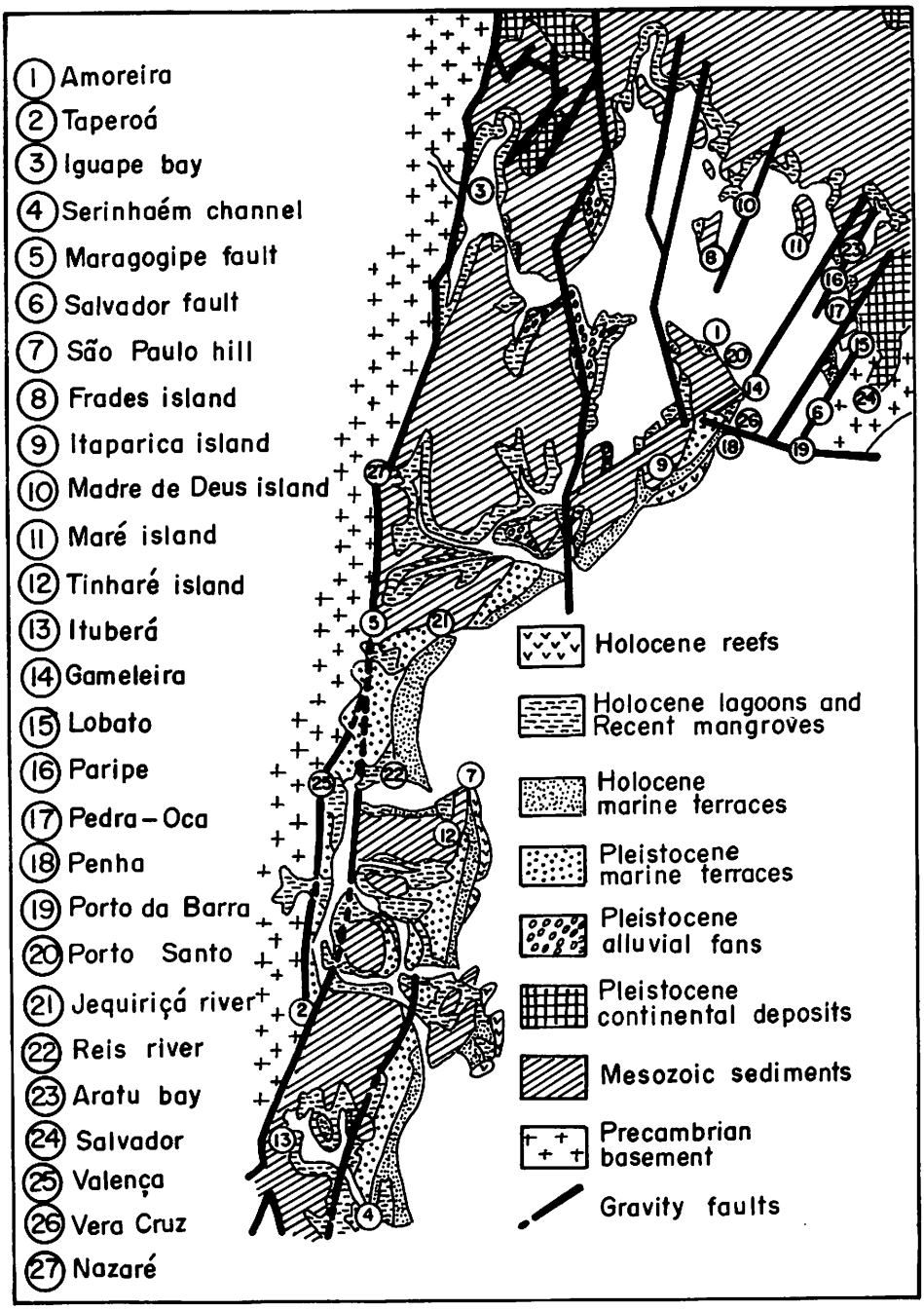

Figure 2. Geological map of southern part of the Reconcavo basin (Martin et al., 1980).

Evidence Related to the Geographic Distribution and Characteristics of the Pleistocene Marine Terraces

As absolute age determinations are lacking, it is not possible to reconstruct relative sea level heights during the penultimate marine transgression (ca. 120,000 years B.P.). However, it is possible to verify if the geographic distribution of the deposits provide some data about possible tectonic activity during the Quaternary. Two distinctive areas, separated by a straight line trending E–W, from Vera Cruz (Itaparica Island) to Nazare, have been identified. At the northern part (Todos os Santos bay) there are no Pleistocene terraces, with the exception of three occurrences situated at the north of Itaparica island and in the Frades and Fontes islands. It is interesting to note that these occurrences are situated within a central band parallel to the margins of the graben. At the southern end of the Vera Cruz–Nazare line, the Pleistocene marine sandy terraces are very well developed. Therefore, it is possible that this line represents an important structural boundary.

Moreover, drainage on Tinhare island is toward the continent, suggesting that the surface of the terrace dips landward, contrary to the original situation, when it was gently sloping toward the ocean. To the north and south of Tinhare island, drainage of Pleistocene terraces is toward the ocean, following the original slope.

Evidence Related to Difference in Level of Holocene Shorelines

To reconstruct the position of an ancient sea level it is necessary to define an indicator in time and space. The position (present height) of the indicators measured in the field is a function of sea level fluctuations (eustasy) and of vertical changes in the earth's crust (tectonism and isostasy). Therefore, it is possible to measure the relative position only. Sea level fluctuations are related to changes in the volume of the ocean water (glacio-eustasy) and in the volume of the oceanic basins themselves (tectono-eustasy), and to deformations of the surface of the geoid (geoidal-eustasy). The first two factors are of regional influence. Two indicators of the same level, when separated by a short distance, must be situated at the same height. Difference in elevation between closely spaced levels can be caused only by crustal deformation.

In a homogeneous sector of the Salvador region, situated to the north of the sedimentary basin, it was possible to construct a relative sea level fluctuation curve for the past 7000 years, based on 66 positions of ancient relative sea levels (Fig. 3). Another sea level fluctuation curve constructed with data from the Precambrian coast to the south of the sedimentary basin, exhibits the same characteristics as the Salvador curve. Both curves seem to indicate that the Eastern Bahia shield has been subjected to the same evolution for the past 7000 years. Therefore,

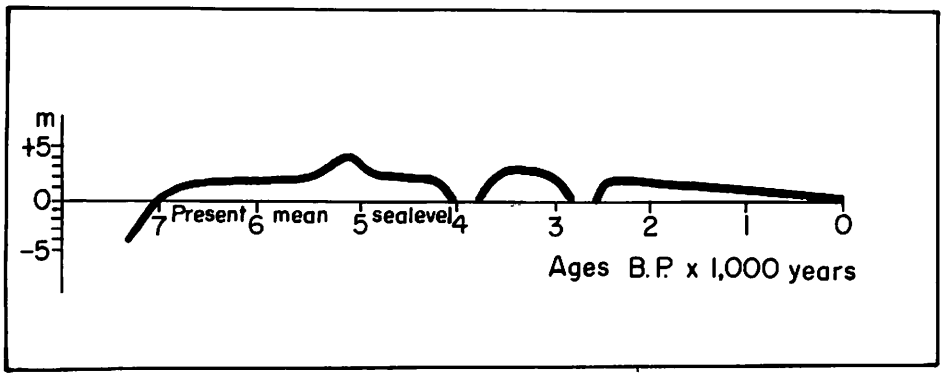

Figure 3. Curve showing the relative sea level fluctuation during the last 7000 years in the Salvador area (Martin et al., 1979).

reconstruction of ancient sea levels in different sectors of the sedimentary basin can be conceived by taking the Salvador curve as reference standard. This will allow us to verify if these sectors have evolved in the same way as the Eastern Bahia shield and to compare sectors among themselves. Table I reveals that some sectors of the sedimentary basin show elevations that are different from those of the Salvador curve. Moreover, it is remarkable that these differences in elevation are not homogenous.

COMPARTMENTATION OF THE RECONCAVO BASIN AS A FUNCTION OF THE DATA SUPPLIED BY THE MORPHOLOGY AND DIFFERENCE IN ELEVATION OF HOLOCENE SHORELINE

The data furnished by the morphology, by the distribution of Pleistocene terraces, and by differences in elevation of Holocene shorelines with respect to the Salvador curve, allow us to subdivide the Reconcavo basin into several compartments (Fig. 3). Firstly, we may distinguish two major units separated by a line trending E–W from Salvador to Nazare and crossing the Itaparica island. The northern unit corresponds to the Todos os Santos bay. In both units a number of compartments maybe recognized (Fig. 4).

Northern Unit

Compartment No. 1

This compartment lies in a narrow zone parallel to the easternmost boundary of the graben. At Pedra Oca, the ancient sea level does not show any difference in elevation with respect to the Salvador curve (Table I and Fig. 5). The Barreiras Formation, which covers the Salvador

TABLE I. Positions of ancient sea levels in several sectors of Todos os Santos Bay compared with positions of the same age on the Salvador curve.

Compartments (See Fig. 4)	Location (See Fig. 2)	Sample No.	Radiocarbon age (y.B.P.)	Position of sea level (m)	Corresponding position in the Salvador curve (m)
1	Pedra Oca	B 50	3260 ± 100	+3,0 (±0,5)	+3,2 (±0,5)
		B 51	3110 ± 105	+3,0 (±0,5)	+3,1 (±0,5)
		B 53	3100 ± 120	+3,0 (±0,5)	+3,1 (±0,5)
		B 52	3030 ± 120	+3,0 (±0,5)	+3,0 (±0,5)
2	Paripe	B 29	6600 ± 180	≃ −1,0	+2,0 (±0,5)
		B 31	5120 ± 120	≃ +1,5	+4,7 (±0,5)
		B 30	4840 ± 120	≃ 0,0	+3,0 (±0,5)
		B 28	4245 ± 100	≃ +0,5	+2,5 (±0,5)
		B 10	2105 ± 70	≃ +0,5	+2,0 (±0,5)
		B 7	2060 ± 100	≃ +0,5	+2,0 (±0,5)
	Aratu bay	B 15	4405 ± 110	≃ 0,0	+2,5 (±0,5)
3	Frequesia	B 174	1685 ± 85	+0,8 (±0,5)	+1,6 (±0,5)
	Maré island	B 176	3110 ± 105	+2,3 (±0,5)	+3,0 (±0,5)
4	Frades island	B 178	3595 ± 120	+3,5 (±0,5)	+3,4 (±0,5)
		B 49	4245 ± 95	+2,5 (±0,5)	+2,5 (±0,5)
		MD1	3550 ± 130	+3,3 (±0,5)	+3,4 (±0,5)
		MD2	3450 ± 120	+3,3 (±0,5)	+3,3 (±0,5)
		Bah.244	1470 ± 100	+1,3 (±0,5)	+1,4 (±0,5)
	Porto Santo	B 43	4525 ± 120	+2,8 (±0,5)	+2,7 (±0,5)
	Penha		2450 ± 95	+2,3 (±0,5)	+2,4 (±0,5)
	Amoreira	B 281	2280 ± 120	+2,0 (±0,5)	+2,2 (±0,5)
	Gameleira	B 283	1915 ± 100	+2,0 (±0,5)	+1,9 (±0,5)
8	Jequiriçá	B 36	5745 ± 140	+2,3 (±0,5)	+2,3 (±0,5)
	Reis river	B 32	4700 ± 160	+2,7 (±0,5)	+2,8 (±0,5)
11	Serinhaém	B 87	2405 ± 100	+2,3 (±0,5)	+2,3 (±0,5)

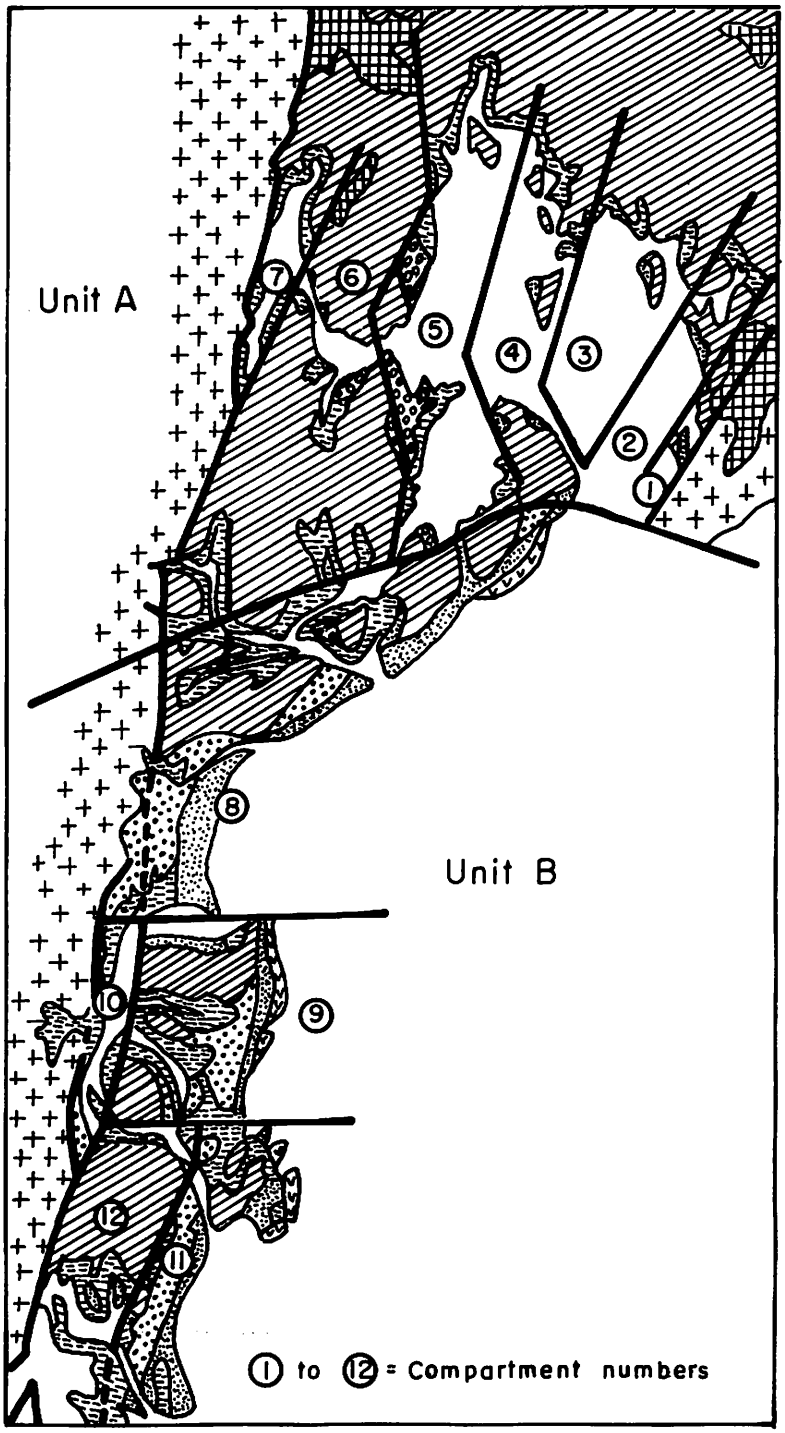

Figure 4. Compartmentation established as a function of Quaternary geological information.

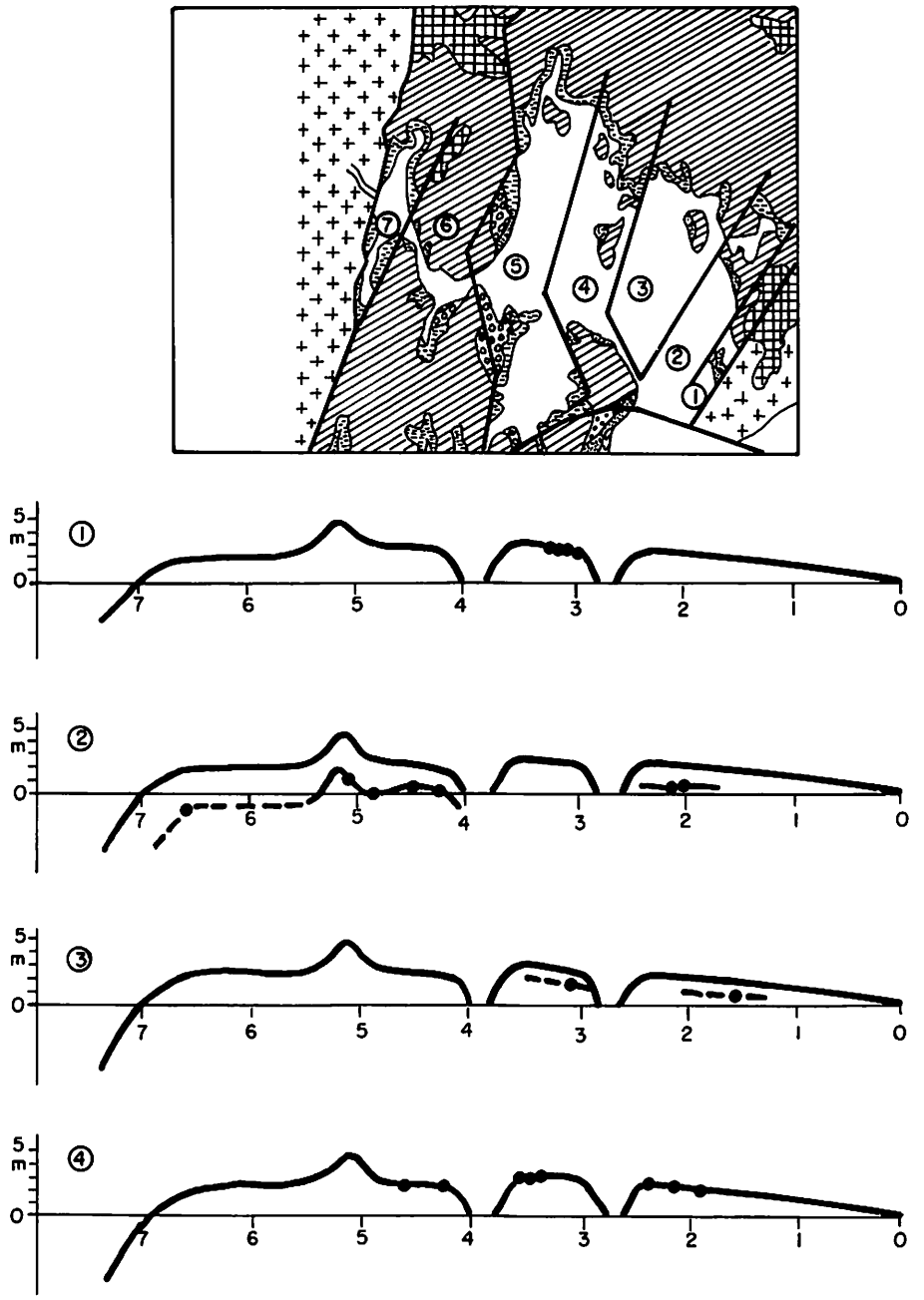

Figure 5. Positions of ancient relative sea levels (dots) in several compartments (1 to 4) compared with the Salvador curve.

fault to the north, was not affected by reactivation. To the south it seems that the fault line was reactivated during the Quaternary, being subjected very recently to subsidence.

Compartment No. 2

This compartment, parallel to the previous one, is separated at the western side by a line running from the Aratu bay entrance to the northern extremity of Itaparica island. Ancient relative sea levels reconstructed for the Paripe and Aratu bay region (Table I and Fig. 1) differ from those of the Salvador curve. The compartment appears to have been in relative subsidence during the Quaternary.

Compartment No. 3

This compartment also lies parallel to the previous ones, bounded at the south by the northern portion of Itaparica island. Evidence of ancient sea levels on the island is in concordance with the Salvador curve. The western boundary of the compartment is probably situated near the rectilinear eastern coast of Frades island. Contrary to the western coast, the eastern cost of this island has no marine terraces. Two ancient relative sea level points lie outside the Salvador curve. The amplitude seems to be less important than in Compartment No. 2.

Compartment No. 4

This compartment, very irregular, embraces the northern part of the Itaparica island and Frades, Madre de Deus, das Vacas, das Bimbarras, and das Flores islands. Only in this area of Todos os Santos bay have Pleistocene marine terraces been found. Ancient relative sea level reconstructions do not show discrepancies with respect to the Salvador curve (Table I and Fig. 5). The western boundary of the compartment corresponds to the western coast of northern Itaparica island and the western coast of das Fontes island. This compartment shows the same tectonic behavior as the Precambrian basement.

Compartment No. 5

The western boundary of this compartment is characterized by important scarps delineating the eastern margin of the Todos os Santos bay. The compartment seems to have been subjected to relative subsidence during the Late Quaternary, since there is no evidence of relative sea levels higher than the present one.

Compartment No. 6

This compartment is situated between Todos os Santos bay and Iguape bay. As this area is situated almost entirely on the continent, no ancient relative sea levels could be reconstructed. Probably, however, it remained stable throughout the Late Quaternary.

Compartment No. 7

This compartment lies at the foot of the cliff of the Maragogipe fault, which forms the western boundary of the graben. It comprises the Iguape bay, which shows clear evidence of subsidence. The compartment probably subsided during the Late Quaternary.

Southern Unit

Compartment No. 8

The northern boundary of this compartment is formed by the Salvador-Nazare line while the southern limit is constituted by the line running E–W from Valença to São-Paulo hill. Two reconstructed ancient relative sea levels obtained in the area agreed with the Salvador curve (Table I), suggesting that during the Late Quaternary its evolution was the same as that of the Precambrian basement.

Compartment No. 9

The southern limit of this compartment is parallel to the E–W line from Valença to São-Paulo hill. To the west it is bounded by the Valença-Taperoa lowlands. As mentioned previously, the rivers on the Pleistocene marine terraces of this area flow landward, indicating that the area tilted toward the continent after the transgressive episode of ca. 120,000 years B.P.

Compartment No. 10

This compartment forms a narrow band at the foot of the Precambrian cliff. It shares its western border with Compartment No. 9. The area is presently occupied by a lagoon. There is no evidence of Holocene sea levels higher than at present. This compartment probably has been subjected to subsidence during the late Quaternary.

Compartment Nos. 11 and 12

Scarce information is available for the area south of Compartment No. 9, but it is possible to delineate two other compartments. The first one, lying seaward, contains Pleistocene marine terraces with a drainage system oriented toward the sea. The second one, lying landward, shows features of subsidence. An ancient relative sea level reconstructed in the first compartment (No. 11), was in agreement with the Salvador curve.

COMPARTMENTATION BASED ON QUATERNARY GEOLOGY AND STRUCTURAL FRAMEWORK OF THE RECONCAVO BASIN

The structural framework of the Reconcavo basin is very well established because it has many producing oil fields. The basin is made up of a series of fault blocks associated with more or less parallel gravity faults. In general, these fault blocks show tilt and differential vertical displace-

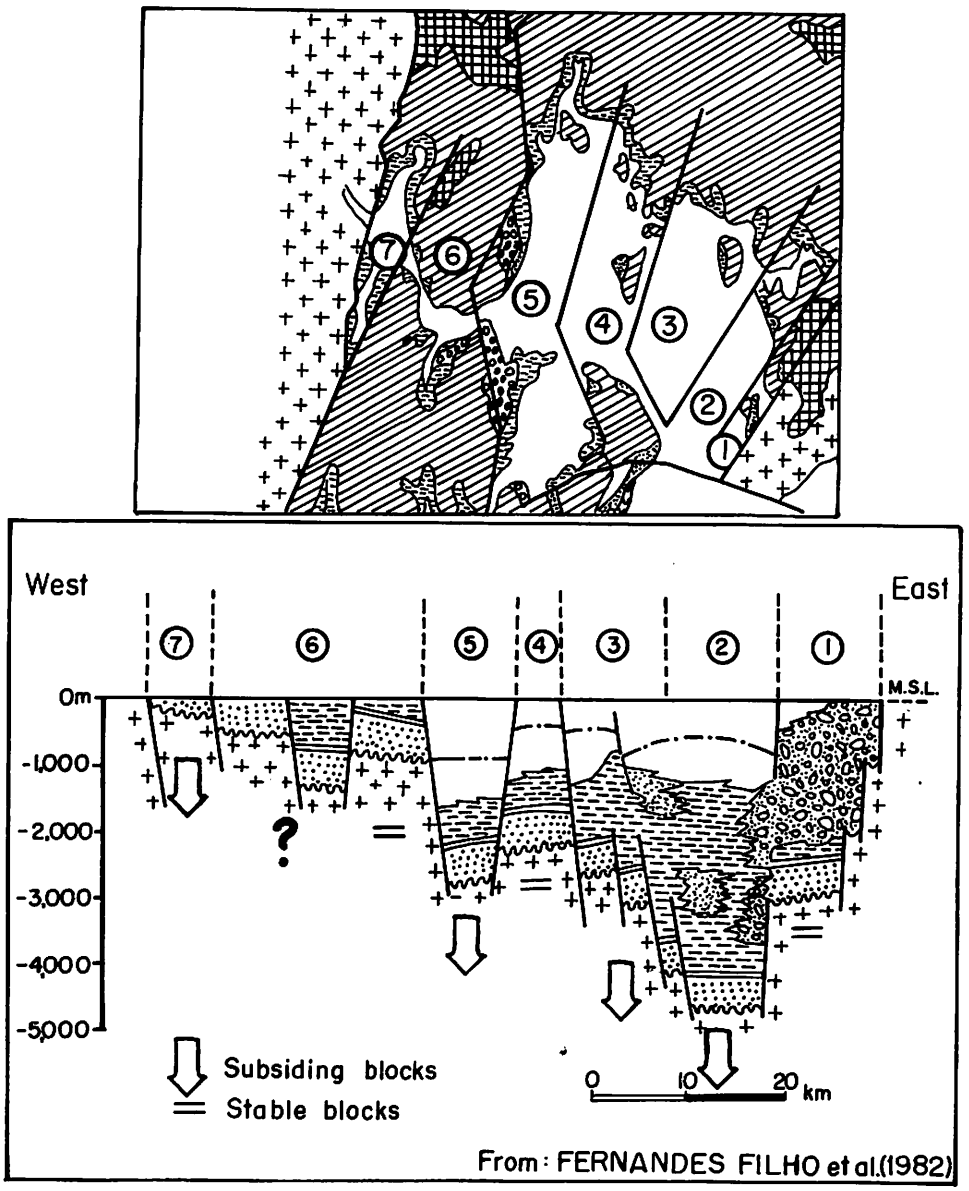

Figure 6. Comparison among compartmentation based on Quaternary geology and the structural framework of the Reconcavo basin.

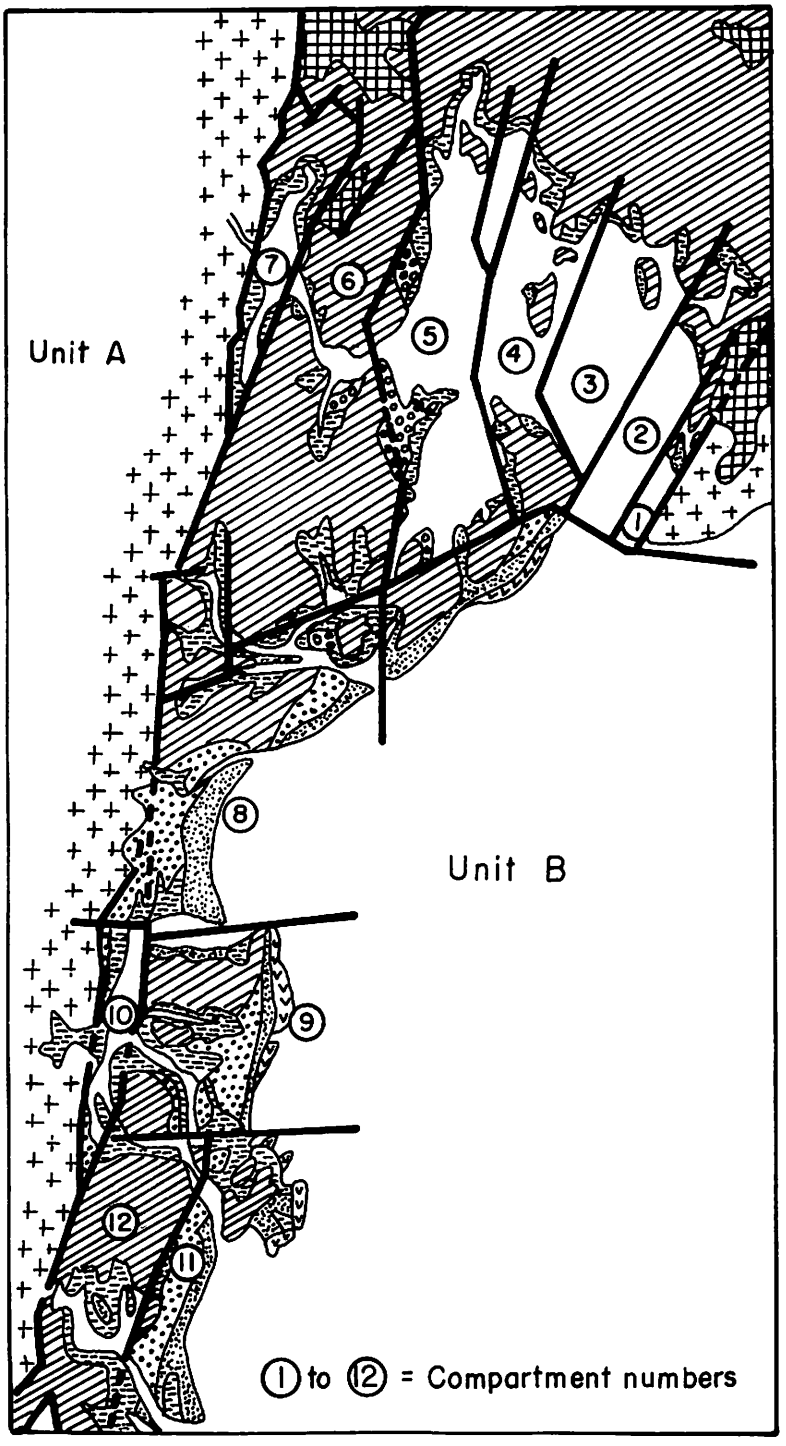

Figure 7. Synthesis map of the compartmentation (structural and Quaternary geology data).

ment. The fault blocks correspond perfectly to the compartment distinguished above on the basis of Quaternary geology. For example, fault block no. 2, characterized by maximum subsidence during the Mesozoic, showed clear evidence of subsidence during the Quaternary, too. Similarly, fault block no. 3 was much less active during both Mesozoic and Quaternary times. Compartment no. 4, which was stable during the Quaternary, is situated on a structural high.

The subsidence which occurred along the western boundary of the basin during the Quaternary only appears south of Iguape bay. Therefore, it does not appear in the cross-section of Figure 6. Information from "deep geology" (oil prospecting) confirms the existence of a northern and a southern unit in the Reconcavo basin (Fernandes Filho et al., 1982). The boundary between these two units corresponds to the Barra fault, which runs through the south of Salvador and through Itaparica island, converging with the Maragogipe fault south of Nazare.

So, we have been able to notice striking agreement between the Quaternary geology and structural framework of the Reconcavo basin (Fig. 7). Moreover, information from the present morphology and from the position of ancient Quaternary shorelines allowed us to infer that some faults were reactivated during the Quaternary.

CONCLUSIONS

Continental margins of Atlantic type are normally considered to be stable areas, but in some parts of Brazil, namely in the Reconcavo basin, noticeable vertical movements have been recorded during the Quaternary. Information from present morphology and ancient Holocene shorelines have been used to demonstrate these tectonic activities. Data from deep geology show that the Reconcavo basin is made up of fault blocks with differential evolution through time. Some of the fault lines bounding the blocks were active, while others remained completely inactive during the late Quaternary.

The authors wish to express their thanks to Dr. Franco Levi and Mr. Erik Lambooy for careful revision of the English text.

References

Almeida, F. F. M. de (1969). Structure and dynamics of the Brazilian coastal area. *International Upper Mantle Symposia* **22B** (VII), 29–38.

Asmus, H. E., and Ponte F. C. (1973). The Brazilian marginal Bassin, in A. E. M. Nairn and F. G. Stelhi (orgs), *The Ocean Basins and Margins*, v. 1, South Atlantic. New-York, London: Plenum Press, 87–132.

Asmus, H. E., and Ferrari, A. L. (1978). Hipótese sobre a causa do tectonismo cenozóico na região sudeste do Brasil. *Série Projeto REMAC* 4, 75–88.

Asmus, H. E., and Porto R. (1980). Difenenças nos estágios iniciais da evolução da margem continental brasileira: possíveis causas e implicações. *An XXXI Congr. Bras. Geol.* 1, 255–239.

Bernat, M., Martin, L., Bittencourt, A. C. S. P., and Vilas-Boas, G. S. (1982). Datations Io/U du plus haut niveau du dernier interglaciaire sur la côte du Brésil. Utilisation du ^{239}Th comme traceur. *C. R. Ac. Sc. Paris* **T296**, 197–200.

Bittencourt, A. C. S. P., Ferreira, Y. A., and Di Napoli, E. (1976). Alguns aspectos da sedimentação na Baía de Todos os Santos. *Revista Brasileira de Geociências* **6** (4), 246–263.

Bittencourt, A. C. S. P., Villas-Boas, G. S., Flexor, J. M., and Martin, L. (1979). Geologia dos depósitos quaternários no litoral do Estado da Bahia, in H. Inda (Ed.) *Geologia e Recursos Minerais do Estado da Bahia*, Textos Básicos 1, 1–21.

Bjornberg, A. J. S., Paraguassu, A. B., and Ganolfi, N. (1972). Sismogênese e neotectônica do sul do Brasil. *XXVI Congresso Brasileiro Geologia* (Abstract), Belém, 74–75.

Branner, J. C. (1920). Recent earthquakes in Brazil. *Bull. Seism. Soc. Amer.* **10** (2), 90–104.

Fernandes Filho, J. A., Muricy Filho, A. F., Silva, O. B., and Zabalaga, H. M. C. (1982). Estágio atual da exploração do petróleo da Bacia do Recôncavo. *Anais XXXII Congresso Brasileiro Geologia* **5**, 2273–2285.

Fulfaro, V. J., and Ponçano, W. L. (1974). Recent tectonic feature in the Serra do Mar region, State of São Paulo, Brazil, and its importance to engineering geology. *Proc. II Intern. Congr. of the IAEG*, São Paulo, 1, theme II, II-7.1 to II-7.7.

Grabert, H. (1960). Die jungtertiare und Altpleisztozane kustengestaltung Mittel-Brasiliens. *Die Erde, Jg.* **91**, 191–205.

Ghignone, J. L. (1978). Geologia dos sedimentos Fanerozóicos do Estado da Bahia, in H. Inda (org. texto) *Geologia e Recursos Minerais da Bahia*, v. 1, SME/CPM-Salvador, 24–113.

Haberhlener, H. (1979). Evolução do conhecimento sismológico no Brasil. *Anais do Simpósio sobre sismicidade Natural e Induzida*, São Paulo, 1–17.

Hasui, Y., Ponçano, W. L., Bistrichi, C. A., Stein, D. P., Galvão, C. A. C. F., Gimenez, A. F., Almeida, M. A., Pires Neto, A. G., Melo, M. S., and Santos, M. C. S. R. (1978). Geologia da Região Administrativa 3 (Vale do Paraíba) e parte da Região Administrativa 2 (Litoral) do Estado de São Paulo. Monografias (IPT) 1, São Paulo, 78 pp.

Howard, A. D. (1962). Escarpa da linha de falha de Salvador. *Boletim Técnico Petrobrás* **5** (3), 59–63.

Inda, H. A., and Barbosa, J. F. (1978). *Texto explicativo para o mapa geológico do Estado da Bahia* (Escala 1:1,000,000), Salvador: SME/CPM, 127 pp.

King. L. C. (1956). A geomorfologia do Brasil Oriental. *Revista Brasileira Geografia* **18** (2), 147–265.

Martin, L., Flexor, J. M., Vilas-Boas, G. S., Bittencourt, A. C. S. P., and Guimarães, M. M. M. (1979). Courbe de variation du niveau rélatif de la mer au cours des 7.000 dernières années sur un sécteur homogène du littoral brésilien (Nord de Salvador, Bahia), In Proceedings of the *1978 International Symposium on Coastal Evolution in the Quaternary*, Suguio, K., Fairchild, T. R., Martin, L., and Flexor, J. M., Eds., São Paulo, 264–274.

Martin, L., Bittencourt, A. C. S. P., Vilas-Boas, G. S., and Flexor, J. M. (1980). *Mapa geológico do Quaternário costeiro do Esta do da Bahia* Escala—1:250,000). Texto explicativo, Salvador: SME/CPM, 57 pp.

Martin, L., Bittencourt, A. C. S. P., and Vilas-Boas, G. S. (1982). Primeira ocorrência de corais pleistocênicos da costa brasileira. Datação da penúltima transgressão. *Ciências da Terra* **2**, 16–17.

Pedreira, A. M. (1976). *Texto explicativo para a carta geológica do Brasil ao milionésimo* (Folha de Salvador, SD-24), Brasília MME/DNPM, 127 pp.

Ponte, F. C. (1969). Estudo morfo-estrutural da Bacia Alagoas-Sergipe. *Boletim Técnico Petrobrás* **12** (4), 439–474.

Putzer, H. (1959). Movimentos epirogênicos quaternários na costa sudeste do Brasil e o problema do sambaqui. *Noticias Geomorfológicas* **2** (4), 39–41.

Sampaio, T. F. (1916). Tremores de terra do Recôncavo da Baía de Todos os Santos. *Revista Instituto Histórico da Bahia* **26** (45), 211–222.

Sampaio, T. F. (1919). Movimentos sísmicos na Baía de Todos os Santos. *Anais Congresso Brasileiro Geografia* **5**, Salvador, 335–367.

Sampaio, T. F. (1920). Tremores de terra na Bahia em 1919. *Revista Instituto Geogr. Hist. Bahia* **27** (46), 183–195.

Suguio, K., and Martin, L. (1976). Brazilian coastline Quaternary formations: The States of São Paulo and Bahia littoral zone evolutive schemes. *Anais Acad. Bras. Ciências* **48**, 325–334.

Tricart, J., and Cardoso Da Silva, T. (1968). Estudos da geomorfologia da Bahia e Sergipe. *Publicação da Fundação para o Desenvolvimento da Ciência da Bakia,* 167 pp.

Information for Contributors

The term "Neotectonics" can be defined as "new, recent, or living movements" and encompasses Neogene to Recent brittle and ductile deformation, vertical motions, tilting, isostatic rebound, seismicity, etc. The field of neotectonics has grown enormously during the last decade and we will provide a forum for researchers who publish in the following disciplines: seismotectonics, geodetic measurements and theory, tectonic geomorphology, mechanics of the lithosphere, isostasy, Neogene to Recent plate motions, as well as magnetics, structural geology, rock mechanics, palynology, paleontology, geochemistry, gravity, and eustasy, whenever these focus primarily on neotectonics.

All manuscripts for submission and correspondence about items under review should be sent to the Editor-In-Chief, Margaret A. Winslow, Dept. of Earth and Planetary Sciences, Science Building, J-106, City College of New York, Convent Avenue at 137th Street, New York, NY 10031 (212) 690-6984.

Correspondence concerning proofs, subscriptions, and all other matters should be sent to the Publisher, Professional Journals, John Wiley & Sons, Inc., 605 Third Avenue, New York, NY 10158.

Neotectonics is published quarterly in English. Abstracts will be in English and may also be in one other language (French, Spanish, German, or Italian). Translations will be provided by the authors. All editorial correspondence with authors will be conducted in English. The journal will contain the following: Research, Professional Reports, Communications and News, Letters to the Editor, Literature Reviews and Abstracts, Recent Contents, and Upcoming Meetings.

A covering letter must accompany each submission, indicating the name, address, and telephone number of the author to whom correspondence and proofs are to be sent.

Submission of a manuscript to the Editor implies that the paper has not been published, and it is not being submitted for publication elsewhere, and that, if the work reported is officially sponsored, it has been released for publication. Under the new copyright law, effective January

Neotectonics: An International Journal of Crustal Dynamics, Vol. 1, 105–107 (1986)
© 1986 John Wiley & Sons, Inc. CCC 0884-8157/86/010105-03$04.00

1978, the transfer of copyright from author to publisher, heretofore implicit in the submission of a manuscript, must now be explicity stated to enable the publisher to assure maximum dissemination of the author's work. The form to be used for this journal appears in the first and last issues of each volume; additional copies may be obtained from the Editor. *A copy of that agreement, signed by the author, is required before a manuscript can be accepted for publication.* (In the case of a "work made for hire," the agreement must be signed by the employer.)

Three copies of the manuscript are required for each submission. All material should be typed double spaced on one side only on standard 8½ × 11-in. (21 × 28-cm) paper with 1-in. (2.5-cm) margins. Any equations or special symbols should be typed wherever possible with all ambiguous symbols clearly identified (e.g., 1, l; x, ×). Number all pages through the reference section, beginning with the abstract.

The paper should be divided in the following way: First order headings are centered capitals; second order headings are centered capital/lower case; third order headings are indented capitals/lower case italic. The Abstract should be 500 words or less.

All *figures* should be cited in text with arabic numbers and captions should be supplied on a separate sheet at the end of the manuscript.

All figures and artwork must be submitted in camera ready form. Xerox copies are not acceptable. Line weight must be even and solid black and all lettering must be large enough to withstand reduction without breaking up or filling in. Ideally, artwork should be submitted twice the final size. The maximum final size of artwork for this journal is 4½ × 7½ in. (11.4 × 19 cm). Artwork is normally reduced to bring lettering down to a 1/12 in. (2 mm) height.

All *tables* should be cited in text with roman numbers and located at the end of the manuscript following the references and any figure captions.

Expository *footnotes* to the text are allowed but should be limited in use. These should be placed at the bottom of the page in the manuscript on which they are cited and should be noted with asterisks and daggers as needed. In no case should a footnote be used simply to indicate a literature citation.

Literature References are generally treated according to the Harvard System with some modifications. In the body of the text they are cited by naming the author (or authors connected by "and" if two, or with et al., replacing all names after the first if more than two) and indicating the year of publication in parenthesis, e.g., "(Jones, 1980)" or "according to Jones and Smith (1983)." Papers cited should be grouped together in a list headed "References," alphabetically arranged by first author's surname, at the end of the body of the paper. There all authors' names and initials are required, followed by the date of publication (in parentheses), followed by the full title of the cited paper. The title of the periodical

follows next, underlined for *italics* and contracted (as in the World List of Scientific Periodicals or Serial Publications Commonly Cited in Technical Bibliographies of the United States Geological Survey), then the volume number (with number of part closed up in parentheses), and finally the page numbers.

Authors will receive *proofs* that *must be corrected and returned within 48 hours*. No new material may be inserted in the text at the proofreading stage. Authors will be charged for alterations. A *reprint order form* is enclosed with the proofs. This form should be completed and returned (with prepayment) with the proofs to the publisher.

Publication Agreement

Under U.S. law, the transfer of copyright from the author should be explicitly stated in writing to enable the publisher to disseminate the author's work to the fullest extent. Please complete a copy of the following Publication Agreement and *include it with all submissions to this journal.* Please note that if the manuscript was a work made for hire, this agreement must be signed by the employer, as author.

Publication Agreement

The undersigned author has submitted a manuscript entitled_____

_____

for publication in_____, published by John Wiley & Sons, Inc.

A. The author transfers to John Wiley & Sons, Inc. the exclusive rights comprised in the copyright of the article, if the article is accepted for publication, except that the author retains the following:

1. All proprietary rights, other than copyright, such as patent rights.
2. The right to make copies of all or part of the work for the author's use in classroom teaching.
3. The right to use, after publication, all or part of this material in a book by the author.
4. The right to make copies of the work for internal distribution within the institution which employs the author.
5. The right to use figures and tables from the work, and up to 250 words of text, for any purpose. .
6. The right to make oral presentation of the material in any forum.
7. The right to veto or approve permission granted by the publisher to a third party to republish all or a substantial part of the article.

In the case of work prepared under U.S. Government contract, the U.S. Government may reproduce, royalty-free, all or portions of the article and may authorize others to do so, for official U.S. Government purposes only, if the contract so requires.

The author agrees that all copies made under any of the above conditions will include notice of the copyright of the publisher.

B. The author warrants that the manuscript is the author's original work. If the work was prepared jointly the author agrees to inform co-authors of the terms of this agreement. It is submitted only to this journal, and has not been published before. (If excerpts from copyrighted works are included, the author will obtain written permission from the copyright owners and show credit to the sources in the manuscript.) The author also warrants that the article contains no libelous or unlawful statements, and does not infringe on the rights of others.

_____

Author's signature and date

Check one:

_____Employer; work made for hire

_____Work of the U.S. Government

_____Author's own work

_____

Typed or printed name

_____

Institution or company

Note to Government Employees

A work prepared by a government employee as part of his/her official duties is called a "work of the U.S. Government," and is not copyrightable. If it is not part of the employee's official duties it may be copyrighted. If this is a work of the U.S. Government, the author may cross out Section A of this agreement and attach a copy of applicable policy of author's agency.

If the work was prepared jointly, and any co-author is not a U.S. Government employee, that author must be delegated by the co-authors to sign the *complete* agreement.

SOVIET SOIL SCIENCE

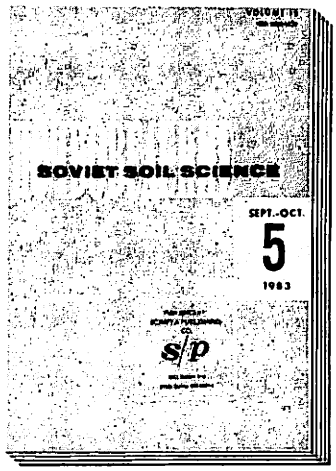

Editor: Andrew P. Mazurak, University of Nebraska

This interdisciplinary journal presents translations from two primary Soviet journals in soil science and agricultural chemistry, as well as papers from other prominent Soviet sources. Each issue contains original research and reviews on soil classification, genesis and geography, soil physics, chemistry, biology, mineralogy, erosion and melioration. There is a strong emphasis on problems encountered with poor, water-logged, Arctic and desert soils, prevalent not only in the Soviet Union, but also in developing Third World countries.

Indexed or abstracted in: Chemical Abstracts, Biological Abstracts and Geo Abstracts.

Volume 18, 1986 Bimonthly $230
Outside U.S. add $20 for surface postage and handling, or add $85 for airmail delivery.

MAIL TO: Subscription Dept., John Wiley & Sons,
605 Third Avenue, New York, NY 10158

Please enter my subscription to:
SOVIET SOIL SCIENCE.
Volume 18, 1986 Bimonthly $230
ISSN: 0038-5832

Outside U.S. add $20 for surface postage and handling, or add $85 for airmail delivery.
( ) Check enclosed. ( ) Bill me.
Charge to my credit card: ( ) MasterCard ( ) VISA

Card #_____ Expiration Date_____

Signature_____

Name_____

Affiliation_____

Address_____

City/State/Postal Code_____

NEO/01

Subscriptions are entered on a calendar year basis. Service will begin when payment is received.
For faster service, PHONE TOLL FREE 1-800-526-5368. In New Jersey, call collect (201) 342-6707.

TRANSACTIONS (DOKLADY) OF THE U.S.S.R. ACADEMY OF SCIENCES: EARTH SCIENCE SECTIONS

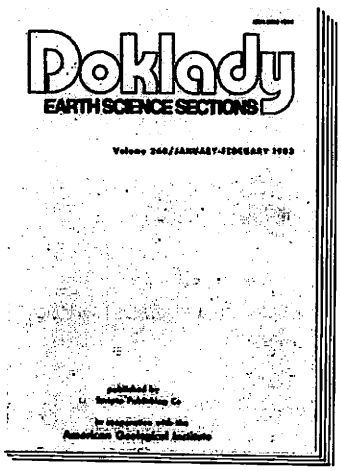

Editor: Jules D. Friedman,
U.S. Geological Survey, Denver

Published in cooperation with the American Geological Institute, this journal presents translations of original research reports from the *Transactions of the Soviet Academy of Sciences*. Each issue brings you the latest Russian research and developments in all aspects of earth science. Designed to serve a broad range of theoretical and applied earth scientists—from physicists to evolutionary biologists—the journal features papers from such important sections of the *Transactions* as: geophysics, seismology, tectonics, general and economics geology, lithology, mineralogy, petrography, geochemistry, paleontology, and oceanology.

Wide-ranging in scope, the journal is an invaluable reference source of information on major Russian advances in all areas of earth science.

Volumes 286–291, 1986 Bimonthly $420
Outside U.S. add $23 for surface postage and handling, or add $115 for airmail delivery.

MAIL TO: Subscription Dept., John Wiley & Sons,
605 Third Avenue, New York, NY 10158

Please enter my subscription to:
TRANSACTIONS (DOKLADY) OF THE U.S.S.R. ACADEMY OF SCIENCES: EARTH SCIENCE SECTIONS.
Volumes 286–291, 1986 Bimonthly $420
ISSN: 0012-494X
Outside U.S. add $23 for surface postage and handling, or add $115 for airmail delivery.
( ) Check enclosed. ( ) Bill me.
Charge to my credit card: ( ) MasterCard ( ) VISA

Card #_____ Expiration Date_____

Signature_____

Name_____

Affiliation_____

Address_____

City/State/Postal Code_____

NEO/02

Subscriptions are entered on a calendar year basis. Service will begin when payment is received.
For faster service, PHONE TOLL FREE 1-800-526-5368. In New Jersey, call collect (201) 342-6707.